Investigating the role of HDAC4 in the progression of Parkinson's Disease in *Drosophila melanogaster*

A thesis presented in partial fulfilment of the requirements for the

degree of

Master of Science

in

Genetics

At Massey University, Manawatu, New Zealand

Rose Lowe

2025

ABSTRACT

Parkinson's disease (PD) is the most common neurodegenerative movement disorder, characterised by the progressive loss of nigrostriatal dopaminergic neurons and the accumulation of α-synuclein-rich protein aggregates known as Lewy bodies. While current therapies manage symptoms, they do not halt disease progression, highlighting the urgent need for curative treatments. Emerging evidence suggests Histone Deacetylase 4 (HDAC4) plays a role in the progression of PD. HDAC4 has been detected in Lewy body inclusions and shown to undergo dysregulated nucleocytoplasmic shuttling in the presence of α-synuclein (*SNCA*), resulting in its nuclear accumulation and the repression of plasticity-related genes. This thesis investigates the role of HDAC4 in PD progression using a *Drosophila melanogaster* model. I found that *HDAC4* overexpression alone mildly impairs locomotor function and nuclear accumulation. However, co-expression of *HDAC4* with *SNCA* results in altered cellular distribution and the formation of large HDAC4 nuclear condensates. These findings suggest that while HDAC4 mislocalisation may contribute to PD pathology, HDAC4 may also play a critical role in maintaining dopaminergic neuron health.

ACKNOWLEDGEMENTS

First and foremost, I would like to express my deepest gratitude to my supervisor, Dr Helen Fitzsimons. Your gentle guidance, encouragement, and infectious enthusiasm created the ideal environment for me to grow both personally and academically. Your depth of knowledge and thoughtful mentorship have been truly invaluable throughout this journey. I feel incredibly lucky to have had you as a mentor and role model. Thank you for believing in me.

To my wonderful lab partners, Hannah, Sarah, Audrey, and Stephana, thank you for making the lab not only a place of learning, but also one filled with laughter and support. Working alongside you all has been one of the highlights of this experience, and I've learned so much from each of you.

To my family, and to my flatmates who became friends for life, your love, encouragement, and grounding presence have carried me through the tougher moments. Whether I needed a listening ear, a burst of positivity, or a well-timed distraction, you were always there. Thank you for being my safe space and cheering me on every step of the way.

Lastly, to my partner, Anthony, thank you for being my rock. Your support, patience, and belief in me, even on the days when I doubted myself, made all the difference. I am so grateful for your love and encouragement through every stage of this journey. I couldn't have done it without you.

To everyone who has played a part in this chapter of my life, thank you, from the bottom of my heart.

TABLE OF CONTENTS

LIST OF TABLES

LIST OF FIGURES

ABBREVIATIONS

AL	Antennal lobe
ANOVA	Analysis of variance
CaMK	Calcium/calmodulin-dependent protein kinase
CO	Codon optimised
CS	Canton special
Cy	Curly
DA	Dopamine/Dopaminergic
Ddc	Dopa decarboxylase
DNA	Deoxyribonucleic acid
DSHB	Developmental studies hybridoma bank
elav	Embryonic lethal abnormal vision
F65A	*Drosophila* HDAC4 hydrophobic core mutant
GAL80ts	Temperature sensitive mutant of GAL80
GFP	Green fluorescent protein
GMR	Glass multimer reporter
HDAC	Histone deacetylase
HSD	Honestly significance difference
KC	Kenyon Cells
L-DOPA	3,4-dihydroxy-L-phenylalanine
MB	Mushroom body
MEF2	Myocyte enhancer factor 2

MMIC	Manawatu Microscopy and Imaging Centre
MPTP	N-methyl-4-phenyl-1,2,3,6-tetrahydropyridine
mtDNA	Mitochondrial DNA
NES	Nuclear export signal
NLS	Nuclear localisation signal
OL	Optic lobe
PBS	Phosphate-buffered saline
PBT	Phosphate-buffered saline with triton X-100
PD	Parkinson's disease
PP2A	Protein phosphatase 2A
PPII	Poly-(L-proline) II
RNAi	RNA interference
Sb	Stubble
SNpc	Substantia nigra pars compacta
TH	Tyrosine hydroxylase
UAS	Upstream activator sequence
w(CS10)	White canton-special
WT	Wild-type
α	Alpha
β	Beta

1 INTRODUCTION

1.1 AGING AND NEURODEGENERATIVE DISEASE

1.1.1 The brain during aging

Aging changes the neuronal complexity and structure of the brain. There is a natural decline in synaptic plasticity, reduced dendritic branching and spine density, chronic neuroinflammation, and white matter deterioration, particularly affecting the prefrontal cortex and hippocampus (Dickstein et al., 2007; Yankner et al., 2008). Not only does age-related deterioration impact learning and memory, but it also increases susceptibility to neurodegenerative diseases. While neuronal damage is normal in aging, considerable and progressive neuronal degeneration occurs in major neurocognitive disorders such as Parkinson's disease (PD), Alzheimer's disease, Prion diseases, Huntington's disease, Frontotemporal dementia, Spinocerebellar ataxia type 1, and Motor neuron disease (Dickstein et al., 2007; Taylor et al., 2002). These diseases are all associated with abnormal changes to the brain as well as dysfunction in cellular systems, including mitochondrial function and protein homeostasis, which together can lead to oxidative stress, neuroinflammation, and eventual neurodegeneration.

Aberrant protein aggregation is also a common feature of several neurodegenerative disorders; for example, the deposition of toxic Huntingtin and Ataxin-1 protein aggregates from the expansion of polyglutamine (CAG) repeats within these proteins results in Huntington's disease and Spinocerebellar ataxia type 1, respectively (Bertram & Tanzi, 2005; Federspiel et al., 2019; Fernandez-Funez et al., 2000). Other neurodegenerative diseases are also associated with abnormal protein deposits, including β-amyloid (Aβ) (Alzheimer's disease), α-synuclein (PD), and microtubule-associated protein tau (frontotemporal dementia with parkinsonism), that correlate with neurodegeneration (Crowther et al., 2005; Dickstein et al., 2007; Taylor et al., 2002). In a small number of cases, familial mutations have been identified in the genes encoding these proteins that promote aggregation, but in most cases these mutations are not present. While it is known these disorders often have a genetic predisposition as well as environmental triggers, the exact underlying mechanisms of both aging and neurodegeneration

are still largely unknown (Bertram & Tanzi, 2005; Mitchell, 2011; Rose, 2009; Whitworth, 2011).

1.1.2 Parkinson's disease

Of these neurodegenerative diseases described in section 1.1.1, PD is the most common neurodegenerative movement disorder, characterised as an age-dependent neurological condition with a progressive course. The mean age of onset is approximately 55 years, and the incidence increases markedly with age, rising from 20 per 100,000 in the general population to 120 per 100,000 at age 70. About 95% of cases are sporadic with no apparent genetic linkage, while the remainder are inherited (Dauer & Przedborski, 2003; Myall et al., 2017; Whitworth, 2011). This disease manifests symptoms such as motor disabilities including rigidity, bradykinesia, hypokinesia, and akinesia, alongside non-motor features like reduced facial expression, decreased voice volume, drooling, and micrographia (small, cramped handwriting). Motor disability often becomes pronounced within 5 – 10 years, even with symptomatic treatment (Dauer & Przedborski, 2003). The prevalence of PD is expected to rise, with predictions indicating an increase of cases in New Zealand from 9,340 in 2013 to 27,200 by 2068. Interestingly, the disease shows a sharp increase in incidence from age 65 and a sharp decline after age 85 (Myall et al., 2017). The non-linear pattern of incidence with age suggests it is more commonly associated with a specific older age group rather than being an aging-dependent condition.

While age is a significant risk factor for PD, the processes that drive neuronal degeneration differ from those that govern normal aging, and certain brain areas are more vulnerable. The substantia nigra pars compacta (SNpc) is largely affected by cell loss in ventrolateral and caudal regions in PD, while normal aging influences the dorsomedial region (Fearnley & Lees, 1991). In early stages, degeneration is concentrated in the ventrolateral substantia nigra, progressing to other brain regions as the disease advances (Balzano et al., 2024). The SNpc, a crucial part of the basal ganglia, consists mainly of dopamine-secreting neurons (Figure 1.1). Dopamine (DA), a key brain monoamine, primarily acts as an inhibitory neurotransmitter and plays a vital role in regulating the excitability of striatal neurons, which help coordinate body

movements (Chinta & Andersen, 2005; Ericsson et al., 2013; Lahiri & Bevan, 2020) (Figure 1.1).

DA is synthesised from tyrosine; an amino acid derived from phenylalanine in the liver. Tyrosine is actively transported into the brain and taken up by dopaminergic (DA) neurons, where it undergoes a two-step conversion. First, tyrosine hydroxylase (TH) catalyses the hydroxylation of tyrosine to L-DOPA (3,4-dihydroxy-L-phenylalanine). The enzyme Dopa decarboxylase (aromatic amino acid decarboxylase; AADC) then rapidly converts L-DOPA into DA in the cytoplasm (Ayano, 2016; Kumer & Vrana, 1996) (Figure 1.1). The biosynthesis of DA depends on the expression and precise regulation of TH, as this enzyme catalyses the first and rate-limiting step in the pathway. This reaction is acutely regulated by neuronal activity and neurotransmitter signalling to maintain neurotransmitter homeostasis in dopaminergic and noradrenergic neurons (Friggi-Grelin et al., 2003; Kumer & Vrana, 1996; Zigmond et al., 1989).

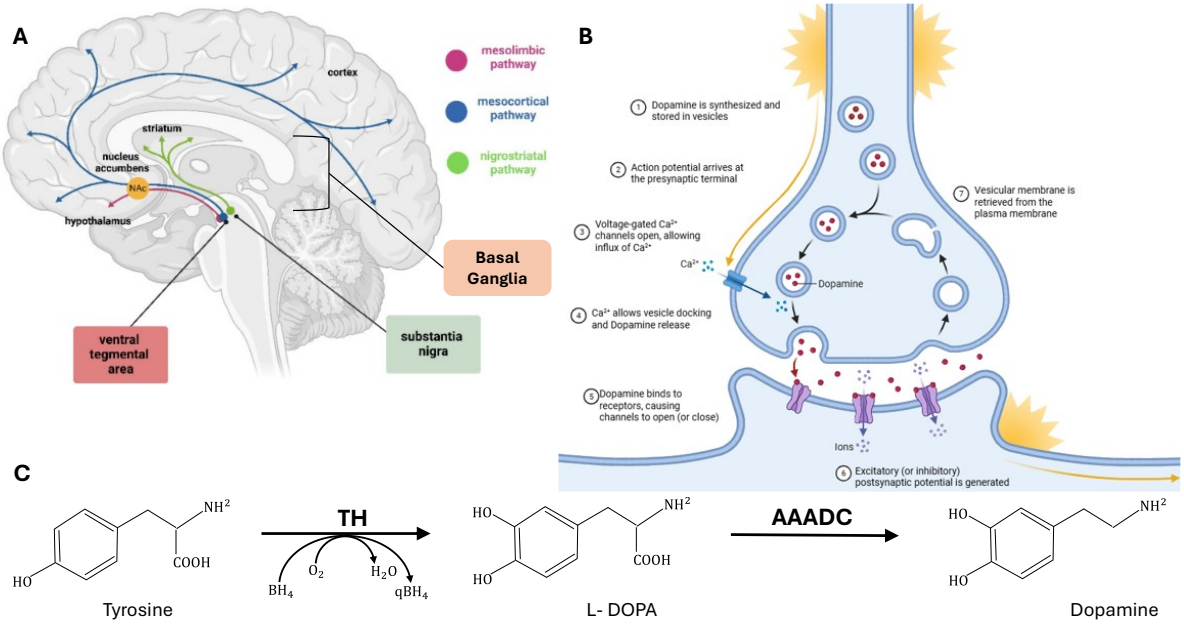

Figure 1.1 – The dopaminergic system

(A) The three dopaminergic pathways in the brain. The mesolimbic pathway (pink), the mesocortical pathway (blue), and the nigrostriatal pathway (green), which extends from the substantial nigra to the striatum. In Parkinson's disease, the nigrostriatal pathway degenerates, leading to a loss of dopamine in the striatum and impaired regulation of the basal ganglia circuitry responsible for voluntary movement. This figure is reproduced and edited from Basso et al. (2024) (DOI: 10.3390/biology13090690), which is distributed under CC BY 4.0 http://creativecommons.org/licenses/by/4.0/. **(B)** Diagram of a dopaminergic synapse in the striatum. Dopamine is released from nigrostriatal terminals and modulates the excitability of medium spiny neurons by acting on D1 (excitatory) and D2 (inhibitory) receptors. In Parkinson's disease, loss of dopamine disrupts this balance, impairing basal ganglia output and motor control. This figure is reproduced and edited with BioRender from Kim, S. (2025) BioRender, https://app.biorender.com/biorender-templates/details/t-6058d4705e753600a05fabc4-chemical-synapse-steps-of-synaptic-transmission. **(C)** Diagram of the dopamine synthesis pathway with tyrosine hydroxylase (TH) catalysing the first and rate-limiting step of conversion of tyrosine to L-DOPA. L-DOPA is then converted to dopamine by aromatic amino acid decarboxylase (AAADC). Original artwork with reference to Alam & Richardson (2020) & Sasaki & Harano (2010).

TH is regulated through gene expression and transcriptional control, as well as phosphorylation and dephosphorylation of multiple serine residues. Phosphorylation increases its affinity for substrates, thereby enhancing activity, whereas dephosphorylation by protein phosphatases reduces TH activity, acting as a negative feedback mechanism (Kumer & Vrana, 1996). Oxidative stress and neurotoxic conditions can downregulate TH function, contributing to neurodegeneration (Kumer & Vrana, 1996). In PD, the degeneration of DA-producing neurons in the SNpc leads to a significant reduction in DA levels. This deficiency results in decreased inhibition of striatal neuron activity, causing excessive firing and making movement control difficult for individuals with PD (German et al., 1989; Maiti et al., 2017).

A small percentage of PD cases are attributed to genetic mutations, with risk genes including *SNCA*, *PINK1, LRRK2, PARK*, Glucocerebrosidase (GBA), and mitochondrial DNA (mtDNA) (Aasly, 2020; Nuytemans et al., 2010; Salles et al., 2024). Most cases have no known genetic cause; therefore, there is a large emphasis on elucidating the molecular pathways involved. Disruption to molecular processes such as mitochondrial function, axonal transport, and protein degradation has been observed to trigger neuropathologies common to both sporadic and inherited forms of PD (Ebrahimi-Fakhari et al., 2012; Henrich et al., 2023; Yang et al., 2025). Environmental toxins, as well as mutations in genes or the misfolding of proteins within these pathways are most commonly the root causes of the pathway dysfunction. Exposure to pesticides, herbicides, fungicides, and insecticides has been strongly linked to the development of sporadic PD (Pezzoli & Cereda, 2013; Van Maele-Fabry et al., 2012). People in rural areas and farmers are particularly at risk due to direct contact or contaminated water sources (Petit et al., 2025). Toxins like 1-methyl-4-phenyl-1,2,3,6-tetrahydropyridine (MPTP) are known to cause Parkinsonism by crossing the blood-brain barrier and converting into the toxic MPP+, which damages DA neurons (Goldman, 2014; Maiti et al., 2017). Other environmental chemicals such as paraquat, maneb, rotenone, and ziram also cause DA neuron degeneration in animal models by disrupting mitochondrial function, particularly Complex I of the electron transport chain, leading to oxidative stress (Goldman, 2014; Maiti et al., 2017). Other environmental exposures, such as polychlorinated biphenyls, solvents, metals, and pollutants, have also been associated with an increased risk of developing the disease; however, the specific pathways they affect are not well known (Goldman, 2014). The current PD treatments

available aim to restore DA levels and manage symptoms through medications, surgical interventions, gene therapy, and supportive therapies (Armstrong & Okun, 2020).

The most effective pharmacological treatment is Levodopa (L-DOPA). While this is converted to DA in the brain, it does not prevent neurodegeneration (Chinta & Andersen, 2005; LeWitt, 2008; Poewe et al., 2017). Surgical interventions such as deep brain stimulation (DBS) are invasive and expensive, while various gene therapies show potential in animal and early human studies but require further research (Bronstein et al., 2011; Deep-Brain Stimulation for Parkinson's Disease Study Group, 2001; Dumbhare & Gaurkar, 2023). While these treatments developed so far help manage PD symptoms, prevent DA degradation, increase DA production, or provide some neuroprotective properties, they are not cures as they do not halt disease progression, emphasising the need for continued research into curative therapies.

The first PD-related gene to be studied and main contributor is *SNCA*, which encodes the α-synuclein protein (Magistrelli et al., 2021; Polymeropoulos et al., 1997). The loss of nigrostriatal DA neurons in PD can be seen alongside the presence of intraneuronal proteinaceous inclusions called Lewy bodies, in which the accumulation of α-synuclein is implicated in its pathology (Dauer & Przedborski, 2003; Poewe et al., 2017). The study by Spillantini et al. (1998) was a landmark discovery demonstrating that α-synuclein is a major component of these Lewy bodies, where electron microscopy revealed that the a-synuclein-containing inclusions form twisted filamentous structures, suggesting that α-synuclein misfolding and aggregation are central to Lewy body formation. Furthermore, autopsies and genetic studies of families with inherited parkinsonism identified duplications and triplications of the *SNCA* gene, along with α-synuclein aggregation and Lewy body pathology, similar to sporadic PD, supporting a link between α-synuclein overexpression and neurodegeneration (Chartier-Harlin et al., 2004; Farrer et al., 2004).

1.2 SNCA

α-synuclein is predominantly localised in the presynaptic terminals and synaptic vesicles of neurons, where it plays a critical role in synaptic vesicle dynamics, including trafficking, docking, and recycling (Bellani et al., 2010; Kahle et al., 2000; Lee et al., 2008; Withers et al., 1997) (Figure 1.2). This protein interacts with membranes and other proteins to modulate neurotransmitter release efficiency (Bellani et al., 2010). Studies on α-synuclein-null mice reveal its functional importance in maintaining synaptic vesicle availability, as these mice exhibit significant deficits in DA release and synaptic vesicle clustering at the active zones of DA neurons (Abeliovich et al., 2000; Cabin et al., 2002). Structurally, α-synuclein exists as a mostly disordered, unfolded polypeptide chain of 140 amino acids with some poly-(L-proline) II (PPII) helical conformation (Jakes et al., 1994; Uversky, 2003) (Figure 1.2). The function of α-synuclein is not fully understood; however, the PPII helical conformation is important for the protein's role in signal transduction, transcription, cell motility, and the immune response (Kelly et al., 2001; Uversky, 2003).

Oligomerisation of α-synuclein has been identified as the biggest contributor to the onset and progression of PD. While individual monomers are unfolded, they can self-associate to form organised secondary structures such as soluble oligomers, leading to amorphous aggregates. These aggregates form highly organised fibrils in the shape of a cross-β-sheet (Uversky, 2003). Lewy bodies seen in PD can form due to inhibition or impairment of α-synuclein degradation, increased expression of, or point mutations in the *SNCA* gene, which can promote misfolding of the protein, causing an unstable conformation. This can induce self-aggregation by binding to additional α-synuclein monomers in a way that exposes distinctive surfaces for optimising new van der Waals interactions, creating unstable structurally unlike oligomers. These oligomers elongate to form proto-fibrils and fibrils, then eventually form Lewy bodies (Melki, 2015; Poewe et al., 2017; Spillantini et al., 1998) (Figure 1.2). While Lewy bodies form in neurons to cause damage in the brain, Lewy body formation can also occur in the digestive tract and behave similarly to prion proteins, where it then spreads through the central nervous system (Maiti et al., 2017; Poewe et al., 2017). The overexpression of α-synuclein in *Drosophila* intestines has demonstrated its potential to aggregate and propagate through

neuronal circuits to the central nervous system, contributing to DA neuronal loss and motor deficits (Liu et al., 2022).

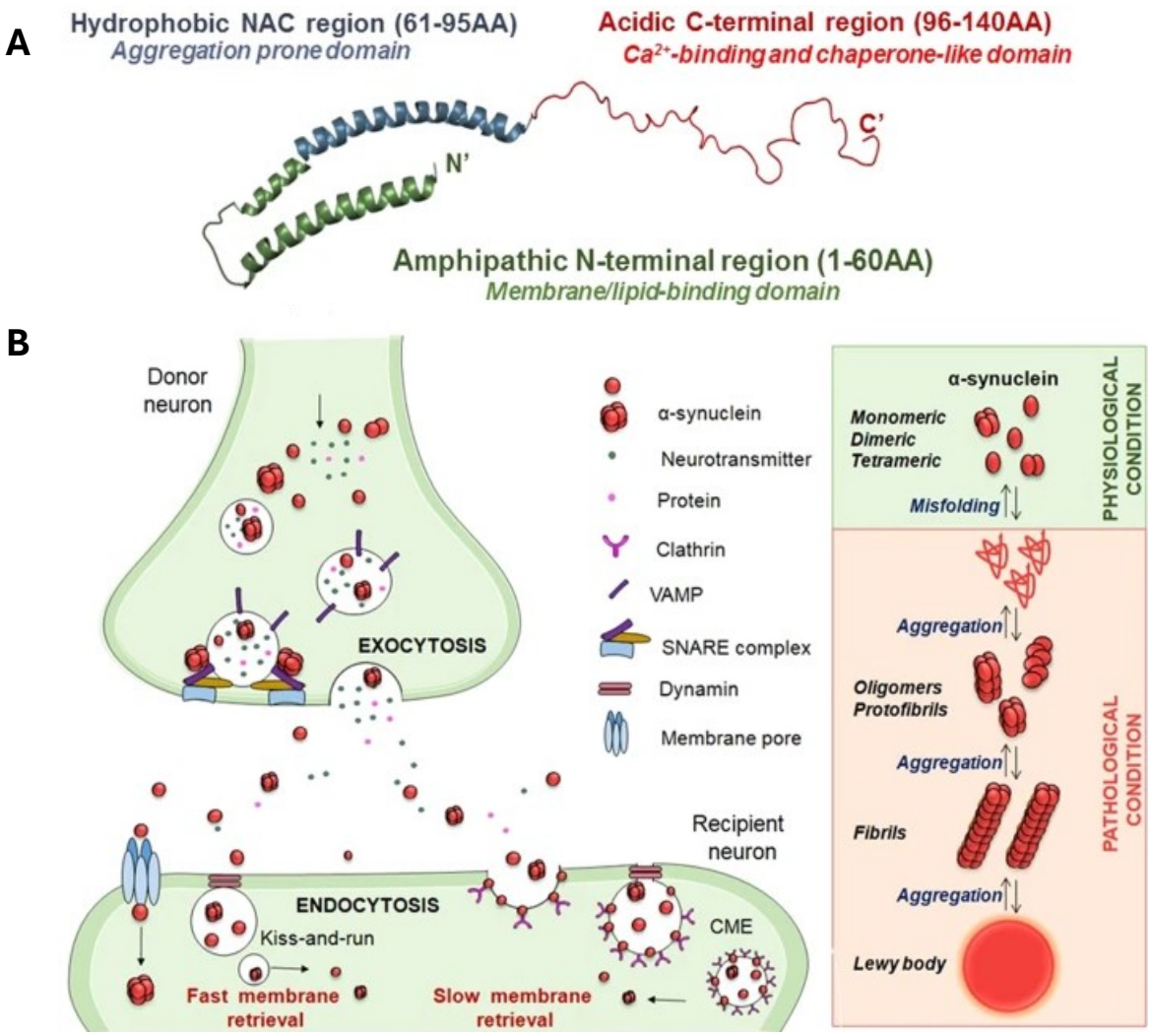

Figure 1.2 - α-synuclein

(A) The structure of α-synuclein, consisting of the N-terminal region (green), the hydrophobic NAC region (blue), and the acidic C-terminal region (red). **(B)** Left panel: α-synuclein is important for synaptic vesicle dynamics, where it regulates exocytosis, SNARE complex function and endocytosis. It modulates vesicle release and recycling via fast (kiss-and-run) and slow (clathrin-mediated) membrane retrieval pathways. Right panel: under physiological conditions (green), α-synuclein exists in different conformations that are balanced between unstructured soluble monomeric and tetrameric forms. Under pathological conditions that promote misfolding (light red), α-synuclein aggregates into oligomers, protofibrils, and fibrils, which eventually form protein inclusions termed Lewy bodies. This figure is reproduced from Calabresi et al. (2023) (DOI: 10.1038/s41419-023-05672-9), which is distributed under CC BY 4.0 http://creativecommons.org/licenses/by/4.0/.

In some cases of PD, mutations in *SNCA* have been identified as the contributing factor to the disease. Polymeropoulos et al. (1997) discovered that a base pair change at position 209 from G to A (G209A) within the *SNCA* gene results in a change from alanine to threonine at position 53 (A53T). This amino acid change disrupts the normal α helical arrangement, extending the adjacent β-sheet, leading to aggregation. Out of seven *SNCA* mutations that have been identified, the A53T mutation is the most frequently observed (Klein & Westenberger, 2012).

Additionally, α-synuclein accumulates in mitochondria, where it impairs Complex I activity, leading to mitochondrial dysfunction, oxidative stress, and neurotoxicity, linking it to PD pathogenesis (Devi et al., 2008). Phosphorylation at different residues significantly affects α-synuclein's neurotoxic properties, with phosphorylation at tyrosine 125 reducing toxicity, while phosphorylation at serine 129 enhances oligomerisation and neurodegeneration (Chen et al., 2009). RNA interference (RNAi) has shown promise in reducing α-synuclein levels, preventing toxic accumulation, and restoring normal cellular functions in affected neurons (Takahashi et al., 2015). Furthermore, α-synuclein's interaction with spectrin alters F-actin dynamics, mislocalising mitochondrial fission protein Drp1, thereby exacerbating mitochondrial dysfunction and neuronal death (Ordonez et al., 2018). Overexpression and aggregation of α-synuclein causes increased production of reactive oxygen species, leading to significant mitochondrial impairment, including reduced mitochondrial membrane potential and ATP production. Mitochondrial respiration is disrupted, further contributing to cellular energy deficits, exacerbating cellular damage (Parihar et al., 2009).

α-synuclein can also accumulate due to impaired molecular pathways in which the structure of this protein is not the direct cause. PD progression is strongly linked to defective protein degradation pathways, including the Ubiquitin-Proteasome System, molecular chaperones, and Autophagy-Lysosomal Pathway. The Ubiquitin-Proteasome System is the primary degradation system for short polypeptides and misfolded proteins. Impaired Ubiquitin-Proteasome System function, such as from a loss of function of parkin and UCH-L1, results in α-synuclein accumulation, contributing to Lewy body formation and neuronal loss (Maiti et al., 2017; McNaught et al., 2001). The Autophagy-Lysosomal Pathway degrades larger protein aggregates, including α-synuclein oligomers and fibrils, through chaperone-mediated autophagy. The chaperone-mediated autophagy specifically degrades α-synuclein via HSC70

and LAMP2A; therefore, impairments in these proteins lead to α-synuclein accumulation and neurotoxicity (Bandhyopadhyay & Cuervo, 2007). Molecular chaperones (Heat Shock Proteins) aid in protein folding, refolding, and degradation by regulating the Ubiquitin-Proteasome System and autophagy-lysosomal pathways to prevent toxic α-synuclein aggregation (Fan et al., 2006; Wyttenbach, 2004). These findings highlight α-synuclein's complex role in neuronal function, synaptic maintenance, and neurodegeneration, making it a crucial target for potential therapeutic strategies in PD. Furthermore, recent research has explored the contribution of histone deacetylases (HDACs) to disease progression, suggesting the Class IIa HDACs play a role in the progression of PD (Choudhary et al., 2009; Seto & Yoshida, 2014). HDAC4 has been detected in Lewy body deposits (Takahashi-Fujigasaki & Fujigasaki, 2006), and α-synuclein was found to dysregulate HDAC4 nuclear retention, leading to neuronal apoptosis in a MPTP PD model (Wu et al., 2017).

1.3 HISTONE DEACETYLASES

HDACs play a crucial role in chromatin remodeling and gene regulation by removing acetyl groups from lysine residues on histone tails, leading to chromatin compaction and gene repression (Bertos et al., 2001; Campos & Reinberg, 2009; Seto & Yoshida, 2014). HDACs are categorised into four classes based on their sequence similarity to yeast proteins, as well as their functional roles and biochemical properties. Class I HDACs (HDAC1, HDAC2, HDAC3, and HDAC8) are typically ubiquitously expressed and are responsible for the majority of cellular deacetylase activity (Fitzsimons, 2015). In contrast, Class II (HDAC4, HDAC5, HDAC6, HDAC7, HDAC9, and HDAC10) and Class IV (HDAC11) HDACs are more tissue-specific in their expression. These HDACs often repress transcription through interactions with transcription factors, though they are also capable of binding non-histone proteins. HDACs in Classes I, II, and IV require a zinc ion for catalytic activity. Class III HDACs, known as Sirtuins (SIRT1–SIRT7), differ in that they rely on NAD^+ as a cofactor for activity and have two enzymatic activities: mono-ADP-ribosyltransferase and HDAC. Notably, not all Sirtuins exhibit deacetylase function despite being classed as one (Campos & Reinberg, 2009; Seto & Yoshida, 2014).

1.3.1 Class IIa HDACs

Class II HDACs are involved in chromatin remodelling, contributing to transcriptional repression through promoter modification via histone deacetylation (Bertos et al., 2001; Lemercier et al., 2000; Miska et al., 1999; Wang et al., 1999). These enzymes exhibit tissue-specific expression, with human HDAC4 being highly abundant in skeletal muscle, brain, and heart (Bertos et al., 2001; Fischle et al., 1999; Grozinger et al., 1999; Wang et al., 1999). Beyond histone regulation, lysine acetylation is an evolutionarily conserved modification that affects numerous cellular processes, including transcription, nuclear transport, metabolism, and protein stability. This modification also interacts with other post-translational modifications (PTMs) such as phosphorylation and ubiquitination, forming an integrated regulatory network that fine-tunes gene expression and cellular function (Choudhary et al., 2009).

While Class I, II, and IV HDACs share a zinc-dependent catalytic mechanism, Class IIa HDACs contain a histidine residue in place of a tyrosine residue in the deacetylase domain. This substitution is believed to reduce the catalytic activity of Class IIa HDACs, as restoring the tyrosine has been shown to reinstate enzymatic function (Lahm et al., 2007; Seto & Yoshida, 2014). Instead, they rely on HDAC3 as their catalytic subunit. HDAC3 forms a stable complex with Class II HDACs through interactions with the co-repressors N-CoR and SMRT, providing its deacetylation activity (Fischle et al., 2002). Class II HDACs possess nuclear localisation signals (NLS) and nuclear export signals (NES), allowing for dynamic nucleocytoplasmic transport (Bertos et al., 2001).

1.3.2 HDAC4

HDAC4, a Class IIa HDAC, is widely expressed in the brain, particularly in regions associated with learning, memory, and motor control, such as the cerebral cortex, hippocampus, striatum, cerebellum, and substantia nigra (Darcy et al., 2010). In many neuronal cell types, it is predominantly localised in the cytoplasm, but can shuttle to the nucleus under specific

conditions such as neuronal activity-induced kinase activation (Chawla et al., 2003; Darcy et al., 2010).

HDAC4 shuttling between the nucleus and cytoplasm is a tightly regulated process, influenced by phosphorylation, protein interactions, and nuclear transport signals. The nuclear entry of HDAC4 requires myocyte enhancement factor 2 (MEF2) binding, which has a more efficient NLS than HDAC4 (Borghi et al., 2001). The phosphorylation of HDAC4 at residues S245, S467, and S632 promotes binding to 14-3-3 proteins, which prevents importin from interacting with the NLS, thereby sequestering HDAC4 in the cytoplasm. This phosphorylation state is regulated by protein phosphatases such as PP1b and PP2A, which therefore promote nuclear entry of HDAC4 (Bertos et al., 2001; Chawla et al., 2003; Grozinger & Schreiber, 2000; Lu et al., 2000b; Seto & Yoshida, 2014). Additionally, PP2A dephosphorylates S298 of HDAC4, a modification necessary for nuclear import (Bertos et al., 2001). A visual representation of HDAC4 shuttling is shown in Figure 1.3. Experimental evidence supporting active shuttling comes from studies using leptomycin B, an inhibitor of the nuclear export receptor CRM1, which causes cytoplasmic HDAC4 to rapidly relocate to the nucleus. This suggests that cytoplasmic sequestration plays a crucial role in regulating HDAC4's function as a corepressor (Bertos et al., 2001; Wang et al., 2000). Neuronal activity influences HDAC4 localisation through calcium signaling, which triggers its export from the nucleus via a calcium/calmodulin-dependent protein kinase (CaMK), relieving its repression of transcription factors and promoting gene expression linked to synaptic plasticity and survival (Chawla et al., 2003). These findings highlight the complex regulatory mechanisms controlling HDAC4 localisation and activity.

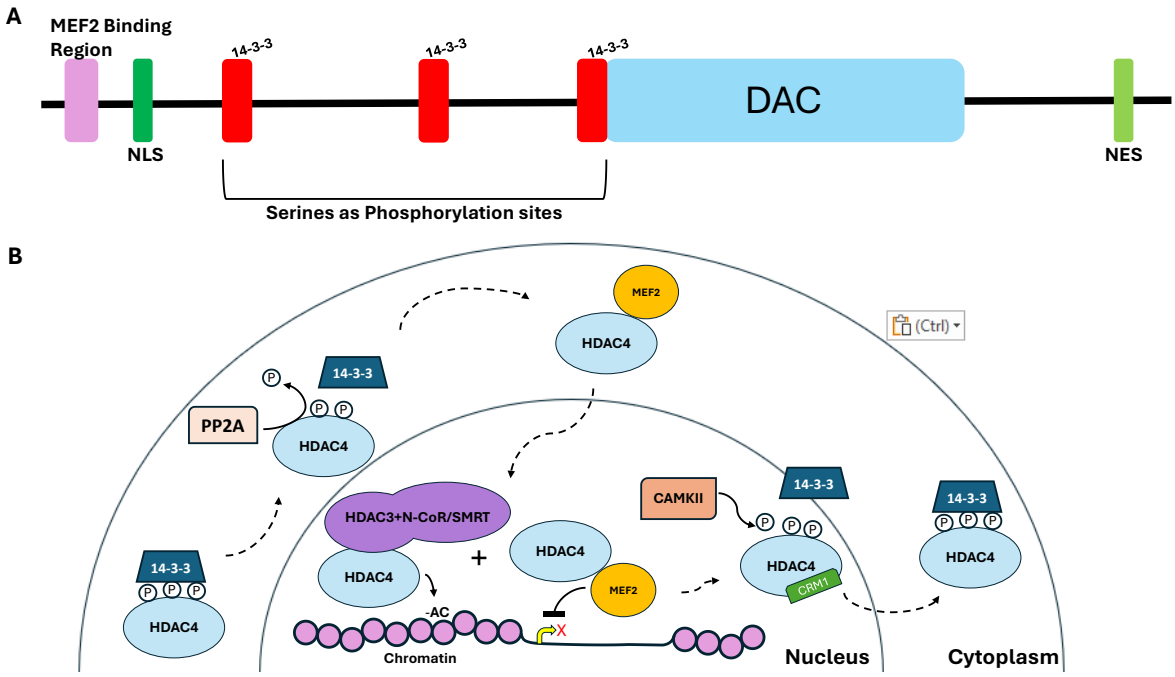

Figure 1.3 – HDAC4 structure and regulation

(A) The domain structure of HDAC4, including the MEF2 binding region, serine residues that when phosphorylated create binding sites for 14-3-3, deacetylase (DAC) domain and nuclear localisation and export signals (NLS/NES). This is an original artwork with reference to Antrobus & Parsons (2022), Chen et al. (2017a), Park & Kim (2020) & Seto & Yoshida (2014). **(B)** HDAC4 nucleocytoplasmic shuttling. In the cytoplasm, HDAC4 is phosphorylated and bound to 14-3-3. PP2A dephosphorylates HDAC4, releasing 14-3-3 and allowing MEF2 to bind. HDAC4 is translocated to the nucleus by MEF2, which contains a more efficient NLS than HDAC4. This allows HDAC4 to repress transcription through two methods; binding to the HDAC3 + N-CoR/SMRT complex to confer histone deacetylation, and repressing MEF2 via direct binding, resulting in decreased transcription of MEF2 mediated genes. When calcium levels rise, CaMKII phosphorylates HDAC4 in the nucleus to allow for 14-3-3 and CRM1 mediated nuclear export. This is an original artwork with reference to Fitzsimons (2015), Mielcarek et al. (2015) & Sando et al. (2012).

1.3.3 HDAC4 in brain function and disease

In the nucleus, HDAC4 represses transcription by repressing transcription factors such as MEF2, which is involved in neuronal survival. It has been shown to repress genes critical for synaptic structure and function (e.g., synaptic vesicle proteins, scaffolding molecules), which modulates synaptic strength and architecture, linking epigenetic control directly to functional plasticity (Chen et al., 2014c; Sando et al., 2012). In glutamatergic neurons, HDAC4 forms complexes with MEF2 in an NMDA receptor-dependent manner to repress genes involved in synaptic plasticity. This was specifically shown in transgenic mice, in which a truncated HDAC4 mutant that localises in the nucleus causes widespread repression of synaptic genes such as CamKIIα and impaired synaptic transmission, leading to deficits in spatial learning and memory (Sando et al., 2012). The intranuclear localisation of HDAC4 is critical for regulating neuronal cell death and survival, as demonstrated in cultured cerebellar granule neurons (CGNs), where nuclear accumulation of HDAC4 in response to cell death represses MEF2- and CREB-dependent transcription (Bolger & Yao, 2005).

The importance of HDAC4 in cognitive function is highlighted in mice with an HDAC4 deletion in excitatory forebrain neurons, which exhibit severe impairments in long-term memory, motor function, and spatial learning. These deficits are associated with impaired long-term potentiation, a key process for synaptic strengthening, as well as altered expression of genes involved in neurotransmission and synaptic remodelling (Kim et al., 2012). Mutations preventing HDAC4's dynamic shuttling further disrupt normal memory formation, reinforcing its role in neuroplasticity (Kim et al., 2012). In *Drosophila*, nuclear accumulation of HDAC4 impairs long-term memory and disrupts axon morphogenesis in the mushroom body (MB), a brain region involved in learning and memory (Main et al., 2021; Tan et al., 2024). Specifically, the studies by Main et al. (2021) and Tan et al. (2024) expressed the 3SA HDAC4 mutant, in which the 3 serines required for 14-3-3 binding and nuclear export are mutated, disrupting the HDAC4 ankyrin repeat binding motif. This mutant caused HDAC4 to accumulate in the nucleus, resulting in defects in MB development as well as impaired memory in *Drosophila*, showing these serines play a role in modulating HDAC4's interactions and localisation.

HDAC4 staining in human hippocampal neurons (Shen et al., 2016), mouse cortex (Darcy et al., 2010), and *Drosophila* MB nuclei (Tan et al., 2024) appears granular, forming punctate

foci that suggest HDAC4 may exist in a subnuclear structure. In human Alzheimer's Disease brains, when HDAC4 accumulates in neuronal nuclei, the number of these foci increases (Shen et al., 2016), and similarly in *Drosophila* neuronal nuclei, increased nuclear accumulation of HDAC4 results in larger foci (Hawley et al., 2025; Main et al., 2021; Tan et al., 2024). Recent evidence suggests that these foci display features of biomolecular condensates *in vitro* (Hawley et al., 2025; Nam & Gwon, 2023). These dynamic subnuclear compartments are formed through oligomerisation of HDAC4, starting from the dimerisation of two HDAC4 molecules via their N-terminal domains. This is dependent on the formation of a hydrophobic core, mediated by a phenylalanine residue, specifically Phe93 in human HDAC4 (Guo et al., 2007) and Phe65 in *Drosophila* HDAC4 (Hawley et al., 2025). Each HDAC4 dimer bridges two separate MEF2A dimers bound to their target DNA, creating a transcriptional repressor complex that regulates gene expression. The dimeric HDAC4–MEF2 complex then further oligomerises to form tetramers and higher-order complexes, forming condensates (Dai et al., 2024) (Figure 1.4). The presence of HDAC4 condensates is associated with impaired MB development in *Drosophila* (Hawley et al., 2025; Tan et al., 2024), and a phenylalanine to alanine mutation in the hydrophobic core disrupts HDAC4's ability to oligomerise. This correlates with reduced nuclear condensation and alleviates the associated neuronal defects, indicating that N-terminal oligomerisation drives condensate formation, and that this is critical to HDAC4's pathogenic activity (Hawley et al., 2025). The disruption of HDAC4 condensation could therefore be a therapeutic strategy to improve outcomes in diseases associated with HDAC4 nuclear accumulation. Specifically, expressing an $HDAC4^{F65A}$ mutation in *Drosophila* PD models may provide insight into whether disruption of HDAC4 reduces PD-like phenotypes.

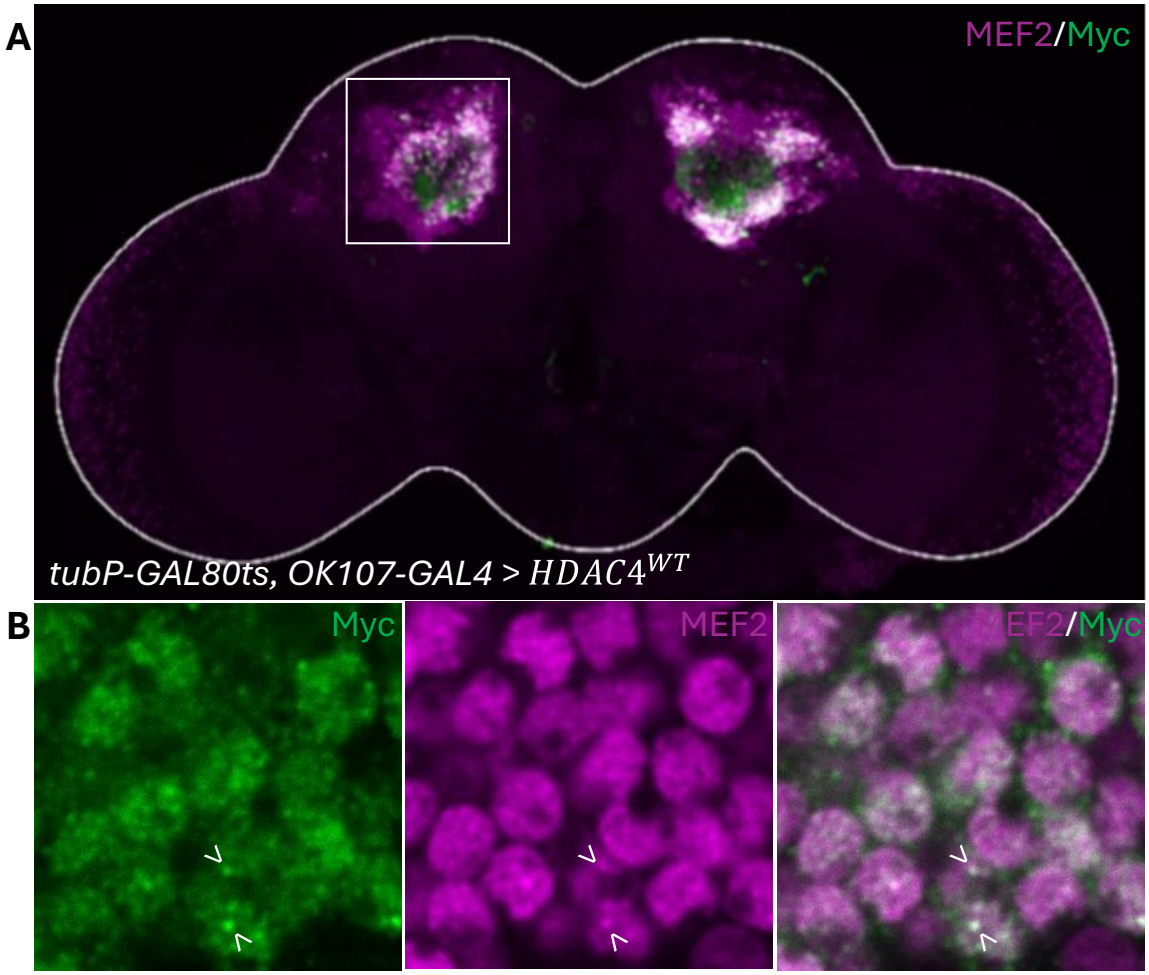

Figure 1.4 - HDAC4 condensate formation

(A) Maximum projection of a whole mount brain expressing HDAC4^{WT}-Myc following immunohistochemistry with anti-MEF2 and anti-Myc. A part of the boxed region is depicted in (B). **(B)** Single optical section images of HDAC4 condensates in the Kenyon cells. Arrowheads point to nuclear condensates of HDAC4. This figure is reproduced from Hawley et al. (2025) (DOI: 10.1101/2025.03.10.642474), which is distributed under CC BY 4.0 http://creativecommons.org/licenses/by/4.0/.

1.3.4 HDAC4 in PD

Recent research has explored the contribution of HDACs to disease progression, in which emerging evidence suggests the Class IIa HDACs play a role in the progression of PD. HDAC4 has been recently identified as a key regulator of gene expression changes in PD neurons. Induced pluripotent stem cell (iPSC)-derived DA neurons from PD patients exhibited HDAC4 mislocalisation to the nucleus, leading to dysregulated gene expression, downregulation of transcription of genes required for both synaptic activity and neuronal development, and upregulation of endoplasmic reticulum (ER) stress-related genes (Lang et al., 2019). Additionally, HDAC4 was shown to accumulate in the nucleus of DA neurons of mice expressing A53T α-Synuclein following the administration of MPTP. This overexpression of nuclear-localised HDAC4 was shown to suppress MEF2A's transcriptional activity and reduce DA neuron survival, highlighting its direct neurotoxic effects and suggesting its involvement in protein aggregation and neurodegeneration (Wu et al., 2017). Conversely, pharmacological inhibition of HDAC4 or knockdown of the gene that encodes it improves neuronal survival and function in PD-derived neurons (Lang et al., 2019). These findings suggest that HDAC4 dysregulation may contribute to neurodegenerative processes and targeting it could represent a potential therapeutic strategy for slowing or preventing PD progression.

1.4 MEF2

The myocyte enhancer factor 2 (MEF2) family of transcription factors participates in diverse gene regulatory programs, including muscle differentiation, T cell apoptosis, growth factor responses, and neuronal survival (Bertos et al., 2001; Black & Olson, 1998; Mao et al., 1999; Youn et al., 1999). Vertebrates express four MEF2 isoforms encoded by distinct genes, *MEF2A, MEF2B, MEF2C*, and *MEF2D* (Lisek et al., 2023). The MEF2 family belongs to the type II MADS domain-containing proteins, which are characterised by a MADS domain at the N terminus (Black & Olson, 1998) (Figure 1.5). This region is important for DNA sequence recognition, and along with the MEF2 domain, these transcription factors bind the MEF2 DNA element, activating transcription of target genes, many of which are involved in muscle and brain function (Black & Olson, 1998; Leifer et al., 1993; Lisek et al., 2023). All isoforms are

expressed throughout the brain at varying levels during development and adulthood. Specifically, MEF2A, C, and D play essential roles in promoting neuronal survival and regulating synaptic plasticity (Lisek et al., 2023)

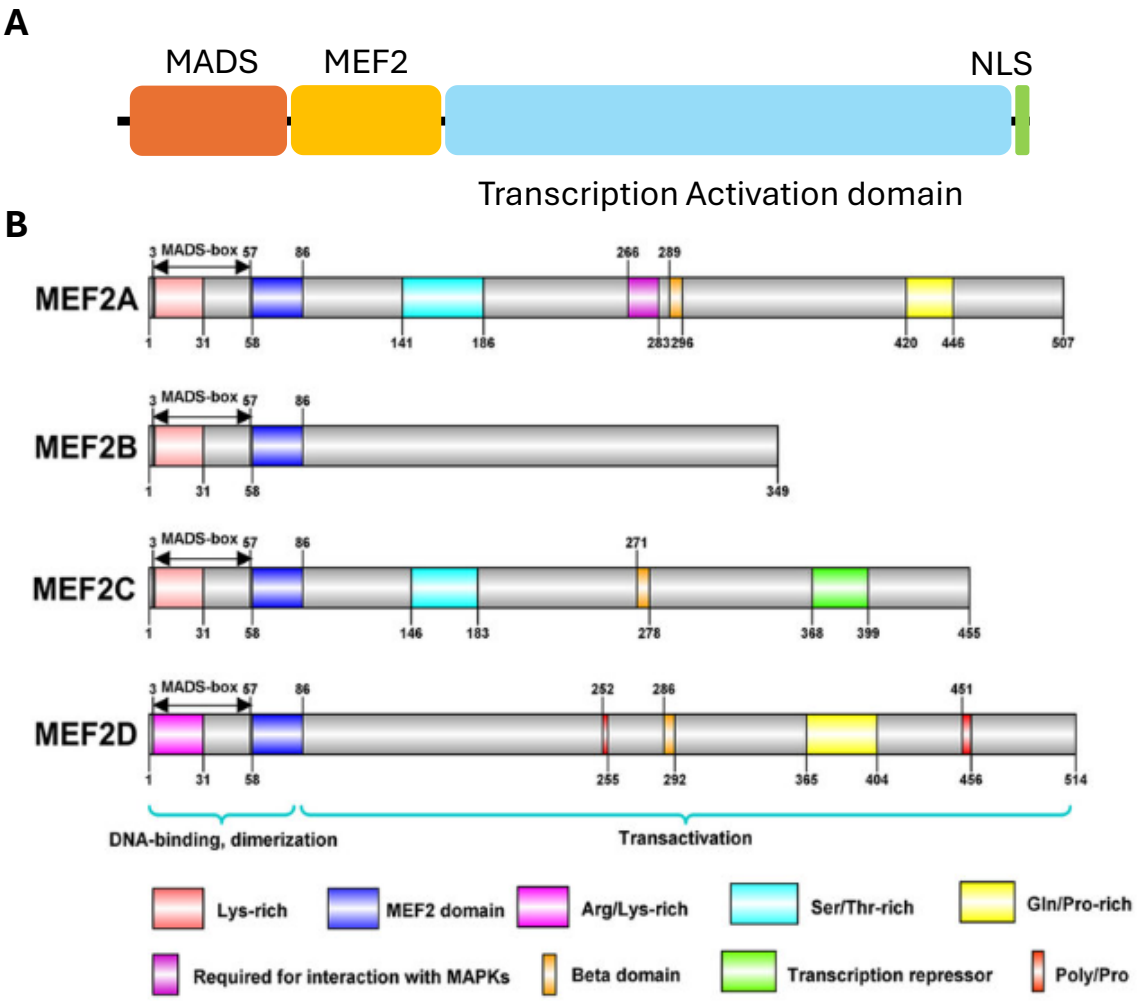

Figure 1.5 – MEF2 structure

(A) Schematic of the MEF2 domain structure common to all MEF2 proteins. This includes the MADS and MEF2 domains, transcription activation domain and nuclear localisation signal (NLS). This is an original artwork with reference to Chaudhary et al. (2021) & McKinsey et al. (2002). **(B)** The structure of human MEF2 proteins, which share similar N-terminal regions containing the MADS-box domain and MEF2 domain. While there is slight variation in the N-terminal domain, the most diversity exists in the structure of the C-terminal transactivation domain between the four proteins. This figure is reproduced from Chen et al. (2017b) (DOI: 10.18632/oncotarget.22899), which is distributed under CC BY 3.0 http://creativecommons.org/licenses/by/3.0/.

1.4.1 MEF2's role in development and disease

MEF2C isoforms are highly expressed in neurons of the cerebral cortex, and this expression declines postnatally, suggesting a role in early cortical lamination and neuronal differentiation (Leifer et al., 1993). *MEF2D* and *MEF2A* expression increase as neurons mature, and as shown in adult mice, *MEF2A* and *MEF2D* exhibit high expression levels in regions such as the olfactory bulb, hippocampus, and cerebellum (Lin et al., 1996). MEF2C is vital for maintaining synaptic balance, as it limits the number and strength of excitatory synapses to ensure proper cognitive function (Barbosa et al., 2008). Neuronal MEF2C knockout in mice leads to increased excitatory synaptic density, enhanced synaptic transmission, and impaired learning and memory, particularly in hippocampus-dependent tasks. These changes were accompanied by altered synaptic plasticity and excessive synaptic connectivity, which can disrupt neural network stability and impair information processing (Barbosa et al., 2008). On the other hand, MEF2D is important for neuroinflammation and resistance to DNA damage-induced apoptosis. Overexpression of *MEF2D* in rats improves microglial activation, mitochondrial function, and cognitive function, while silencing *MEF2D* impairs these processes (Shi et al., 2022). Knockdown of MEF2D in cerebellar granule neurons sensitises them to etoposide-induced apoptosis, whereas a phosphomimetic MEF2D mutant restores survival (Chan et al., 2014). Together, these findings highlight the critical role of MEF2 transcription factors in regulating neuronal development, synaptic homeostasis, and survival under both physiological and pathological conditions.

MEF2 activation is highly responsive to intracellular calcium signalling, linking it to neuronal activity. This calcium-dependent switch converts MEF2 from a repressor to an activator of transcription (Black & Olson, 1998; Fischle et al., 2001), triggering anti-apoptotic gene expression that protects neurons during development and in response to synaptic stimulation (Mao et al., 1999). Electrophysiological analyses further confirm that MEF2C-deficient neurons exhibit stronger excitatory synaptic currents, underscoring MEF2C's role as a crucial regulator or "brake" on excitatory connectivity (Barbosa et al., 2008). Ultimately, MEF2, particularly MEF2C, functions as a key transcriptional effector that links synaptic activity with genetic programs for neuroprotection, making it essential for neuronal health, learning, and memory throughout life (Mao et al., 1999).

1.4.2 The interaction between MEF2 and HDAC4

MEF2 transcription factors were the first identified to interact with class IIa histone deacetylases HDAC4 and HDAC5 (Bertos et al., 2001; Lemercier et al., 2000; Miska et al., 1999; Sparrow et al., 1999; Wang et al., 1999). This interaction is mediated by a specific 30-residue region located between the MADS box and MEF2-specific domain within the MEF2 DNA-binding domain, which is necessary for HDAC4 binding (Bertos et al., 2001; Lu et al., 2000b). A conserved motif shared among MITR (splice variant of HDAC4), HDAC4, HDAC5, and HDAC7 is responsible for MEF2 binding, further highlighting the specificity of this regulatory interaction (Bertos et al., 2001). MEF2 and HDAC4 co-localise in neuronal nuclei in mammalian cells (Borghi et al., 2001) as well as in Kenyon cells (KC), the intrinsic neurons of the MB, in *Drosophila* (Fitzsimons et al., 2013) (Figure 1.6), where this complex regulates transcriptional activity (Borghi et al., 2001; Chan et al., 2003). The interaction of HDAC4 and MEF2 results in the repression of plasticity-related genes, whereby HDAC4 binds MEF2 through its N-terminal domain to repress its activity (Fitzsimons, 2015; Youn et al., 2000). HDAC4 phosphorylation resulting in nuclear export relieves repression of MEF2 (Fitzsimons, 2015; Lu et al., 2000b). When CaMK activity is low, or HDAC4 remains unphosphorylated, it accumulates in the nucleus, repressing transcription of MEF2-dependent genes (Wang et al., 2000). Overexpression of 14-3-3 proteins promotes cytoplasmic retention of HDAC4, while dephosphorylation by PP2A allows its nuclear re-entry in a MEF2-dependent manner (Fitzsimons, 2015; Wang et al., 2000). HDAC4's NLS is weak and does not allow efficient nuclear localisation on its own and instead relies on MEF2 binding for nuclear entry; mutations in the MEF2 binding site have been demonstrated to result in cytoplasmic retention in both mammalian cells (Borghi et al., 2001) and *Drosophila* KC (Main et al., 2021; Tan et al., 2024).

The detrimental effects of nuclear HDAC4 accumulation on MB development, as mentioned in section 1.3, depend on its ability to bind MEF2. HDAC4 condensates sequester MEF2, and mutations in the MEF2 binding site, which disrupt this interaction, alleviate the neurodevelopmental defects (Hawley et al., 2025; Tan et al., 2024). However, this is not simply due to increased repression of MEF2, as RNAi-mediated knockdown of MEF2 significantly reduces the HDAC4-induced defects, rather than exacerbating them, which would be expected

if the defects were a result of reduced activity of MEF2. Increased nuclear HDAC4 also stabilises MEF2 protein (Tan et al., 2024). Preliminary data using the neurodevelopmental model explored whether disruption of the HDAC4-MEF2 interaction would reduce nuclear HDAC4-induced developmental defects, as *HDAC4* overexpression alone accumulates in the nuclei of the MB (Hawley, 2024; Main et al., 2021). Expression of a truncated *HDAC4* consisting of the N-terminal region with the α helix and the MEF2 binding domain (*HDAC4*$^{M1\text{-}L285}$), along with wild-type (WT) *HDAC4*, resulted in exclusion of HDAC4 from the nucleus, and an improvement in MB development. This was likely due to HDAC4$^{M1\text{-}L285}$ binding and titrating out MEF2, such that it no longer bound HDAC4, which prevented nuclear entry of HDAC4. These data suggest that the presence of MEF2 is required for nuclear HDAC4 to exert its negative effects on neuronal development (Hawley, 2024).

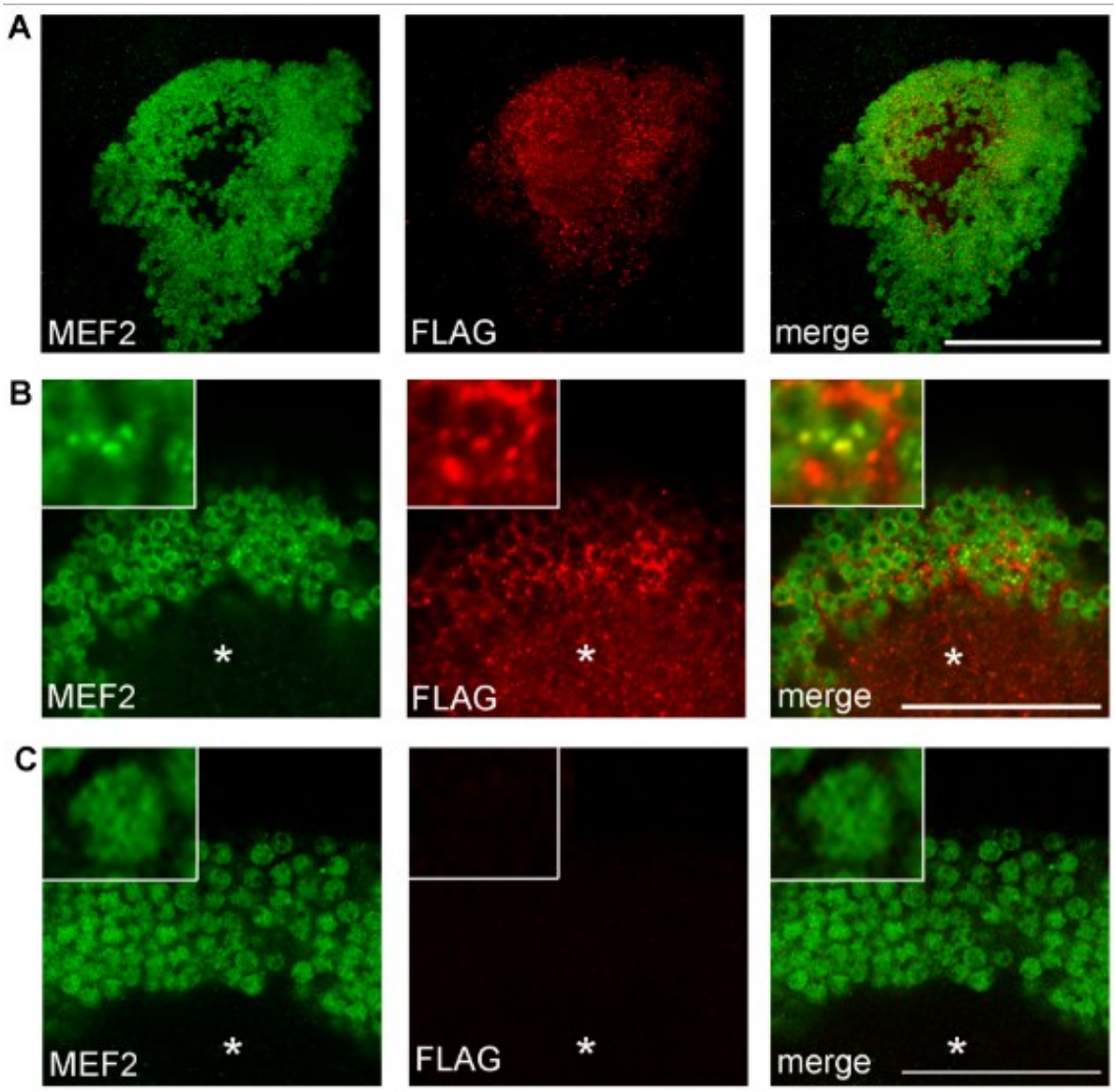

Figure 1.6 – MEF2 and HDAC4 co-localisation in Kenyon cells

(A) Maximal projection through the posterior of a brain expressing MEF2 (green) and HDAC4 (red) in Kenyon cells. Scale bar = 50 μm. **(B)** An optical section (1 μm) through the Kenyon cells shows MEF2 in nuclei whereas HDAC4 is largely cytoplasmic aside from a subset of cells in which HDAC4 is observed in nuclei, where it recruits MEF2 into punctate foci. Inset shows a single cell body at 5.4x magnification. Scale bar = 25 μm. **(C)** In the control, MEF2 is evenly distributed across the nucleus. Asterisk labels the calyx (dendritic field). Scale bar = 25 μm. This figure is reproduced from Fitzsimons et al. (2013) (DOI: 10.1371/journal.pone.0083903), which is distributed under CC BY 4.0 http://creativecommons.org/licenses/by/4.0/.

Under pathological conditions such as oxidative stress, excitotoxicity, and neurodegeneration observed in PD, MEF2 function becomes significantly impaired. Factors such as mitochondrial dysfunction, protein aggregation, and ubiquitin-proteasome system failure further compromise MEF2 activity (Lisek et al., 2023). Specifically, mitochondrial MEF2D plays a vital role in neuronal survival; its inhibition leads to reduced Complex I activity, elevated hydrogen peroxide levels, diminished ATP production, and increased vulnerability to stress-induced neuronal death (She et al., 2011). In both PD models and postmortem brain samples of individuals with PD, MEF2D and mitochondrial ND6 are reduced, with toxins such as MPTP and rotenone disrupting MEF2D's mitochondrial function (She et al., 2011; Wang et al., 2014). Moreover, oxidative stress induces MEF2D oxidation, impairing its DNA-binding capacity and promoting aggregation, as observed in both experimental models and PD patient brains, in which oxidative inactivation of MEF2D correlates with increased neuronal death (Gao et al., 2014). Additionally, MEF2D undergoes degradation via chaperone-mediated autophagy in the cytoplasm, and disruption of this process by α-synuclein leads to the accumulation of inactive MEF2D in the cytoplasm and neuronal death (Yang et al., 2009). In $SNCA^{A53T}$ mutant neurons, elevated nitrosative stress results in MEF2C S-nitrosylation, disrupting its regulation of PGC1α, which results in impaired mitochondrial function and increased apoptosis (Ryan et al., 2013). Together, these findings illustrate that MEF2 dysregulation, driven by multiple converging pathological processes, plays a central role in PD progression, and disruption of the HDAC4-MEF2 interaction warrants further investigation as a potential target for therapeutic intervention.

1.5 THE USE OF *DROSOPHILA* AS A MODEL FOR NEURODEGENERATIVE DISEASE

Given the complexity of the human nervous system, the use of model organisms has been essential in the study of neurological diseases. *Drosophila melanogaster*, commonly known as the fruit fly, offers numerous advantages as a model for investigating human brain disorders (Jeibmann & Paulus, 2009; McGurk et al., 2015). It supports a wide range of sophisticated genetic techniques, including time- and tissue-specific inducible promoters, enabling precise control over gene expression (Jeibmann & Paulus, 2009; McGurk et al., 2015). With its short lifespan and high reproductive rate, *Drosophila* facilitates rapid generation turnover, significantly speeding up experimental workflows. Although its genome contains fewer protein-coding genes than humans (14,000 vs 20,000–25,000), many fundamental molecular pathways are conserved between the two species, making it an invaluable tool for genetic research (Jeibmann & Paulus, 2009; McGurk et al., 2015; St Johnston, 2002). Notably, approximately two-thirds of human disease-associated genes have homologs in *Drosophila*, enabling the exploration of disease mechanisms *in vivo* (McGurk et al., 2015; Reiter et al., 2001; Rubin et al., 2000). Functional analyses such as behavioural assays are well established, further enhancing their utility in studying gene function (Jeibmann & Paulus, 2009).

Although the fly nervous system is less anatomically complex than that of mammals, it contains a well-organised central nervous system of approximately 200,000 neurons (Raji & Potter, 2021), with neurons and glia protected by a blood–brain barrier, mirroring key aspects of vertebrate neuroanatomy (McGurk et al., 2015). Additionally, external morphological traits such as bristles, wing structures, and compound eyes provide easily scorable phenotypes for genetic screening under a stereomicroscope (St Johnston, 2002). Practical advantages also include the lack of meiotic recombination in males and the presence of only four chromosomes, simplifying genetic crosses (St Johnston, 2002). The genetic tractability, evolutionary conservation of key pathways, and robust experimental toolkit of *Drosophila* make it a powerful model for investigating the molecular and cellular basis of human brain diseases (Jeibmann & Paulus, 2009).

1.5.1 Spatial and temporal control of gene expression

In human disease, mutations can result in loss of function, increased function, gain of new functions, or a combination of these. To model these effects in *Drosophila*, researchers commonly introduce the human disease gene into flies, allowing analysis of its biological consequences and the pathways involved (McGurk et al., 2015). This is often achieved using the GAL4/UAS system, a widely used genetic tool. The foundational work by Brand and Perrimon (1993) demonstrated that the yeast GAL4 protein could activate transcription in *Drosophila*, paving the way for its use in fly genetics. The system consists of two key components: a GAL4 driver line that expresses the GAL4 transcription factor in a specific tissue or cell type, and a responder line containing the gene of interest downstream of an Upstream Activating Sequence (UAS) (Duffy, 2002; Fischer et al., 1988; Figure 1.7). When these lines are crossed, GAL4 binds to the UAS and drives targeted gene expression. GAL4 itself is an 881-amino acid protein from *Saccharomyces cerevisiae*, originally identified as a regulator of galactose-inducible genes such as *GAL1* and *GAL10*. It contains separable DNA-binding and transcriptional activation domains and activates transcription by binding to four 17-base pair sequences in the region between these genes, forming the UAS, which functions similarly to enhancers in multicellular organisms (Giniger et al., 1985). The GAL4/UAS system supports a variety of applications, including gain- and loss-of-function analyses, lineage tracing, and genetic mosaic studies, thus enabling a deeper understanding of development and disease (Duffy, 2002). An advanced version of the system, known as TARGET, incorporates a temperature-sensitive mutant of the GAL80 repressor ($GAL80_{ts}$), which permits precise spatial and temporal regulation of gene expression. At permissive temperatures (18°C), $GAL80_{ts}$ binds to and inhibits GAL4, preventing gene expression. When the temperature is raised to non-permissive temperatures (30°C), $GAL80_{ts}$ is inactivated, allowing GAL4 to drive expression of the target gene. Between 18°C and 30°C, GAL4 exhibits linear temperature-dependent increases in activity (McGuire et al., 2004; Schwartz et al., 2016). The fine-tuning and refinement of this system allow researchers to control gene function at specific developmental stages and in selected tissues (Duffy, 2002; McGuire et al., 2004).

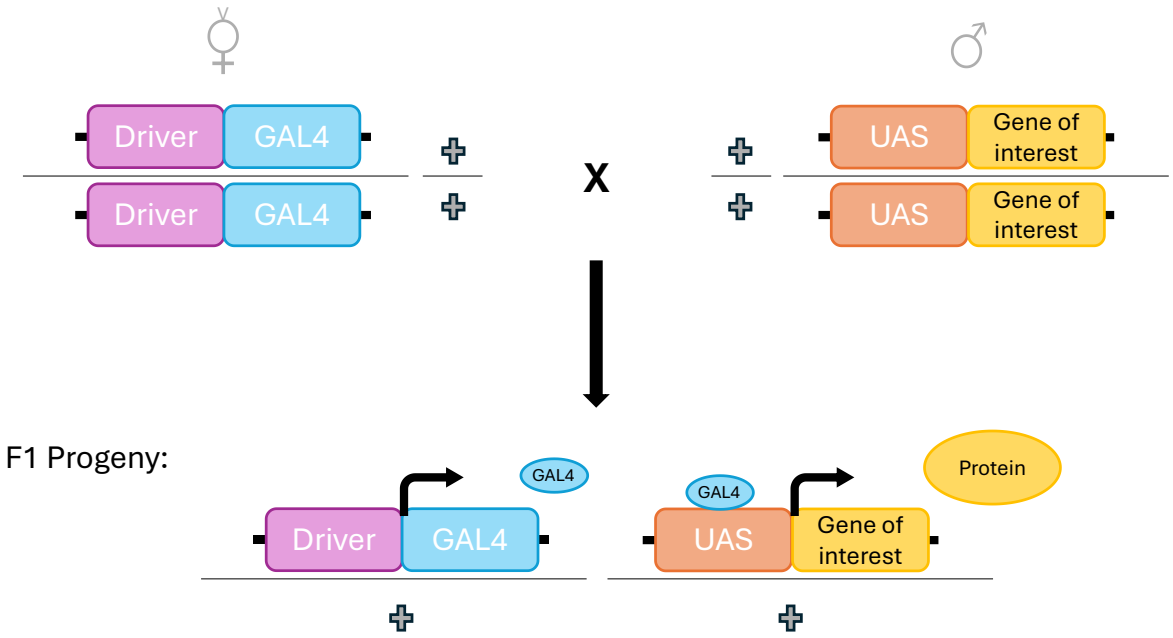

Figure 1.7 – The UAS-GAL4 system

The UAS/GAL4 system for the temporal and spatial control of gene expression in *Drosophila.* Virgin females containing the GAL4 gene under the control of the driver of choice are crossed to males containing UAS fused upstream of the gene of interest. The progeny of this cross will carry one copy of the UAS-transgene and one copy of the GAL4 driver. GAL4 will bind the UAS, leading to expressing the gene of interest in the tissue-specific pattern of the driver.

1.5.2 The *Drosophila* brain

The *Drosophila* brain, though significantly smaller than the human brain with an estimated 200,000 neurons (Raji & Potter, 2021), is a compact yet highly complex and well-organised structure. Despite its size, the fruit fly brain shares key features with vertebrate nervous systems, including conserved neuronal genes, molecular pathways, and neurotransmitter systems (Pandey & Nichols, 2011). This conservation makes *Drosophila* a powerful model for studying neural function and disease. Three regions of the *Drosophila* brain necessary for receiving sensory and visual information, as well as learning and memory formation are the mushroom body (MB), antennal lobes (AL), and optic lobes (OL) (Rein et al., 2002; Figure 1.8).

The MB is a key brain region in *Drosophila*, sharing many similarities with the vertebrate cerebellum (Li et al., 2020). This network is critically involved in learning, memory, and the integration of sensory information such as olfactory, visual, and thermosensory cues (Aso et al., 2009; Heisenberg et al., 1985; Li et al., 2020). The main neurons that make up the MB are the KCs. Their dendrites form the calyx, where they receive input from the sensory regions such as the ALs (Yasuyama et al., 2002). The axons of the KCs are bundled into lobes and are characterised into 3 subtypes, γ (33%), α′/β′ (18%), and α/β (49%), and they receive both olfactory and non-olfactory inputs (De Belle & Heisenberg, 1994; Dubnau et al., 2001; Heisenberg et al., 1985; McBride et al., 1999).

The AL comprises densely packed neuropils termed glomeruli, each serving as a functional unit for processing olfactory information. Olfactory sensory neurons (OSNs) express odorant receptor (OR) genes (Fishilevich & Vosshall, 2005), and project from the antennae into specific glomeruli, establishing the primary input pathways for olfactory signals. Projection neurons (PNs) receive input from OSNs within the glomeruli and transmit processed information to the MB. Local interneurons (LNs) interconnect different glomeruli, facilitating complex processing and modulation of olfactory signals within the AL (Silbering et al., 2008; Stocker et al., 1990; Figure 1.8).

In the adult fly, the eye consists of a highly organised lattice of approximately 700–800 ommatidia, each comprising a precise arrangement of eight photoreceptor neurons (R1-R8), cone cells, and pigment cells (Cagan & Ready, 1989; Ready et al., 1976). Visual signals

initiated by the ommatidia are transmitted through photoreceptor axons to the optic lobe (OL), which is composed of three primary neuropils: the lamina, medulla, and lobula complex (Fischbach & Dittrich, 1989). Specifically, the R7 and R8 photoreceptors send their axons into the medulla, where they form synaptic connections that launch the brain's visual processing pathways (Takemura et al., 2008).

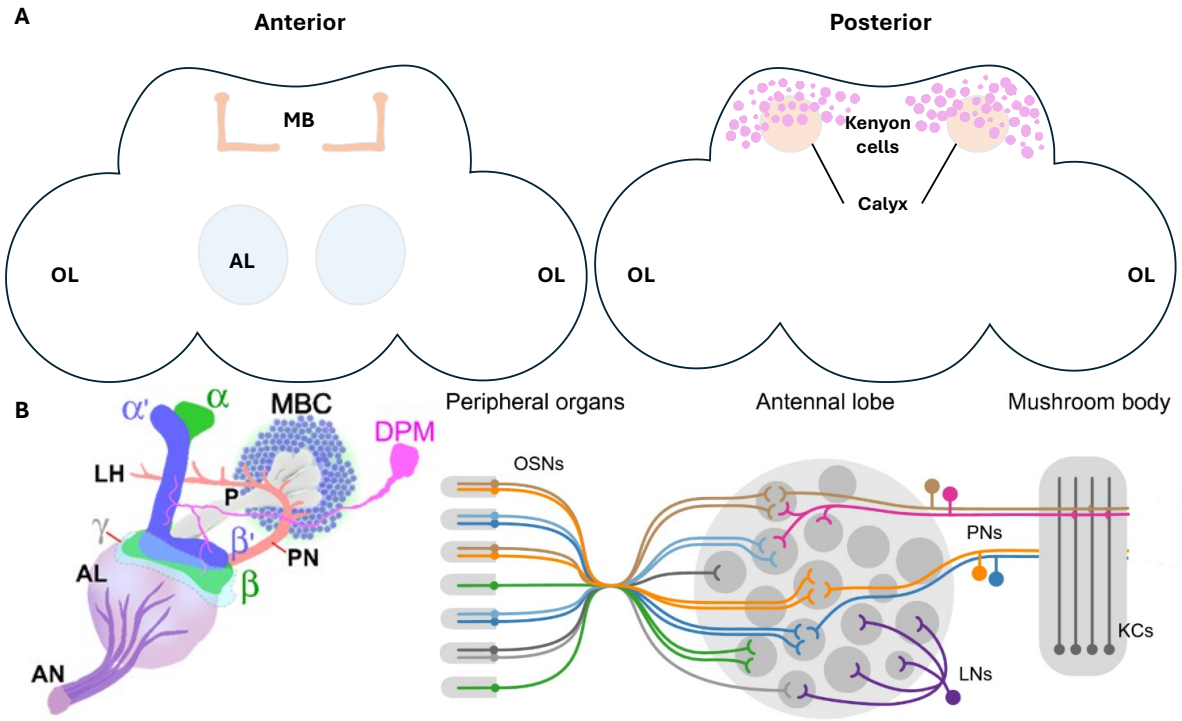

Figure 1.8 – The *Drosophila* brain

(A) Schematic of the *Drosophila* brain showing the location of the mushroom body (MB), and antennal lobes (AL) on the anterior and the Kenyon cells and calyx are located on the posterior side. The optic lobes (OL) span the brain on either side of the center. **(B)** Left: circuitry from the antennal lobe to the MB and lateral horn. Olfactory receptor neurons transmit information via the antennal nerve (AN) to the AL, where they synapse onto projection neurons (PNs). PNs transmit olfactory information to higher brain centres including the MB and the lateral horn. In the MB, Kenyon cells extend axons anteriorly through the peduncle (P). The axons of α/β and α′/β′ neurons bifurcate to form the vertical (α and α′) and horizontal (β and β′) lobes of the MB. The axons of γ neurons form the horizontal lobe (γ). This figure is reproduced from Kasuya et al (2009) (DOI: 10.3389/neuro.02.011.2009), which is distributed under CC BY 4.0 http://creativecommons.org/licenses/by/4.0/. Right: schematic of the *Drosophila* olfactory circuit. Olfactory sensory neurons (OSNs) identify sensory cues in the antennae and send axons to the antennal lobe. OSNs converge onto specific glomeruli where they synapse with PNs and local interneurons (LNs). Most PNs innervate only one glomerulus (brown, orange, blue), but some are multiglomerular (pink). LNs tend to innervate many glomeruli (purple). PNs then send axons to the MB and beyond. This figure is adapted from Zhao & McBride (2020) (DOI: 10.1007/s00359-020-01399-6), which is distributed under CC BY 4.0 http://creativecommons.org/licenses/by/4.0/.

1.5.3 *Drosophila* dopaminergic neuronal network

Human DA neurons are located primarily in two specific brain regions, the hypothalamus and the brain stem, whereas in *Drosophila* there are approximately 130 DA neurons per brain hemisphere, which are organised into distinct clusters; PPL1, PPL2, PPM1/2, PPM3, PAM, and PAL (Dasgupta, 2016; Mao & Davis, 2009; Nässel & Elekes, 1992) (Figure 1.9). These clusters are arranged symmetrically about the midline and project to key brain regions, including the MB lobes (Nässel & Elekes, 1992). DA neurons in *Drosophila* play essential roles in modulating locomotion, arousal, sleep, feeding, and learning. For example, the PPL1 cluster is involved in aversive learning, while the PAM cluster is linked to reward processing, which closely mirrors the mammalian DA system (Aso et al., 2014; Liu et al., 2012; Welberg, 2009) (Figure 1.9). DA neurons provide modulatory input to the MB and are critical for synaptic plasticity and memory formation (Riemensperger et al., 2011). The connectome reveals detailed pathways through which DA neurons interact with KCs and MB output neurons, highlighting mechanisms for reinforcement learning (Li et al., 2020). Additionally, MB output neurons connect to descending neurons, linking the MB to motor control circuits and demonstrating how learned information can influence behaviour (Li et al., 2020). The conservation of DA neuron function between flies and mammals enables the use of *Drosophila* to investigate PD mechanisms.

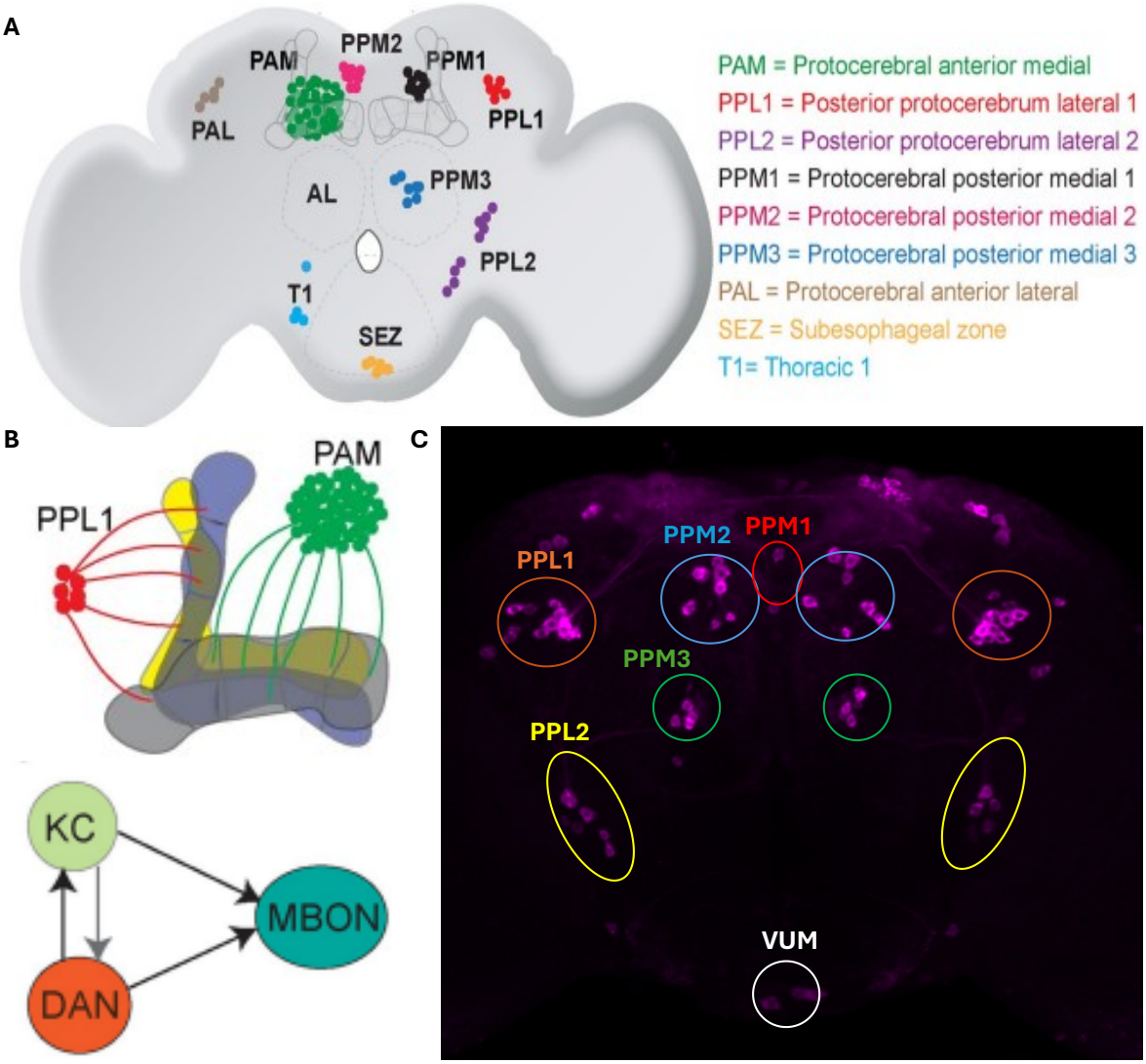

Figure 1.9 – *Drosophila* dopaminergic neuron network

(A) Schematic representation of the main clusters of dopaminergic neurons in the *Drosophila* brain. **(B)** Upper: PPL1 and PAM neurons project to the MB, circuitry required for aversive learning and reward processing. Lower: representation of the interaction between dopaminergic neurons (DAN), Kenyon cells (KC) and MB output neurons (MBON). This figure is reproduced from Siju et al (2021) (DOI: 10.1007/s00441-020-03371-x), which is distributed under CC BY 4.0 http://creativecommons.org/licenses/by/4.0/. **(C)** Maximum projection of whole mount wildtype brains following immunohistochemistry with anti-TH (a marker of DA neurons) at 1:250 dilution. PPM1, PPM2, PPM3, PPL1, PPL2 and VUM neurons are highlighted, which are the most vulnerable to α-synuclein-mediated neurodegeneration.

1.5.4 Modelling PD in *Drosophila*

While *Drosophila* naturally contain homologues of many human disease-causing genes, *SNCA* is not one of them. Instead, using the GAL4/UAS system, *Drosophila* models have been developed to express human α-synuclein, which leads to DA neuron degeneration and motor deficits in flies, modelling aspects of PD pathology. These models have been instrumental in dissecting the molecular mechanisms underlying PD and in identifying genetic and environmental factors that contribute to the disease (Jeibmann & Paulus, 2009; Whitworth, 2011; Xiong & Yu, 2018). The accelerated loss of DA neurons leading to a progressive and irreversible decline in locomotor function seen in human PD is recapitulated in *Drosophila* through two assays, a negative geotaxis climbing assay and tyrosine hydroxylase (TH) immunostaining of the brain (Barone & Bohmann, 2013). As TH is required for the biosynthesis of DA (see Section 1.1.2), it is present in all DA neurons (Friggi-Grelin et al., 2003). Locomotor function is assessed in flies via their natural negative geotaxis response to measure climbing up the side of a vial, in which the proportion of flies that climb above 5cm is used to calculate the climbing index (see methods section 2.5). Wild-type (WT) flies have a lifespan of up to approximately 100 days and display healthy locomotor function, measured by a climbing index of 0.79 or higher through the first 50 days, with a more pronounced reduction in performance toward the end of life at days 60 and 70 (White et al., 2010). *Drosophila* DA neurons also do not degenerate with age in healthy WT flies, as shown via TH immunostaining (White et al., 2010). With this as a healthy baseline reference, behaviour models of PD have been established through the observation of DA neuron degeneration, decline of locomotor function, and reduced lifespan (Table 1.1). Feany and Bender (2000) were the first to demonstrate that overexpression of human α-synuclein in *Drosophila* induces hallmark PD-like phenotypes, recapitulating key features of PD. Furthermore, Lewy body-like structures in *Drosophila* DA neurons stained positive for α-synuclein and were ultrastructurally composed of filaments with granular material (Jeibmann & Paulus, 2009; Kuzuhara et al., 1988). This model laid the groundwork for using *Drosophila* to study PD mechanisms. Since this study, many others have reported expression of α-synuclein leads to these PD-like phenotypes; however, others have reported little to no effect, in particular with degeneration of DA neurons and climbing deficits (Table 1.1). Specifically, some studies found more widespread neuronal degeneration when α-synuclein is expressed (Auluck et al., 2002; Periquet et al., 2007);

however, others found degeneration of some clusters but not others (Agostini et al., 2023; Jahromi et al., 2021) or no degeneration at all (Pesah, 2005). While the observed variable phenotypes raise some questions about the effects of transgenic α-synuclein expression, a few explanations may account for this, such as the GAL4 driver *SNCA* transgenic line (Whitworth, 2011). The *Drosophila* α-synuclein models provide insight into the cellular and molecular mechanisms underlying PD, including the roles of protein aggregation, mitochondrial dysfunction, and oxidative stress. (Whitworth, 2011; Xiong & Yu, 2018). The variable phenotypes make establishing a robust *Drosophila* model of PD in our laboratory crucial for understanding the role of HDAC4 in the onset and progression of PD. Once clear PD phenotypes are observed in our laboratory, this can be compared to strategies that reduce HDAC4 nuclear accumulation, condensation, or disrupt the HDAC4-MEF2 interaction to accurately decipher whether this can decrease neurodegeneration in the model.

Drivers	α-synuclein variants	Neurodegeneration	Motor function/lifespan/behavioural effects	Cellular effects	Reference
TH-GAL4	α-Syn-WT (codon-optimized)	Survival of PPL1 and PPM1/2 neurons ↓	Locomotor activity ↓ Lifespan ↓	α-synuclein aggregate formation	(Agostini et al., 2023)
elav-GAL4	α-Syn-WT α-Syn-A53T	ND	Lifespan: α-Syn-WT ↓ & α-Syn-A53T = NSC	Phosphorylation of α-Syn-WT ↑, α-Syn-A53T ↑ Resistance to proteinase-K digestion: α-Syn-WT ↑, α-Syn-A53T ↑↑ Accumulation of misfolded and aggregated α-Syn-WT = NSC, α-Syn-A53T ↑↑	(Arsac et al., 2021)
Ddc-GAL4	α-Syn-WT	Survival of dorsomedial DA neurons (PPM1/2) ↓	ND	Formation of LB- and LN-like inclusions	(Auluck et al., 2002)
elav-GAL4 *GMR-GAL4*	α-Syn-WT α-Syn-S129D α-Syn-S129A	Overall survival of DA neurons: α-Syn-WT ↓, α-Syn-S129D ↓, α-Syn-S129A = NSC Retinal degeneration: α-Syn-WT ↑, α-Syn-S129D ↑↑, α-Syn-S129A = NSC	ND	Inclusion formation with Ser129 phosphorylation inhibition ↑ Inclusion formation correlates with increased proteinase K resistance	(Chen & Feany, 2005)

elav-GAL4 *GMR-GAL4*	α-Syn-WT α-Syn-Y125F α-Syn-S129D α-Syn-S129A	Overall survival of DA neurons: α-Syn-WT = ↓, α-Syn-Y125F = ↓ (compared to α-Syn-WT), α-Syn- S129D = ND, α-Syn- S129A = ND Retinal degeneration: α-Syn- Y125F ↑ (compared to α-Syn-WT), α-Syn-S129D = ND, α-Syn-S129A = ND	Motor function: α-Syn-WT = NSC, α-Syn-Y125F ↓, α-Syn-S129D ↓	Increased phosphorylation ameliorates α-Syn neurotoxicity α-Syn toxicity = accumulation of soluble high-molecular-weight oligomers	(Chen et al., 2009)
nSyb-GAL4	α-Syn-A30P	PPM2 neuron survival: ↓	Motor function: ↓ Age-dependent walking deficits: ↑ Anxiety phenotype: ↑	The addition of L-Dopa rescued motor function deficits	(Chen et al., 2014a)
elav-GAL4 *TH-GAL4* *Or83b-GAL4* *Cha-GAL4*	α-Syn-A30P	ND	Motor function: ↓ Olfactory function: ↓	α-Syn-A30P ↑ in DA neurons = age-dependent deficit in odor acuity and odor discrimination. Oxidative stress exacerbated olfactory deficits	(Chen et al., 2014b)

Rh1-GAL4	α-Syn-WT (codon-optimized)	Age dependent retinal function: ↓ Retinal neuron degeneration: ↑	ND	Autophagic vacuole formation in the retina: ↑ Synaptic terminal area in lamina: ↑ Synaptic vesicle density in lamina: ↓	(Chouhan et al., 2016)
Ddc-GAL4 *elav-GAL4* *GMR-GAL4*	α-Syn-WT α-Syn-A30P α-Syn-A53T	Dorsomedial DA neuron survival: α-Syn-WT = ↓, α-Syn-A30P = ↓, α-Syn-A53T = ↓ Retinal degeneration: α-Syn-WT ↑, α-Syn-A30P = ↑, α-Syn-A53T = ↑	Motor function: α-Syn-WT = ↓, α-Syn-A30P = ↓, α-Syn-A53T = ↓		(Feany & Bender, 2000)
Ddc-GAL4 *TH-GAL4*	α-Syn-WT α-Syn-A53T α-Syn-A76P	ND	Irregular sleep behaviour Irregular circadian locomotor activity		(Gajula Balija et al., 2011)
elav-GAL4 *Ddc-GAL4* *GMR-GAL4*	α-Syn-WT α-Syn-E46K	PPM1/2, PPL2 & PAM neuron survival: α-Syn-WT = ↓, α-Syn-E46K = ↓↓ Retinal neuron degeneration: α-Syn-WT = ↑, α-Syn-E46K = ↑↑	Motor function: α-Syn-WT = ↓, α-Syn-E46K = ↓↓ Locomotor activity: α-Syn-WT = ↓, α-Syn-E46K = ↓ Longevity: α-Syn-WT = NSC, α-Syn-E46K = ↓	Higher sensitivity to ethanol vapour Higher sensitivity to Paraquat toxicity	(Jahromi et al., 2021)

elav-GAL4	α-Syn-WT α-Syn-A30P α-Syn-A56P α-Syn-A53T α-Syn-A30P/A56P/A76P (TP)	Survival of DA neurons: α-Syn-WT = ↓, α-Syn-A53T = ↓, α-Syn -A56P = ↓, TP = ↓↓	Motor function: α-Syn-WT = NSC, α-Syn-A53T = ↓, α-Syn -A56P = ↓, TP = ↓↓	Formation of soluble α-Syn oligomers compared to WT: α-Syn-A30P = NSC, α-Syn-A56P = ↑, α-Syn-A53T = NSC, TP = ↑↑	(Karpinar et al., 2009)
elav-GAL4	α-Syn-WT α-Syn-NLS α-Syn-NES	Survival of DA neurons: α-Syn-WT = ↓, α-Syn-NLS = ↓, α-Syn-NES = NSC	ND	Number of apoptotic cells: α-Syn-WT = ↑, α-Syn-NLS = ↑, α-Syn-NES = NSC Acetylation levels = α-Syn-NLS = ↓, α-Syn-NES = NSC	(Kontopoulos et al., 2006)
ESG-GAL4 *TH-GAL4* *Ddc-GAL4*	α-Syn-WT	PPM1/2, PPL1 & PPM3 neuron survival: ↓	Lifespan: ↓ Motor function: ↓	intestinal expression of α-syn results in intestinal dysplasia and aggravates the pathogenesis of brain-induced PD	(Liu et al., 2022)

elav-GAL4	α-Syn-WT α-Syn-E46K α-Syn-H50Q α-Syn-G51D	PAL neuron survival: α-Syn-WT = NSC, α-Syn-E46K = ↓, α-Syn-H50Q = ↓, α-Syn-G51D = ↓ PPM1/2 neuron survival: α-Syn-WT = NSC, α-Syn-E46K = NSC, α-Syn-H50Q = NSC, α-Syn-G51D = ↓↓ PPM3 neuron survival: α-Syn-WT = NSC, α-Syn-E46K = ↓, α-Syn-H50Q = ↓, α-Syn-G51D = ↓↓ PPL1 neuron survival: α-Syn-WT = NSC, α-Syn-E46K = NSC, α-Syn-H50Q = NSC, α-Syn-G51D = ↓↓ PPL2 neuron survival: α-Syn-WT = ↓, α-Syn-E46K = ↓↓, α-Syn-H50Q = ↓↓, α-Syn-G51D = ↓↓	Motor function: α-Syn-WT = ↓, α-Syn-E46K = ↓↓, α-Syn-H50Q = ↓↓, α-Syn-G51D = ↓↓ Lifespan: Syn-WT = NSC, α-Syn-E46K = ↓, α-Syn-H50Q = ↓, α-Syn-G51D = ↓	Oligomer and amyloid formation compared to α-Syn-WT: α-Syn-E46K = ↑, α-Syn-H50Q = ↑, α-Syn-G51D = ↑	(Mohite et al., 2018)
TH-GAL4	α-Syn-WT (codon optimised)	PPM1/2 & PPL1 neuron survival: ↓	Motor function: ↓	Swollen mitochondria in PPL1 Neurons Fragmented mitochondria in PPM3 Neurons	(Narwal et al., 2024)

Ddc-GAL4 *elav-GAL4*	α-Syn-WT α-Syn-Δ71-82 α-Syn-1-120	Overall neuron survival: α-Syn-WT = ↓, α-Syn-Δ71-82 = NSC, α-Syn-1-120 = ↓	ND	Accumulation of aggregated α-Syn-WT = ↑, α-Syn-Δ71-82 = NSC, α-Syn-1-120 = ↑	(Periquet et al., 2007)
elav-GAL4 *Ddc-GAL4* *GMR-GAL4*	α-Syn-WT	PPM2 neuron survival: NSC Retinal neuron degeneration: NSC	Motor function: NSC		(Pesah, 2005)
GMR-GAL4 *nSyb-GAL4*	α-Syn-WT α-Syn-A30P α-Syn-A53T α-Syn-E46K α-Syn-H50Q α-Syn-G51D	Retinal neuron degeneration: NSC	Motor function: α-Syn-WT = ↓↓, α-Syn-A30P = NSC, α-Syn-A53T = ↓, α-Syn-E46K = ↓, α-Syn-H50Q = ↓, α-Syn-G51D = ↓↓		(Sakai et al., 2019)
TH-GAL4	α-Syn-WT (codon optimised)	PPL1 neuron survival: ↓	ND	α-Syn mediated neurodegeneration is prevented by GstS1 and Gclm mutation of the Eip55E gene enhances α-Syn induced neurodegeneration	(Trinh et al., 2008)
nSyb-QF2	α-Syn-WT	TH positive cells: ↓	Motor function: ↓	Disruption of the spectrin cytoskeleton and mislocalization of ankyrin	(Maor et al., 2023)

nSyb-QF2 *nSyb-GAL4*	α-Syn-WT	ND	Motor function: ↓	α-Syn-mediated motor function loss is prevented by nicotine Aggregated α-Syn decreased with nicotine	(Olsen et al., 2023)
Syb-QF2 *repo-GAL4*	α-Syn-WT	TH positive cells: ↓	Motor function: ↓	Formation of α-Syn inclusions Upregulation of proteolysis and cell surface receptor signaling genes	(Olsen & Feany, 2019)
elav–GAL4 *TH-GAL4* *Syb-QF2*	α-Syn-WT α-Syn-S129A α-Syn-S129D	Number of cortical neurons in the anterior medulla: ↓	Motor function: ↓	α-Syn-mediated motor function loss is resuced by Act5C, Drp1 and α-spectrin Increase in vacuole formation Increased caspase activation in neurons Increase in F-actin in neurons Increase in mitochondrial elongation	(Ordonez et al., 2018)

Table 1.1 - Phenotypes associated with *Drosophila* Parkinson's Disease models

↓ = Decreased compared to control, ↑ = Increased compared to control, NSC = No significant change, ND = Not determined, NLS = Nuclear localisation signal, NES = Nuclear export signal

1.6 AIMS AND OBJECTIVES

1. **Determine whether the expression of α-synuclein causes neurodegeneration in the *Drosophila* model of this disease.**

   The PD (α-synuclein) model in *Drosophila* will be characterised by confirming expression of α-synuclein and measuring neurodegeneration. Neurodegeneration will be measured via the loss of tyrosine hydroxylase staining (a marker of DA neurons) and motor function via a climbing assay. The expression patterns of various GAL4 drivers will also be analysed for optimal expression of α-synuclein in DA neurons.

2. **Characterise the subcellular distribution and expression levels of *HDAC4* in neurons and determine whether this is altered in the presence of α-synuclein.**

   The subcellular distribution and expression levels of *HDAC4* in neurons in the presence of α-synuclein will be characterised to determine whether its distribution is altered in the presence of α-synuclein, whether it forms condensates and whether it codistributes with MEF2.

3. **Determine whether disease progression can be slowed by interfering with HDAC4 aggregation, HDAC4 distribution or reducing *HDAC4* expression in the *Drosophila* model of this disease.**

   Mutants that are predicted to prevent nuclear HDAC4 accumulation ($HDAC4^{M1\text{-}L285}$), disrupt HDAC4 aggregation ($HDAC4^{F65A}$) or reduce *HDAC4* expression (HDAC4 RNAi) will be co-expressed with α-synuclein to determine if this improves phenotypes (tyrosine hydroxylase staining and climbing ability) resulting from expression of *SNCA*.

2 MATERIALS AND METHODS

2.1 *DROSOPHILA MELANOGASTER* FLY STRAINS

The *Drosophila* fly strains used in this study are listed in Table 2.1, which states both the shorthand name and their full genotype. All fly strains in this thesis are referred to by the shorthand name only. As listed in this table, some strains were generated within this lab while others were purchased from stock centres overseas and imported in compliance with New Zealand MPI (Ministry of Primary Industries) and HSNO (Hazardous Substances and New Zealand Organisms) regulations and approvals. In this thesis, FlyBase-approved gene symbols/names are used. Gene names and genotypes are italicised, while protein names and phenotypes derived from genotypes are not. For proteins named after a gene, the first letter is capitalised. These *Drosophila* gene and protein nomenclature guidelines are outlined at https://wiki.flybase.org/wiki/FlyBase:Nomenclature.

Integrated Construct	**Chromo-somal Linkage**	**Genotype**	**Source**
UAS-CD8::GFP	2	*y^1w*; P{UAS-mCD8::GFP.L}LL5*	BDSC[1] #5137
UAS-GFP	2	*w*; P{w+mC=UAS-2xEGFP}AH2*	BDSC #6874
UAS-mCD8::RFP	3	*w[*]; P{y[+t7.7] w[+mC]=10XUAS-IVS-mCD8::RFP}attP2*	BDSC #32218
NP3558-GAL4	X	*y[*] w[*] P{w[+mW.hs]=GawB}HDAC4[NP3558] / FM7c* Kyoto #104540	Kyoto Stock Center
ELAV^{C155}-GAL4	1	*w[CS10];P{w[+mW.hs]=GawB}elav[C155]*	BDSC #458
GMR-GAL4	2	*w[*]; P{w[+mC]=GAL4-ninaE.GMR}12*	BDSC #1104
nSyb-GAL4	3	*y[1] w[1118]; P{y[+t7.7] w[+mC]=nSyb-GAL4.P}attP2*	BDSC #51941
OK107-GAL4	4	*w[*]; P{w[+mW.hs]=GawB}OK107 ey[OK107]*	BDSC #854

Ddc-GAL4	2	*w[1118]; P{w[+mC]=Ddc-GAL4.L}4.3D*	BDSC #7010
Ddc-GAL4 #1/TM3,Sb	3	*w[1118]; P{w[+mC]=Ddc-GAL4.L}Lmpt[4.36] ?TM3,Sb*	BDSC #7009
Ddc-GAL4 #2/CyO	2	*w[1118]; P{w[+mC]=Ddc-GAL4.L}4.3D/CyO*	BDSC #7010
UAS-SNCA^{WT}	3	*w[*]; P{w[+mC]=UAS-Hsap\SNCA.F}5B*	BDSC #8146
UAS-SNCA^{A30P}	3	*w[*]; P{w[+mC]=UAS-Hsap\SNCA.A30P}40.1*	BDSC #8147
UAS-SNCA^{A53T}	3	*w[*]; P{w[+mC]=UAS-Hsap\SNCA.A53T}15.3*	BDSC #8148
UAS-SNCA^{co} (codon optimised) #1/CyO	2	*w[1118]; P{w[+mC]=UAS-SNCA.J}1/CyO*	BDSC #51375
UAS-SNCA^{co} (codon optimised) #2/TM3,Sb	3	*w[1118]; P{w[+mC]=UAS-SNCA.J}7/TM3, Sb[1]*	BDSC #51376
HDAC4::GFP (cantonised)	1	*w[CS10], P{w[+mC]=PTT-GA}HDAC4[CA07134] (cantonised)*	BDSC #50817
UAS-DmHDAC(WT)-myc	3	*w[67c23]; P{w[mC+]=UAS-DmHDAC4(WT)-myc}attP2:(3L)68A4*	Genetivision, USA
UAS-DmHDAC4$^{M1-L285}$	3	*w[67c23]; P{DmHDAC4[M1-L285]-myc, w[+mC}attP2(3L:68A4).*	Genetivision, USA
DmHDAC4^{F65A}-myc	3	*w[CS10]; P{w[+mC]=UAS-DmHDAC4[F65A]-myc}attP2(3L:68A4)*	Genetivision, USA
UAS-Hdac4 RNAi	3	*w[CS10]; P{GD9446}v20522 Cantonized*	[2]VDRC #20522
UAS-DmHDAC4-myc; OK107-GAL4	3,4	*w[CS10];P{y[+t7.7]=CaryP}attP2, UAS-DmHDAC4(WT)-myc; P{w[+mW.hs]=GawB}OK107 ey[OK107]*	This study, produced by combining BDSC #854 and UAS-DmHDAC4-myc
UAS-SNCA^{co}/CyO; UAS-DmHDAC4^{WT}	2,3	*w[1118]; P{w[+mC]=UAS-SNCA.J}1/CyO; P{w[+mC]UAS-DmHDAC4(WT)-myc}attP2:(3L)68A4*	This study, produced by combining BDSC #51375 and UAS-DmHDAC^{WT}-myc
UAS-SNCA^{co}/CyO; UAS-DmHDAC4$^{M1-L285}$	2,3	*w[1118]; P{w[+mC]=UAS-SNCA.J}1/CyO;P[w[+mC]=[UAS-DmHDAC4[M1-L285]-myc]}attP2(3L:68A4)*	This study, produced by combining BDSC #51375 and UAS-

			DmHDAC4$^{M1-L285}$
UAS-SNCA^{co}/CyO; UAS-DmHDAC4^{F65A}	2,3	*w[1118]; P{w[+mC]=UAS-SNCA.J}1/CyO;P{w[+mC=UAS-DmHDAC4[F65A]-myc]}attP2(3L:68A4)*	This study, produced by combining BDSC #51375 and DmHDAC4^{F65A}-myc
UAS-SNCA^{co}/CyO; UAS-DmHDAC4 RNAi	2,3	*w[1118]; P{w[+mC]=UAS-SNCA.J}1; P{GD9446}v20522*	This study, produced by combining BDSC #51375 and VDRC #20522
UAS-SNCA^{co}/CyO; UAS-GFP	2	*w[1118]; P{w[+mC]=UAS-SNCA.J}1,P{w+mC=UAS-2xEGFP}AH2/CyO*	This study, produced by combining BDSC #51375 and #6874
HDAC4::GFP; Ddc-GAL4	1,2	*w[1118], P{w[+mC]=PTT-GA}HDAC4[CA07134]; P{w[+mC]=Ddc-GAL4.L}4.3D*	This study, produced by combining BDSC #7010 and #50817

Table 2.1 - *Drosophila melanogaster* stock lines

[1]BDSC, Bloomington *Drosophila* Stock Center.

[2]VDRC, Vienna *Drosophila* Resource Center.

2.1.1 Fly stock maintenance

All *Drosophila* stocks were maintained on standard medium at 22°C with a 12-hour light-dark cycle. Standard medium was made by combining 10 g agar, 40 g yeast, 110 g polenta cornmeal, and 1 L of dH_2O and simmering this mixture for 2 min with constant stirring. After taking this off heat, 130 g white sugar, 20 mL molasses and 3.3 g of Moldex (methyl 4-hydroxybenzoate) dissolved in 37 mL 96% ethanol was added and mixed in thoroughly. For 30 mL vials (Labserv, Cat #LBS3680), 8 mL of food was used, while 100 mL bottles for larger quantities of flies required 40 mL of food. Once the media was set, it was sprinkled with yeast to encourage egg laying and plugged with either a foam plug (Genesee scientific, Cat #59-200) (vials) or a sponge plug (Jaece, Cat #L800-C) (bottles). To subculture stocks, every 3 weeks, adult flies were turned onto new food and left to lay eggs for 3-4 days before being removed. Three generations of each stock were maintained, the oldest of which was replaced by a newer generation after each round of subculturing.

2.2 GENETIC CROSSES

Genetic crosses for functional analyses were performed with virgin females that were crossed with the appropriate strain of males to provide the desired heterozygous genotype. Females were collected within 8 h of emerging, as adult *Drosophila* do not mate within 10 h of eclosion at 25°C (Seong et al., 2023). To ensure only virgins were collected, bottles/vials containing emerging adults were checked in the morning, in which only adults that had signs of recent eclosion were collected. This includes visible meconium, a swollen and pale abdomen, folded wings, and a swollen head. These females were placed in a separate vial, and any mature females were discarded. Once cleared in the morning, all females that emerged within the following 6-8 h were collected. Vials were then set with three to five virgin females and the same number of males. When a larger number of progeny was required, bottles were set with 12-15 virgin females and the same number of males. Adults were removed before the progeny emerged. The F1 heterozygous progeny were then used for analyses. Most crosses for functional analyses were raised at 25°C; however, *Ddc-GAL4* crossed to *SNCA* and *HDAC4* rescue constructs were raised at 18°C. This includes *Ddc-GAL4 > UAS-SNCA*; $HDAC4^{M1\text{-}L285}$,

Ddc-GAL4 > UAS-SNCA; HDAC4 RNAi and *Ddc-GAL4 > UAS-SNCA; HDAC4^{F65A}* as well as *Ddc-GAL4 > UAS-SNCA; UAS-CD8::GFP* and *Ddc-GAL4 > UAS-SNCA* when analysed alongside the *HDAC4* rescue constructs.

2.3 IMMUNOHISTOCHEMISTRY ON WHOLE-MOUNT *DROSOPHILA* BRAINS

2.3.1 *Drosophila* brain isolation and immunohistochemistry

Whole flies were fixed in PFAT-DMSO (4% paraformaldehyde in 1X phosphate buffered saline (Sigma Aldrich, Cat. #P4417), 5% dimethyl sulfoxide, 0.1% Triton X-100) and incubated for 1 h on a nutator, before being washed in 1xPBT (1X phosphate buffered saline+0.5% Triton X-100) 3 times for 5 min each. Brains were dissected under a stereomicroscope with fine forceps (Dumont Inox #5), then post-fixed in PFAT-DMSO for 20 min. Brains were then stored at -20ºC in 100% methanol.

Fixed brains stored at -20ºC were rehydrated in 50% methanol/PBT solution before washing 4 x 5 min in PBT and blocking in immunobuffer (5% Normal goat serum (Gibco^{TM}, Cat # 16210064)) for 3 h at room temperature. Primary antibody diluted in immunobuffer was added and incubated overnight at room temperature. Brains were then incubated in secondary antibody diluted in immunobuffer at 4ºC overnight before being mounted on slides in antifade (90% glycerol, 0.2% n-propyl gallate, 1X PBT). Slides were prepared by sealing two coverslips onto each slide with an approximately 0.5 cm gap in between them, to create a channel to allow mounting of brains with a coverslip without damaging them. The coverslips, sealed with nail polish, were kept in the dark at 4ºC until needed for imaging. Antibodies used are listed in Tables 2.2 and 2.3.

Target	Host	Source	Catalogue #	Dilution
GFP	Mouse	DSHB[1]	12A6	1:200
TH	Rabbit	Sigma-Aldrich	AB152	1:250
c-Myc	Mouse	DSHB	9E10	1:100
MEF2	Rabbit	Bruce Paterson[3]	n/a	1:500
HA-Tag (C29F4)	Rabbit	Cell Signalling Technology	3724	1:200
SNCA	Mouse	DSHB	H3C	1:200

Table 2.2 - Primary antibodies used for immunohistochemistry

[1]DSHB, Developmental Studies Hybridoma Bank.

[3]Bruce Paterson, National Cancer Institute, Bethesda, MD, USA.

Name	Target Species	Host Species	Source	Catalogue #	Dilution
Alexa Anti-Mouse 555	Mouse	Goat	Invitrogen	A-21422	1:500
Alexa Anti-Mouse 647	Mouse	Goat	Invitrogen	A-21240	1:500
Alexa Anti-Rabbit 647	Rabbit	Goat	Invitrogen	A-21244	1:500
Alexa Anti-Rabbit 555	Rabbit	Goat	Invitrogen	A-21428	1:500

Table 2.3 - Secondary antibodies used for Immunohistochemistry

2.3.2 Confocal microscopy imaging and analysis

Slides were acclimated at room temperature for at least 30 min before imaging. The brains were imaged using a Zeiss LSM900/Airyscan 3 super-resolution confocal microscope in the Manawatu Microscopy and Imaging Centre (MMIC) using 10x air, 20x air, and 40x oil objectives. Optical sections of 1-2 μm were obtained. Each image was analysed and processed using ImageJ. Figures are shown as either single sections or maximum projections, as indicated.

2.4 EVALUATION OF LOCOMOTOR FUNCTION

Locomotor function was assessed with the startle-induced negative geotaxis assay (Barone & Bohmann, 2013), which measures the ability of flies to climb up the side of a vial. Male flies were collected at eclosion and separated into 20 flies per vial with 5-7 vials per genotype, equating to a total of 100-140 flies per genotype. The assay was carried out every Monday, Wednesday, and Friday, starting from 3 days old until all flies stopped climbing. The assay was carried out at the same time each day to avoid any differences in climbing activity due to circadian rhythms.

To conduct the assay, flies were gently tapped into empty vials and left for 2 min to acclimate to the vial. Each vial was placed in front of a sheet of paper marked with horizontal lines at 1 cm intervals. The vials were then tapped gently but firmly 10 times to collect the flies at the bottom, and then they were given 10 seconds to climb up the side of the vial. A photo was taken at 10 seconds, and the proportion of flies that climbed above 5 cm was calculated. Dead flies were included in calculating the climbing score. Flies were turned onto fresh food when required throughout the experiment (approximately every 3-7 days).

2.5 ASSESSMENT OF EYE PHENOTYPES

The glass multimer reporter GAL4 driver (*GMR-GAL4*) promotes expression in developing photoreceptors of the eye (Freeman, 1996). Female *GMR-GAL4* flies were crossed to *UAS-SNCA*^{WT}, *UAS-SNCA*^{A30P}, *UAS-SNCA*^{A53T}, *UAS-SNCA*^{CO1}, or *UAS-SNCA*^{CO2} males. Adult progeny from these crosses were placed into Eppendorf tubes and euthanised by freezing at -20°C for 48 h before their eyes were imaged with a stereomicroscope (Olympus SZX16). Three females and three males from each genotype were randomly selected, and their eyes were imaged by positioning each fly so one eye was visible, and a series of images was captured at successive focal planes (Z positions) using CellSens imaging software. These Z-stack images were combined into a maximum intensity projection using the Adobe Photoshop Auto-Align Layers and Auto-Blend Layers functions to produce a single composite image.

2.6 STATISTICAL ANALYSIS

To determine whether differences between the results of two groups were statistically significant or not, an unpaired t-test was performed. For comparisons of greater than two genotypes, statistical significance was assessed using a one-way ANOVA with post-hoc Tukey's HSD test with significance set at $\alpha = 0.05$.

3 RESULTS

3.1 ESTABLISHMENT AND CHARACTERISATION OF THE PD MODEL IN *DROSOPHILA*

3.1.1 Confirmation of expression of human *SNCA* in the *Drosophila* brain

Elevated levels of α-synuclein, which accumulates in intracellular aggregates, are a pathological hallmark of PD, and increasing evidence suggests that the soluble oligomeric forms of α-synuclein may be the primary toxic species contributing to DA neuron degeneration (Dauer & Przedborski, 2003; Poewe et al., 2017). This neuronal loss underlies the motor decline and decay in cognitive function observed in PD patients. The *Drosophila* models expressing normal and mutant forms of α-synuclein have been established that recapitulate PD-like phenotypes such as neurodegeneration, motor function deficits and α-synuclein aggregation (Dauer & Przedborski, 2003; Jeibmann & Paulus, 2009; McGurk et al., 2015). This model has not been tested in our laboratory, and there is evidence in the literature for significant variation in phenotypes observed depending on the driver and the specific α-synuclein lines that are employed (Table 1.1), therefore the first step of this project was to establish and characterise a PD model in our laboratory.

The *nSyb-GAL4* driver facilitates pan-neuronal expression and has been successfully used to drive expression of α-synuclein, resulting in α-synuclein aggregation (Olsen et al., 2023; Olsen & Feany, 2019; Ordonez et al., 2018), climbing and walking deficits (Chen et al., 2014a; Maor et al., 2023; Olsen et al., 2023; Ordonez et al., 2018; Sakai et al., 2019), and neurodegeneration (Chen et al., 2014a; Maor et al., 2023; Olsen & Feany, 2019; Ordonez et al., 2018). The first step in characterisation of this model in our laboratory was to confirm the expression of α-synuclein. Female virgin *nSyb-GAL4* females were crossed to *UAS-SNCA* or control WT *Canton S (CS)* males to utilise the UAS/GAL4 system for driving α-synuclein expression across the whole brain. The brains of progeny were processed for immunohistochemistry, in which the primary antibody anti-α-synuclein H3C was used. This is a monoclonal antibody

that recognises the C-terminus and binds to both monomeric and aggregated forms of α-synuclein (Perrin et al., 2003).

The H3C antibody detected α-synuclein in a specific pattern at 1:20 dilution, as seen by the difference in detection patterns between the control and *UAS-SNCA* brains (Figure 3.1B, C). α-synuclein expression was detected in the OLs, ALs, and faint expression was detected in the MB lobes. This is consistent with the characterised pattern of expression for *nSyb-GAL4*, which, although it drives expression pan-neuronally, is not equally expressed in all neuronal cell types, with the highest expression in the OLs and ALs (Figure 3.1A). While these images are low resolution to show whole brain expression, α-synuclein subcellular localisation within the MB appears to localise primarily to the MB lobes, which consist of bundled axons, rather than to the cell bodies or nuclei. The absence of a peri-nuclear "halo" suggests α-synuclein is predominantly localised to neurites rather than in the cytoplasm. The even staining across the whole brain seen in the control appears non-specific with high background due to the high concentration of antibody compared to that in the literature (Olsen et al., 2023; Ordonez et al., 2018). The staining for the 1:100 dilution was faint, indicating that this was below the optimal concentration (Figure 3.1B). Both antibody dilutions used here for immunohistochemistry were much lower than what is commonly used (Olsen et al., 2023; Ordonez et al., 2018), suggesting α-synuclein expression is low or α-synuclein was unusually difficult to detect. This difficulty is investigated further in section 3.1.5, in which the detection of human α-synuclein expressed by the WT *SNCA* gene was compared with that expressed by a *SNCA* transgene that had been codon optimised for expression in *Drosophila.*

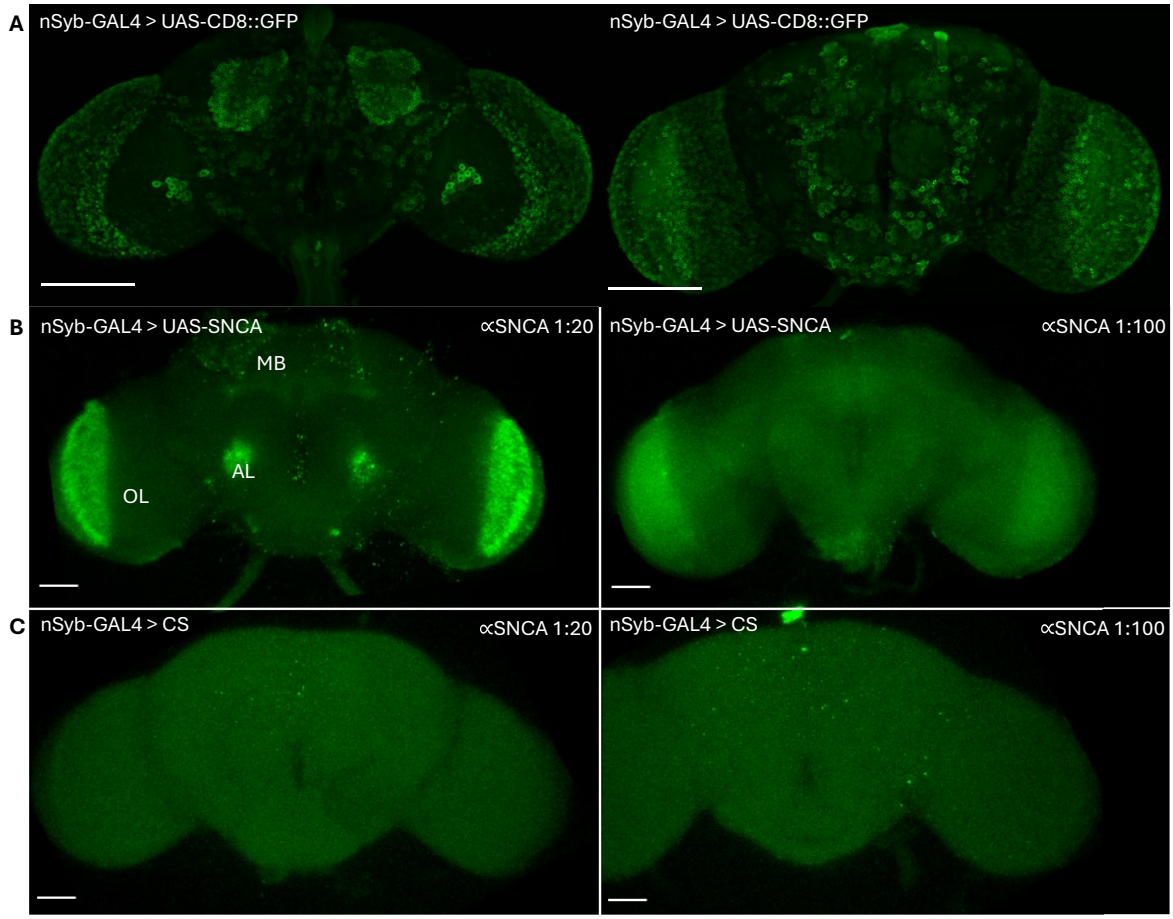

Figure 3.1 - Confirmation of expression of human *SNCA* in the *Drosophila* brain

(A) A Representative image of the *nSyb-GAL4* expression pattern as seen from an anterior (right) or posterior (left) view. Maximum projections of brains of flies expressing mCD8::GFP under the control of *nSyb-GAL4* were stained with anti-GFP to assess distribution. Reproduced from Hawley et al. (2023) (DOI: 10.17912/micropub.biology.000885), which is distributed under CC BY 4.0 http://creativecommons.org/licenses/by/4.0/. **(B)** and **(C)** Maximum projections of anterior whole mount *nSyb-GAL4>UAS-SNCA* (B) and *nSyb-GAL4 CS* (C) brains following immunohistochemistry with anti-*SNCA* (H3C) at 1:20 dilution (left) and 1:100 dilution (right). *CS* = canton special control; OL = optic lobe, MB = mushroom body lobes, AL = antennal lobe. Scale bar = 50 μm.

3.1.2 Characterisation of the α-synuclein-induced impairment in motor function

Expression of α-synuclein in the *Drosophila* brain has been shown to impair motor function as a result of neurodegeneration of motor neurons (Agostini et al., 2023; Jahromi et al., 2021; Liu et al., 2022), which can be quantitatively assessed via the negative geotaxis climbing assay. Flies have an innate desire to climb, termed negative geotaxis, which can be measured to provide an assessment of locomotor function (Barone & Bohmann, 2013). To assess climbing ability, *nSyb-GAL4* females were crossed to *UAS-SNCA* and control *CS* males, and the progeny were collected within 48 h of eclosion. They were transferred to fresh vials (n = 20 per vial) and the negative geotaxis assay was performed every 2-3 days to assess their locomotor function (Section 2.5). The climbing ability of both α-synuclein and control flies consistently declined over the 31-day period with minimal day-to-day variation (Figure 3.2). There was no significant difference between the α-synuclein and control flies. The climbing ability of the control flies (*nSyb-GAL4>CS*) decreased steadily from day 10, which is much faster than expected based on previous assessments that indicate that the locomotor function of *CS* flies remains intact during aging, with a climbing score of around 0.7 or higher for at least 25 days (Haywood & Staveley, 2004; Jahromi et al., 2021). This suggested that the *CS* stock may have had reduced physiological vigour, which was evident from the observation that 40% of these flies died before the end of the assay. This is significantly earlier than seen in the literature and compared to the average *Drosophila* lifespan of up to 100 days (Magwire et al., 2010; Piper & Partridge, 2018; White et al., 2010). While these results indicate there isn't a significant difference between the two genotypes, the poor performance of the controls prevents assessment of whether expression of α-synuclein led to a progressive decline in motor function. During the climbing analysis, it was noticed that the automatic light/dark cycle timer in the fly behaviour lab was inadvertently bumped so that the flies were no longer on a 12:12-hour light/dark cycle and had been exposed to 24 h light conditions, which may have affected the results. Constant light conditions significantly disrupt the circadian rhythms and locomotor activity of *Drosophila* as normal rhythmic patterns are abolished, leading to arrhythmic locomotor behaviour (Cho et al., 2016; Konopka et al., 1989; Leloup & Goldbeter, 2000).

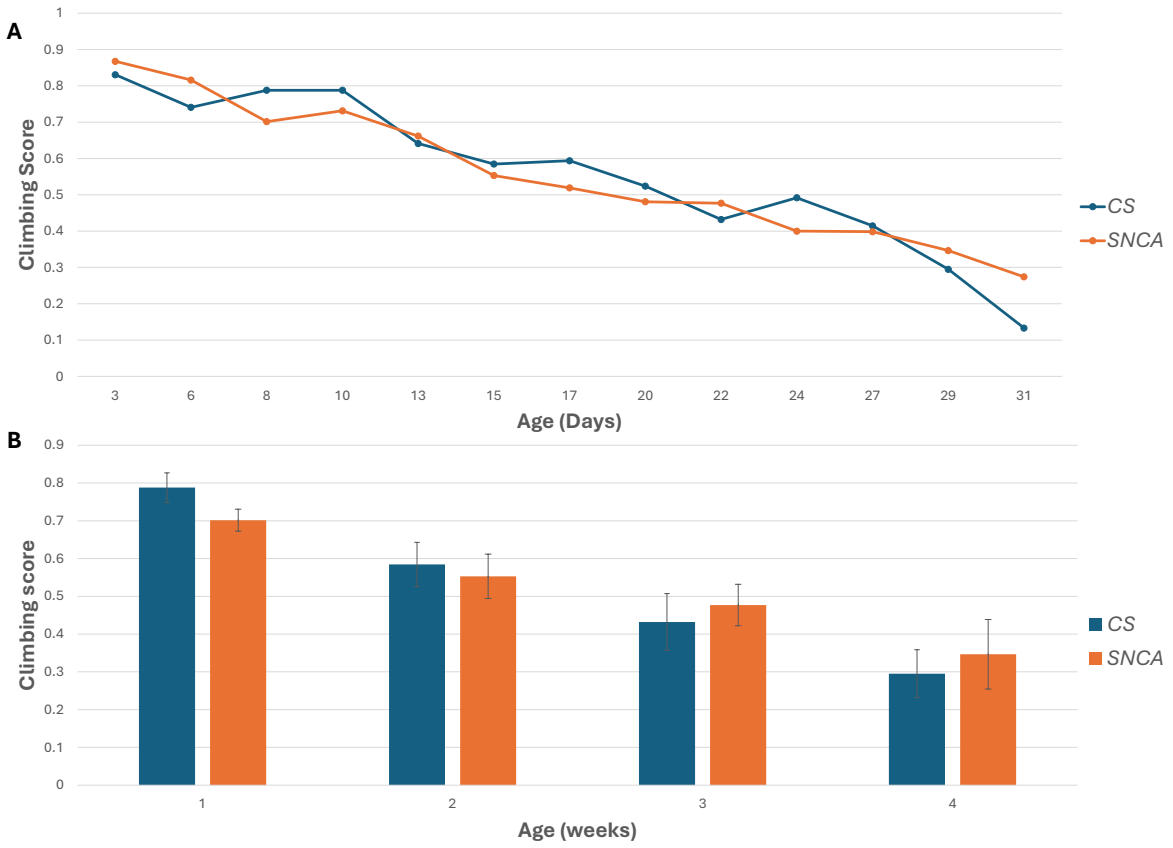

Figure 3.2 – Assessment of motor function following pan-neuronal expression of α-synuclein

Assessing the effect of *nSyb-GAL4 > UAS-SNCA* expression on motor function via a negative geotaxis assay. 140 flies of each genotype were tested over 30 days. Data is shown both via a line graph over days (A) and a bar graph of motor function at each week (B). Climbing score = the percentage of flies climbed above 5cm in 10 seconds. Error bars indicate mean ± standard error of the mean. *CS* = canton special, used as the control with the genotype *nSyb-GAL4 CS*.

In addition to the poor climbing performance of the control strain, the decline of climbing in α-synuclein flies was slower than has been previously reported (Jahromi et al., 2021; Ordonez et al., 2018). The immunohistochemistry results (Figure 3.1) indicate that α-synuclein expression appears modest; therefore, it is possible that it might not be expressed at a high enough level to impair motor function. Two approaches were consequently adopted: to assess whether *nSyb-GAL4* is the most appropriate driver for expression of α-synuclein as a *Drosophila* PD model, and to identify whether a different control strain would be more suitable.

To address the possibility that *nSyb-GAL4* may not be driving expression of α-synuclein in DA neurons at sufficiently high levels, the climbing of flies expressing *SNCA* driven by *nSyb-GAL4* was compared to a second pan-neuronal driver, *elav-GAL4*. At the same time, flies were also generated in which *HDAC4* was expressed to assess if neurodegeneration occurs when *HDAC4* is overexpressed in *Drosophila* neurons. The nuclear accumulation of HDAC4 is associated with impairment of motor performance in a rodent model (Wu et al., 2017); therefore, this will establish whether increasing HDAC4 also impairs motor function in the *Drosophila* model. It is important to note that in comparing Figures 3.2 and 3.3, the first experiment was terminated after 31 days when it became clear that the controls were impaired, whereas in the current experiment, the climbing ability was assessed until all flies stopped climbing; therefore, the scales are slightly different. With this consideration, it is clear that the *nSyb-GAL4>CS* and *nSyb-GAL4>UAS-SNCA* flies deteriorated at the same rate as observed in Figure 3.2. Both the flies expressing *elav-GAL4*-driven α-synuclein and the *elav-GAL4* controls performed even more poorly (Figure 3.3). This led me to question whether pan-neuronal drivers were optimal for expression of α-synuclein in DA neurons; however, it was ambiguous as to whether this was a result of the *CS* genetic background or insufficient α-synuclein expression.

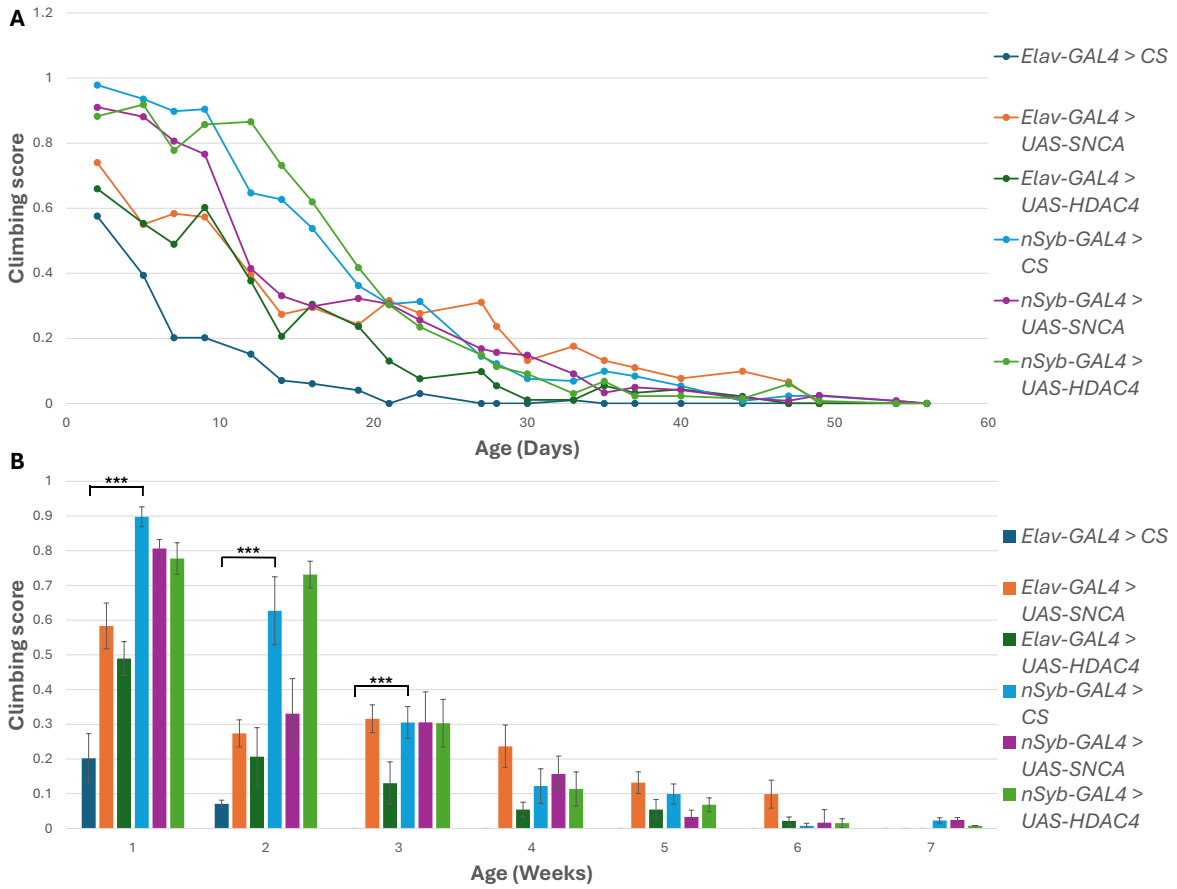

Figure 3.3 - Evaluation of motor function with *elav-GAL4* and *nSyb-GAL4* driven α-synuclein and HDAC4 expression

Assessing the effect of pan-neuronal *SNCA* expression on motor function via a negative geotaxis assay. 100 flies of each genotype were tested over 55 days. Data is shown both via a line graph over days (A) and a bar graph of motor function at each week (B). Climbing score = the percentage of flies climbed above 5cm in 10 seconds. Error bars indicate mean ± standard error of the mean. *CS* = canton special. (one-way ANOVA, Week 1: $F(5, 30) = 24.0966$, $p = 1.13 \times 10^{-9}$, Week 2: $F(5, 30) = 9.2175$, $p = 2 \times 10^{-5}$, Week 3: $F(5, 30) = 9.2175$, $p = 2 \times 10^{-5}$, Week 4: $F(5, 30) = 2.0562$, $p = 0.099$, Week 5: $F(5, 30) = 2.6422$, $p = 0.0429$, Week 6: $F(5, 30) = 3.2065$, $p = 0.0195$, Week 7: $F(5, 30) = 0.6122$, $p = 0.6913$. Post-hoc Tukey's HSD, $p<0.5$ = *, $p<0.1$ = **, $p<0.01$ = ***).

To address this, different control strains were tested. w^{1118} is also a commonly used control strain. Genetic backgrounds were compared by crossing *CS* females to males of the *CS*, w^{1118}, *w(CS10)* and *yw* strains and assessing climbing ability. w^{1118} flies showed a much slower climbing deficit than all other strains (Figure 3.4); therefore, all fly strains were outcrossed for 5 generations to w^{1118} to place them in this genetic background.

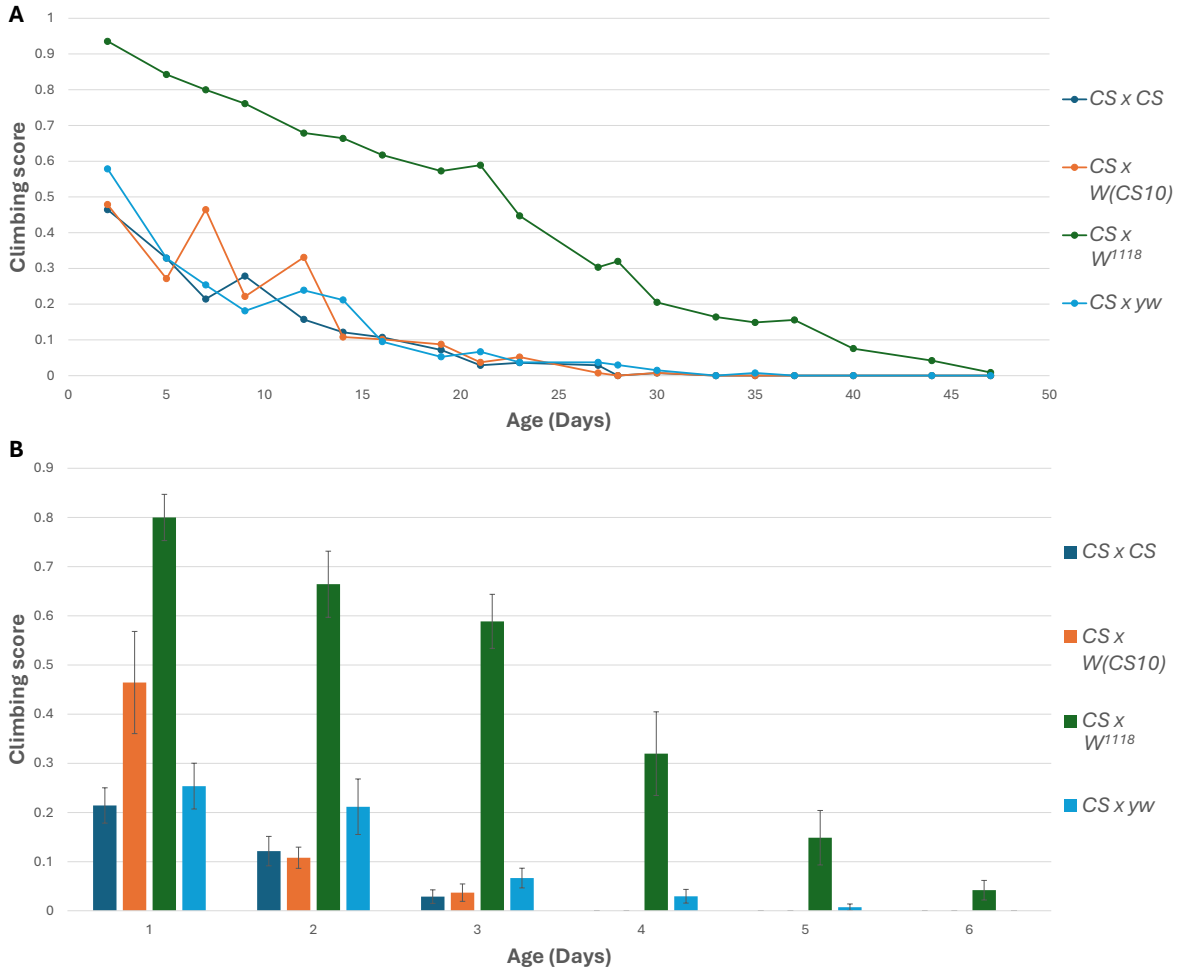

Figure 3.4 – Assessing motor function of *Drosophila* control strains

Assessing the motor function of common control strains via a negative geotaxis assay. 140 flies of each genotype were tested over 44 days. Data is shown both via a line graph over days (A) and a bar graph of motor function at each week (B). Climbing score = the percentage of flies climbed above 5cm in 10 seconds. Error bars indicate mean ± standard error of the mean. *CS* = canton special.

3.1.3 Assessment of *nSyb-GAL4* and *elav-GAL4* mediated expression in DA neurons

It was clear that the *CS* strain showed poor climbing ability; however, as mentioned above, despite this, the decline in motor function for *nSyb-GAL4 > UAS-SNCA* was slower than expected. *nSyb-GAL4* and *elav-GAL4* are both pan-neuronal drivers; however, their expression patterns differ (Hawley et al., 2023). *nSyb-GAL4* drives higher expression in the OLs, ALs, and down the midline of the brain, while *elav-GAL4* drives slightly higher expression in the MB. Since DA neurons are the primary target for α-synuclein expression in *Drosophila* models of PD, it was important to assess the relative expression levels of each driver in these neurons. To address this, anti-tyrosine hydroxylase (anti-TH) staining was used as a marker to visualise the DA clusters. The detection of TH is well established as an accurate marker of DA neurons (Friggi-Grelin et al., 2003). Figure 3.5 demonstrates clear imaging of the DA neurons with anti-TH, specifically the PPM1/2, and PPL clusters for DA neuron characterisation, which have been found to be the most susceptible to α-synuclein-mediated neurodegeneration (Jahromi et al., 2021). This clearly characterises the distribution of DA neurons in the brain and shows that the TH antibody works well.

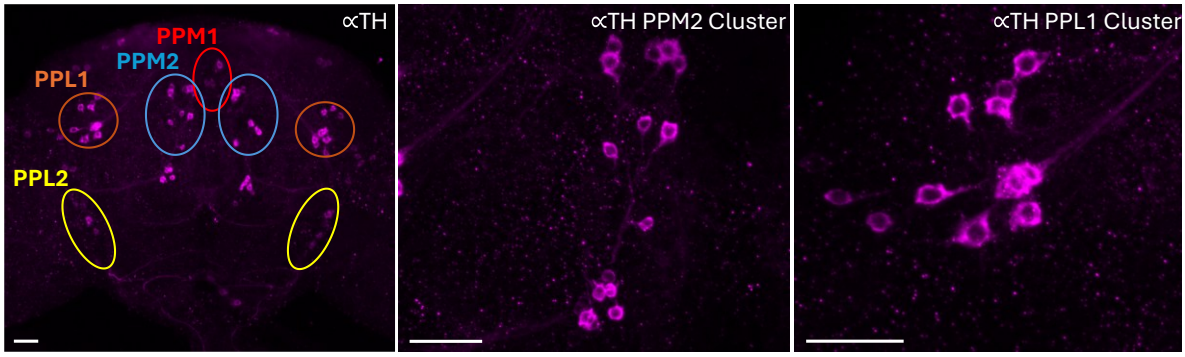

Figure 3.5 - DA neuron characterisation

Maximum projections of whole mount WT brains following immunohistochemistry with anti-TH at 1:250 dilution. The PPM1/2, and PPL clusters are labelled, which have been found to be the most susceptible to a-synuclein-mediated neurodegeneration. Scale bar = 20 µm.

Both the *nSyb-GAL4* and *elav-GAL4* drivers were crossed to the reporter strain *UAS-CD8::GFP* to compare the expression pattern of these drivers and determine their level of expression in DA neurons specifically. Green fluorescent protein (GFP), originally isolated from Aequorea jellyfish, is a protein that exhibits a bright, green fluorescence that allows for visualisation of gene expression and cell processes (Tsien, 1998). CD8::GFP is a fusion of GFP with the transmembrane domain of mouse CD8, which targets GFP to the cell membrane of cells to allow clear visualisation of cell bodies and neuronal projections (Lee & Luo, 1999). Widespread GFP expression was detected with both *elav-GAL4* and *nSyb-GAL4* drivers. There was some overlap with TH, however the level of expression driven by either driver in DA neurons was very low (Figure 3.6).

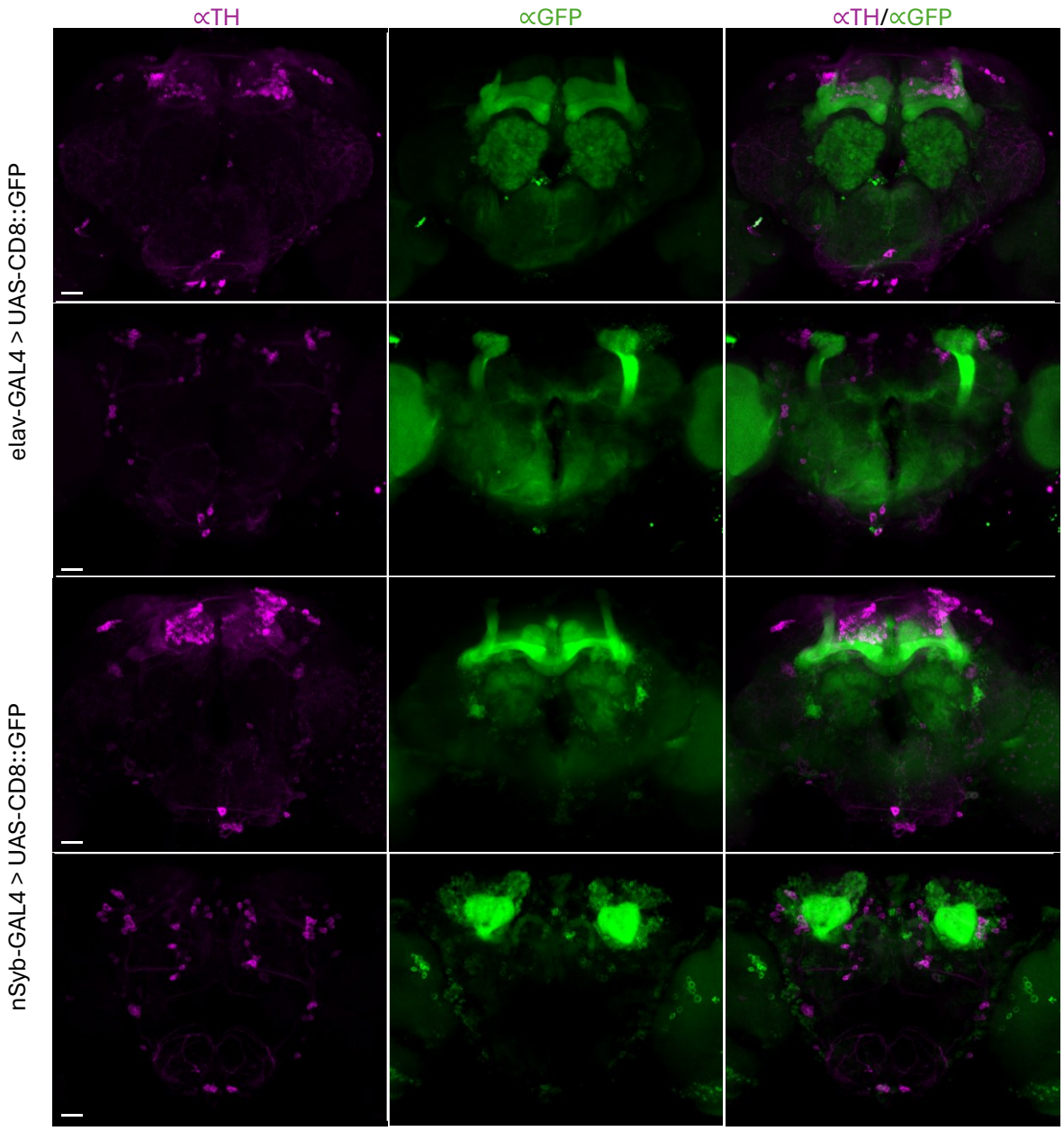

Figure 3.6 - Comparison of patterns of expression of pan-neuronal drivers in the *Drosophila* brain.

Maximum projections of anterior and posterior whole mount *elav-GAL4 > UAS-CD8::GFP* (upper) and *nSyb-GAL4 > UAS-CD8::GFP* (lower) brains following immunohistochemistry with anti-TH at 1:250 dilution (magenta) and anti-GFP at 1:200 dilution (green). Overlapping signal of GFP and TH appears white in the merged image. Scale bar = 20 μm.

3.1.4 Assessment of *Ddc-GAL4*-driven expression in DA neurons

Due to pan-neuronal-driven expression showing low levels of expression in DA neurons, the *Ddc-Gal4* driver, which drives high expression in dopaminergic and serotonergic neurons, (Haywood et al., 2002; Konrad & Marsh, 1987), was characterised as a potential alternative driver to facilitate high expression of α-synuclein in DA neurons. It was hypothesised that this would result in a more severe neurodegeneration phenotype (Hodgetts & O'Keefe, 2006; Konrad & Marsh, 1987).

The climbing ability of flies expressing α-synuclein under control of *Ddc-GAL4* was then assessed. This assay overlapped with assessing the impact of *nSyb-GAL4* and *elav-GAL4*-driven expression of α-synuclein on motor function; therefore, *UAS-SNCA* was still in the *CS* background while *Ddc-GAL4* was in the w^{1118} background. As a result, progeny were generated in a mixed strain. The climbing ability of controls was improved compared to those in the *CS* background, however there was still only a modest climbing deficit shown when *UAS-SNCA* was driven with *Ddc-GAL4* (Figure 3.7). To confirm expression of α-synuclein, the brains of progeny were processed for immunohistochemistry with anti-TH and anti-α-synuclein, however no α-synuclein was detected (Figure 3.8), which brought the identity of the *Ddc-GAL4* stock into question. The experiment was repeated with *UAS-CD8::GFP*, and no GFP expression was observed (data not shown), indicating that the *Ddc-GAL4* stock was either mis-identified or had lost the transgene cassette.

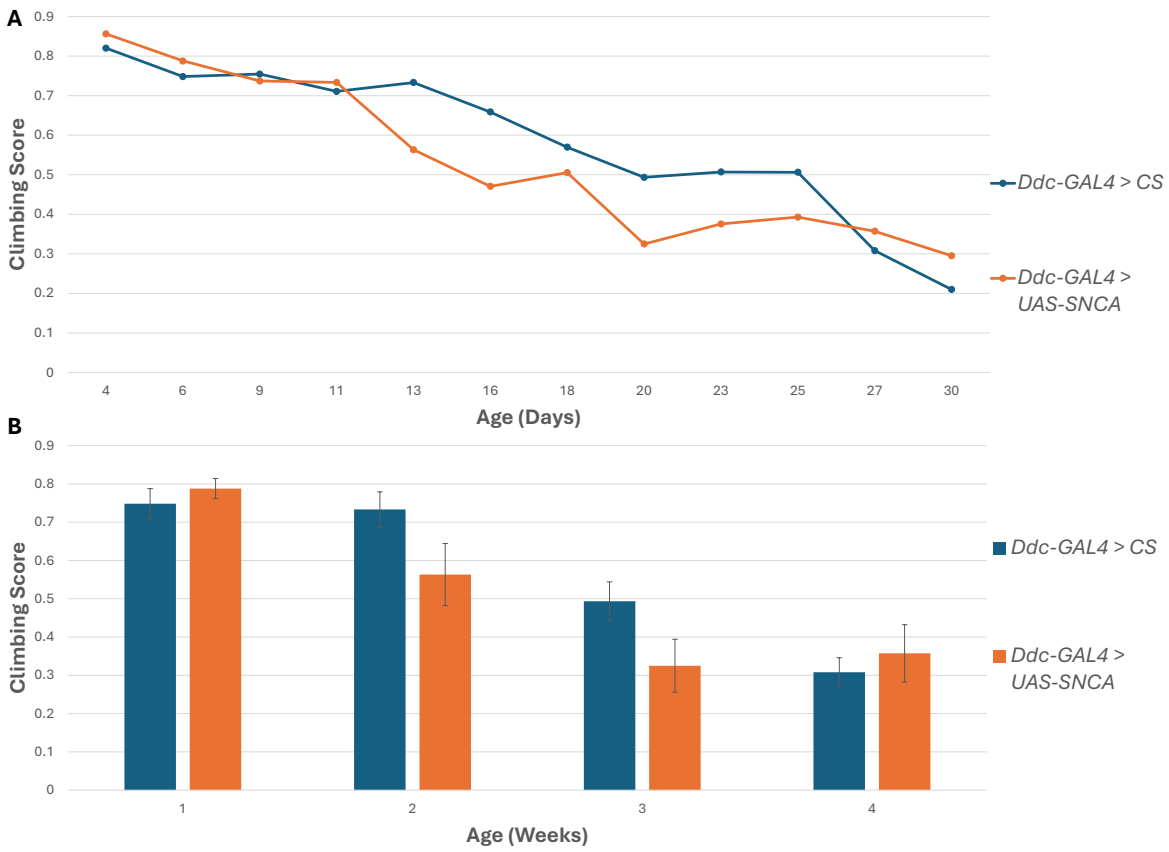

Figure 3.7 - Assessing *Ddc-GAL4* driven expression of *SNCA* on motor function

Assessing the effect of *SNCA* expressed in the *Ddc-GAL4* driver pattern on motor function via a negative geotaxis assay. 140 flies of each genotype were tested over 30 days. Data is shown both via a line graph over days (A) and a bar graph of motor function at each week (B). Climbing score = the percentage of flies climbed above 5cm in 10 seconds. Error bars indicate mean ± standard error of the mean. *CS* = canton special.

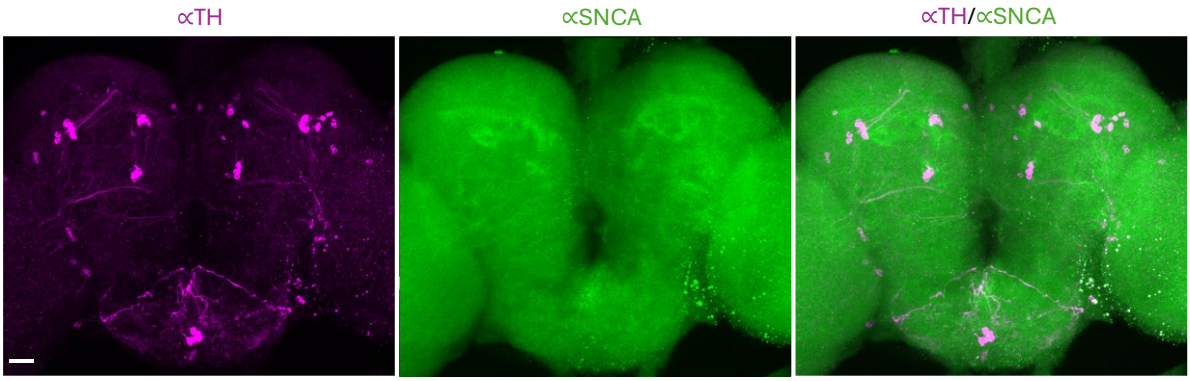

Figure 3.8 - Assessment of *Ddc-GAL4* driven *SNCA^{WT}* expression in DA neurons

Maximum projections of whole mount *Ddc-GAL4>UAS-SNCA* brains following immunohistochemistry with anti-*SNCA* (green) at 1:20 dilution and anti-TH (magenta) at 1:250 dilution. Gain intensity was increased in an effort to detect a signal, resulting in high background. Scale bar = 20 µm.

Two new *Ddc-Gal4* stocks (*Ddc-GAL4*$^{4.36}$ and *Ddc-GAL4*$^{4.3D}$, herein referred to as *Ddc-GAL4 1* and *Ddc-GAL4 2,* respectively) were obtained and crossed to *UAS-CD8::GFP* to verify expression in DA neurons (Figure 3.9). The expression pattern was consistent with that previously observed (Xie et al., 2018; Yarali & Gerber, 2010), with GFP expression overlapping with TH in DA neurons, in particular the PPM and PPL1/2 clusters. The GFP-expressing neurons that don't overlap with TH are likely to be serotonergic as *Ddc-GAL4* drives expression in both neuronal subtypes (Hodgetts & O'Keefe, 2006; Jahromi et al., 2021; Konrad & Marsh, 1987).

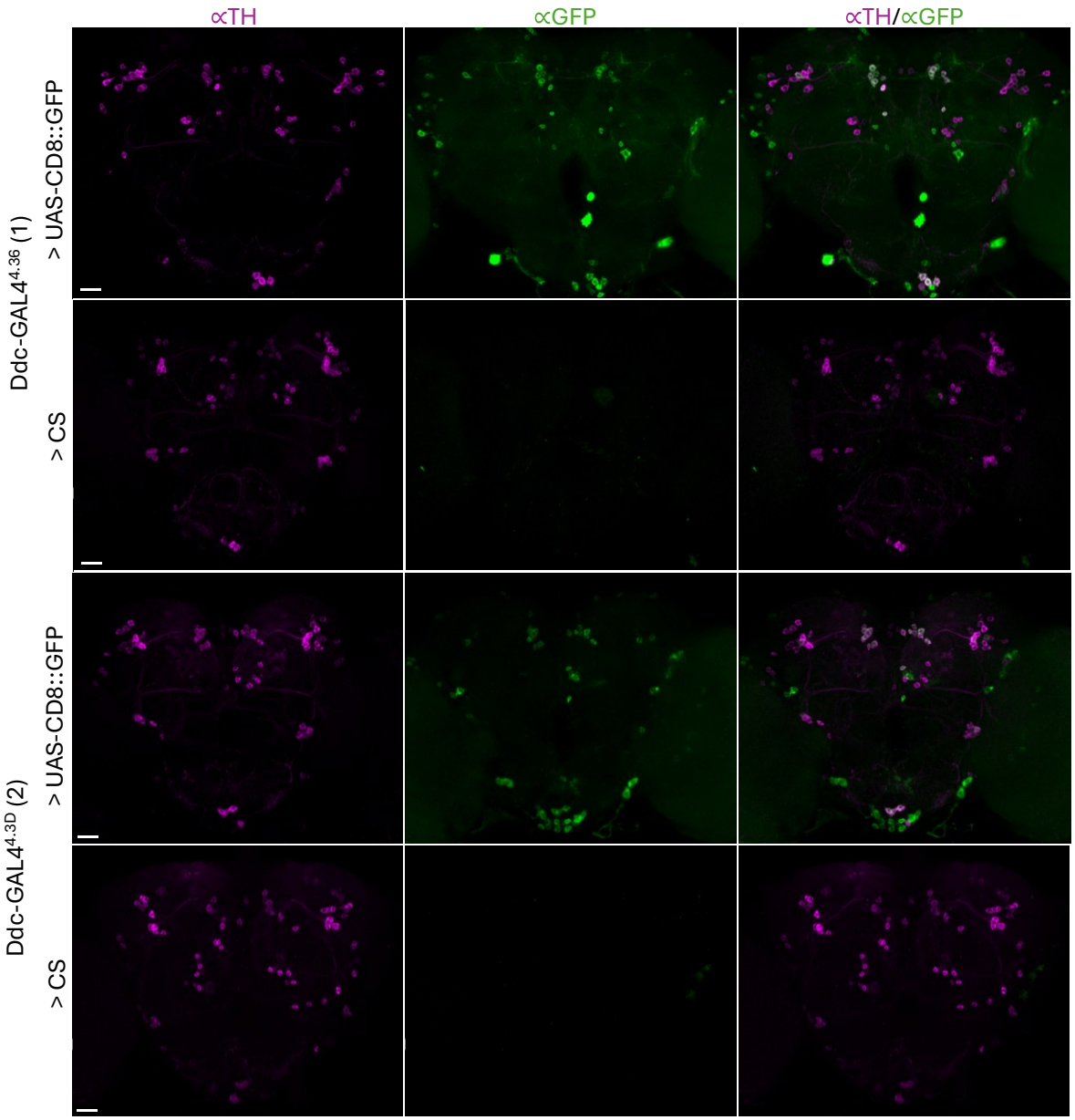

Figure 3.9 - Assessing *Ddc-GAL4*$^{4.36}$ (1) and *Ddc-GAL4*$^{4.3D}$ (2) driven expression in the *Drosophila* brain

Maximum projections of whole mount *Ddc-GAL4 1* (upper) and *Ddc-GAL4 2* (lower) driven brains crossed to *UAS-CD8::GFP* or *CS* following immunohistochemistry anti-TH at 1:250 dilution (magenta) and anti-GFP at 1:200 dilution (green). Scale bar = 20 µm.

3.1.5 Comparison of expression of *SNCA* transgenes

Due to the difficulty detecting α-synuclein, it was hypothesised that WT human α-synuclein was not expressed at sufficiently high levels for robust detection, or alternatively, the protein was not particularly stable in *Drosophila* neurons, which would also explain the modest climbing deficit. To that end, two new fly strains were obtained that carry UAS fused upstream of a human *SNCA* transgene that had been codon-optimised for expression in *Drosophila* (herein referred to as *SNCA* CO 1 and 2). It is known that codon optimisation results in higher expression, due to organisms preferring different codons (Gustafsson et al., 2004). Expression of CO α-synuclein was compared in DA neurons with the rationale that higher expression would lead to accelerated neurodegeneration and a more severe climbing defect. Despite the driver showing robust GFP expression, α-synuclein was still low when detected with the H3C antibody at 1:200 dilution, suggesting that WT human α-synuclein does not accumulate to high levels in *Drosophila* neurons. *Ddc-GAL4*-driven expression of *SNCA*^{CO1} and *SNCA*^{CO2} showed robust expression at the same antibody dilution and confocal settings (Figure 3.10). Expression was detected primarily in the PPM1/2 neurons, with some potential low expression in PPL1 and PPL3 clusters, as determined by co-distribution with TH.

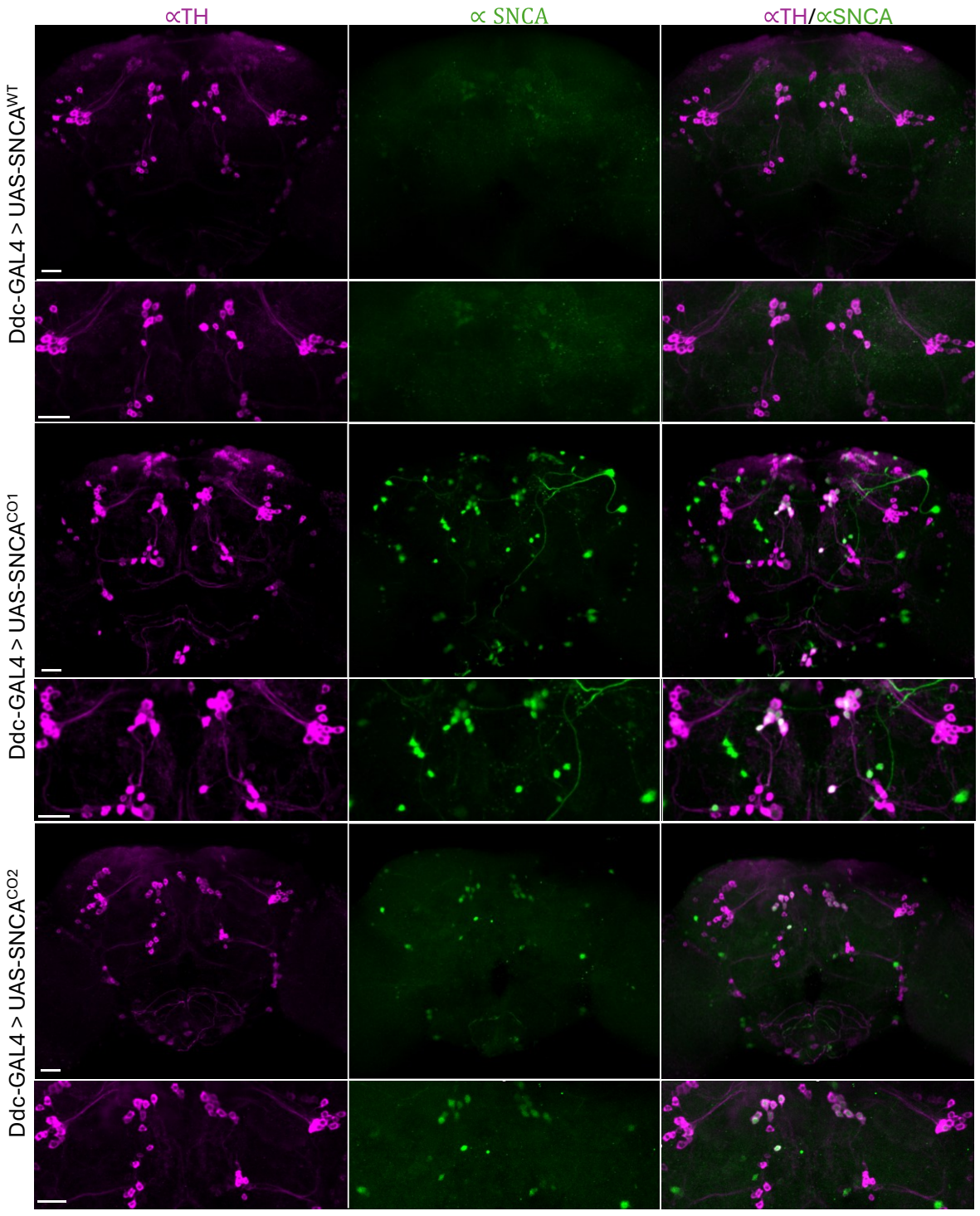

Figure 3.10 - Comparison of expression of WT and codon optimised *SNCA* transgenes

Figure 3.10 Cont. - Comparison of expression of WT and codon optimised *SNCA* transgenes

Maximum projections of whole mount brains expressing $SNCA^{WT}$, $SNCA^{CO1}$ or $SNCA^{CO2}$ driven by *Ddc-GAL4* following immunohistochemistry anti-*SNCA* (green) at 1:200 dilution and anti-TH (magenta) at 1:250 dilution. Scale bar = 20 μm.

3.1.6 Assessment of neurodegeneration induced by α-synuclein

Once robust expression of α-synuclein was detected in DA neurons, the next step was to determine whether this promotes age-dependent neurodegeneration. Neurodegeneration of DA neurons over 30 days was assessed by comparing the survival of TH neurons between 1-day-old and 30-day-old flies. *Ddc-GAL4* females were crossed to *UAS-SNCA CO* males, and brains of progeny harvested at one and 30 days post eclosion (Agostini et al., 2023; Mohite et al., 2018; Narwal et al., 2024; Trinh et al., 2008). Decreased intensity of TH staining has been shown to correlate with degeneration of DA neurons (Kastner et al., 1993). Figures 3.11 show there is some decrease in fluorescence in the neurons of the 30-day-old flies compared to the 1-day-old flies, specifically in the PPM2 neurons. PPM1, PPM2, PPM3, PPL1, and PPL2 neurons are thought to be more vulnerable to α-synuclein-mediated neurodegeneration, although there are discrepancies due to other variables such as different drivers, methodologies, and transgenes used (Table 1.1) (Agostini et al., 2023; Jahromi et al., 2021; Liu et al., 2022). The images in Figure 3.11 show high overlap between α-synuclein and TH in PPM1/2 neurons, suggesting they would be the most affected. In this case, it appears PPM2 and possibly PPL2 are decreased in intensity while the serotonergic neurons are still bright after 30 days, which indicates neurodegeneration of DA neurons. While this shows some indication of neurodegeneration, it is a preliminary assessment; a clear determination would require quantitation of a larger number of brains over a longer time course.

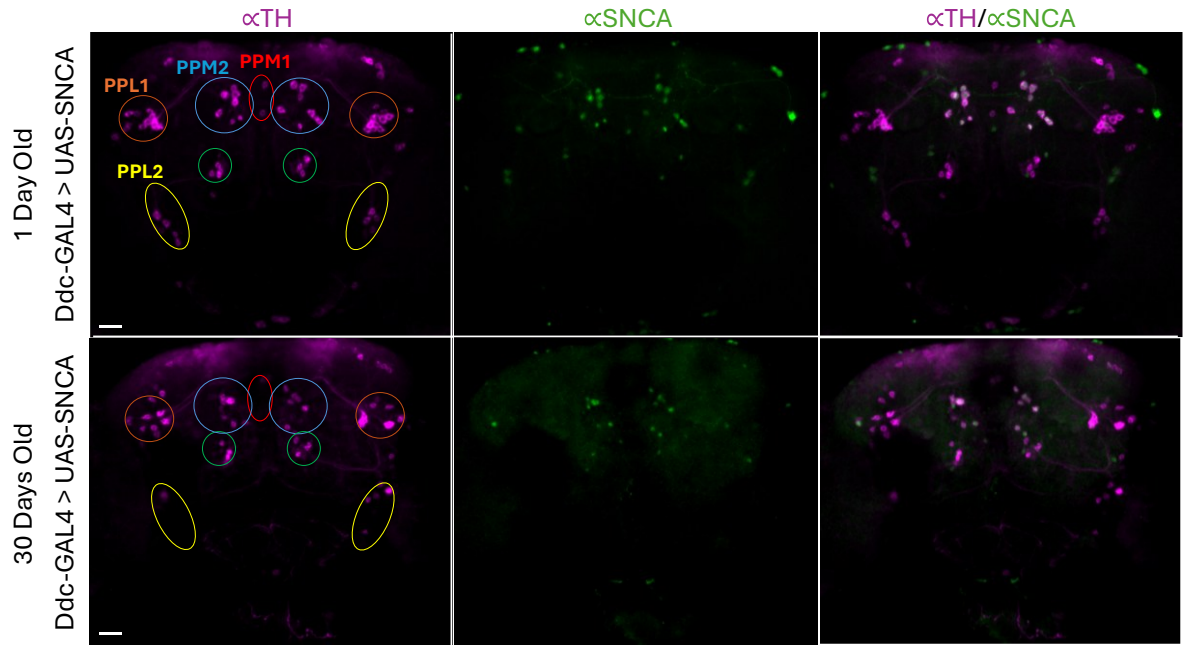

Figure 3.11 - Assessment of neurodegeneration induced by α-synuclein

Maximum projections of whole mount *Ddc-GAL4>UAS-SNCA* brains at 1 day old (upper panel) and 30 days old (lower panel) following immunohistochemistry anti-*SNCA* at 1:200 dilution (green) and anti-TH at 1:250 dilution (magenta). Labelled PPM and PPL DA neuron clusters show decreased intensity of TH staining, indicating neurodegeneration. Scale bar = 20 μm.

3.1.7 Assessment of eye defects induced by α-synuclein

To further confirm that CO α-synuclein results in neurodegeneration, the impact of its expression on the eye was examined, as the eye is a well-established model for assessing neurodegenerative processes due to its highly organised structure and sensitivity to cellular toxicity (Iyer et al., 2016; Nitta & Sugie, 2022; Tsachaki & Sprecher, 2012). *GMR-GAL4*, which drives expression in the eye (Hay et al., 1997), was crossed to both CO human *SNCA* as well as WT *SNCA* and *SNCA* mutants A30P and A53T (Figure 3.12). Expression of CO *SNCA* resulted in a defective eye, with fused and misaligned ommatidia, whereas expression of WT α-synuclein or either mutant did not result in a significant phenotype compared to CS, which aligns with the previous experiments showing that WT α-synuclein does not produce a notable disease phenotype. This also establishes that expression of α-synuclein *Drosophila* eye could be used as a model to examine therapeutic strategies. Interestingly, there also appears to be a difference in severity of phenotypes between males and females expressing CO α-synuclein, with the female eyes displaying a more severe phenotype. *GMR-GAL4* and *UAS-SNCA*^{CO1} are on chromosome 2, and *UAS-SNCA*^{CO2} is on chromosome 3; therefore, it cannot be an X-linked difference. This could be due to differences in hormonal or developmental pathways.

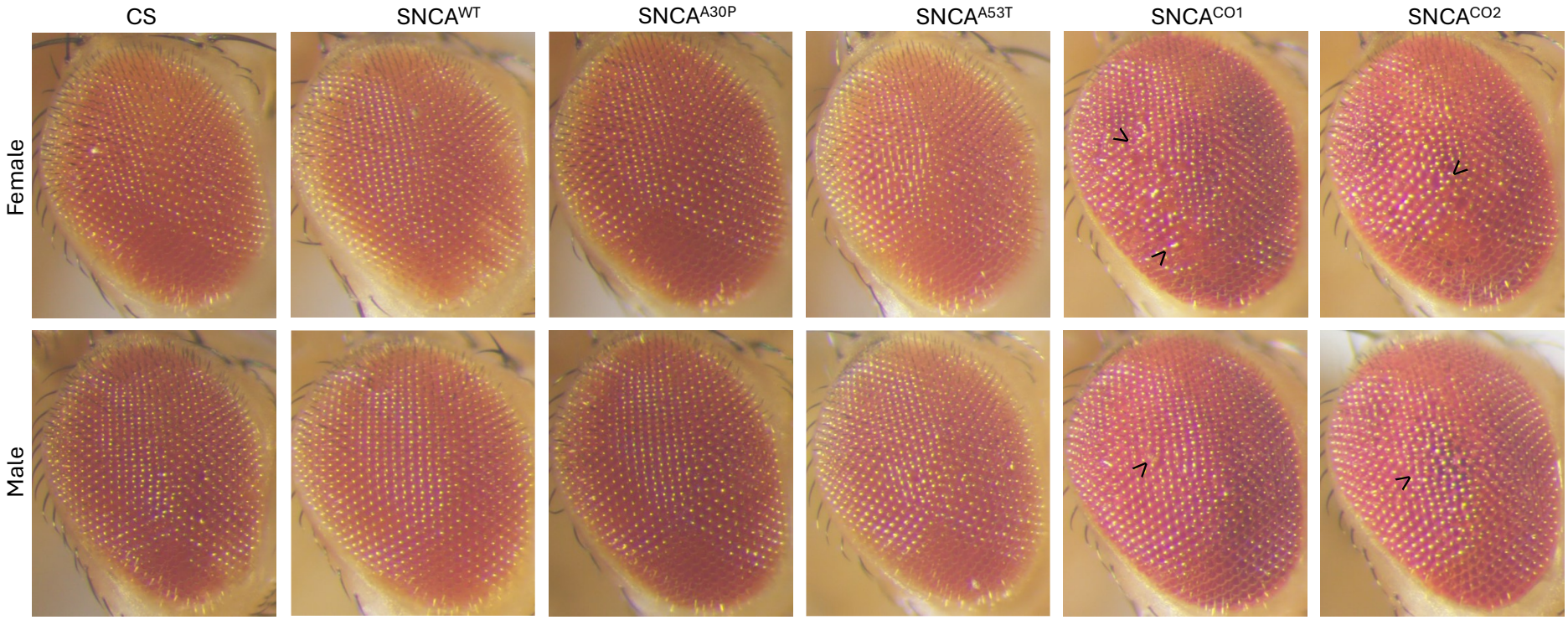

Figure 3.12 - Assessment of eye defects induced by α-synuclein

Each panel shows photos of the compound eye of transgenic flies (*GMR-GAL4>CS, GMR-GAL4>UAS-SNCA^{WT}, GMR-GAL4>UAS-SNCA^{A30P}, GMR-GAL4>UAS-SNCA^{A53T}, GMR-GAL4>UAS-SNCA^{CO1}, GMR-GAL4>UAS-SNCA^{CO2})*. Arrowheads point to misaligned ommatidial arrays.

3.1.8 Characterisation of expression of HDAC4 in DA neurons

Endogenous *HDAC4* expression was characterised to determine whether it was expressed in DA neurons in *Drosophila*. HDAC4 has been detected in Lewy bodies and identified as a key regulator of gene expression changes in PD neurons (Lang et al., 2019; Takahashi-Fujigasaki & Fujigasaki, 2006). Additionally, MEF2 and HDAC4 have been shown to co-localise in neuronal nuclei in mammalian cells (Borghi et al., 2001) as well as in KCs in *Drosophila* (Fitzsimons et al., 2013). Under pathological conditions observed in PD, HDAC4 accumulates in the nucleus, and MEF2 function becomes significantly impaired. In the rodent model, HDAC4 translocates from the cytoplasm into the nucleus in DA neurons. Once in the nucleus, HDAC4 actively represses MEF2, leading to widespread dysregulation of neuroprotective gene expression resulting in enhanced neuronal apoptosis (Wu et al., 2017). This raises the possibility of decreasing neurodegeneration by interfering with HDAC4 and MEF2 binding, thus decreasing nuclear HDAC4. This strategy would rely on both proteins being expressed in DA neurons in *Drosophila,* which has not been examined.

As an HDAC4 antibody was unavailable to detect endogenous HDAC4, an alternative approach was required to label HDAC4-expressing neurons. Instead, *NP3588-GAL4* was crossed to *UAS-CD8::GFP* to express GFP in the pattern of endogenous *HDAC4* expression. The *NP3588* driver is an *HDAC4*-trapped p[GAL4]-driven expression where the GAL4 P element transposon is inserted 3144 bp downstream from the 3' end of the 2nd exon of the endogenous *HDAC4* gene, therefore expressing GAL4 in the HDAC4 pattern (Fitzsimons et al., 2013). Expression was low outside of the KCs; however, faint staining was observed in some DA neuron clusters, shown in Figure 3.13 in which the intensity has been increased to allow visualisation more clearly. Increasing the intensity to focus on these neurons showed overlap between HDAC4 and TH in PPL2 and PPM3 neurons, with some co-distribution in PPL1, PPM2, and VUM neuron clusters (Figure 3.13). These neuronal populations have been shown to be susceptible to neurodegeneration in the *Drosophila* model of PD (Agostini et al., 2023; Jahromi et al., 2021; Liu et al., 2022). This suggests that dysregulation of HDAC4 in these neurons could cause motor dysfunction and neurodegeneration in *Drosophila,* however this is yet to be established.

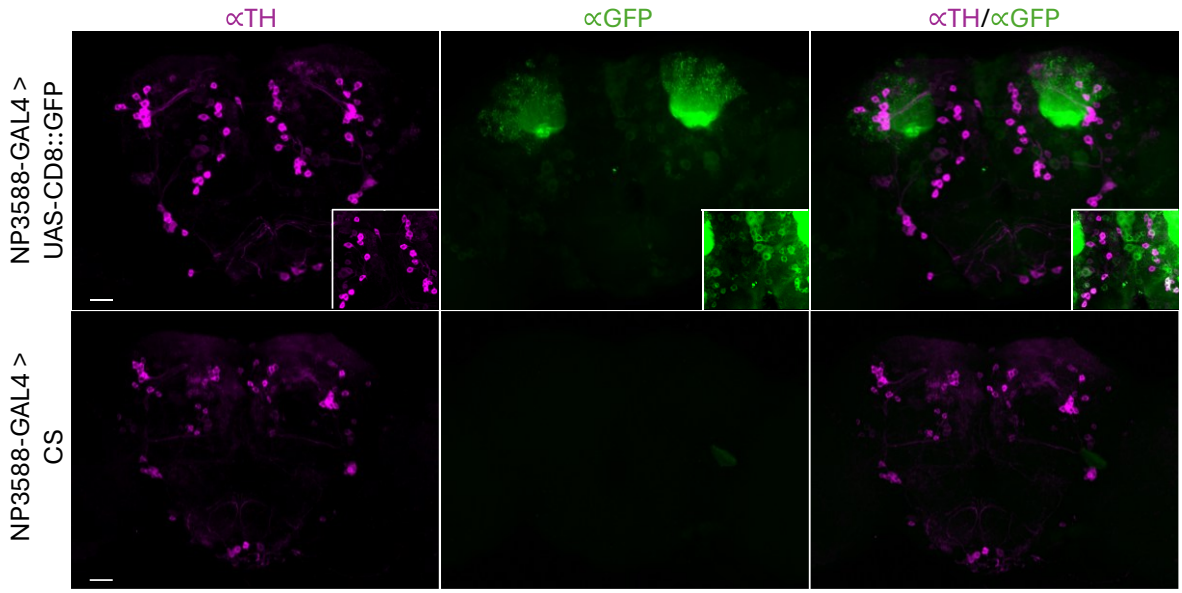

Figure 3.13 – Characterisation of HDAC4 expression in DA neurons

Maximum projections of whole mount *NP3588-GAL4 > UAS-CD8::GFP* (upper panel) and *NP3588-GAL4 CS* (lower panel) brains following immunohistochemistry with anti-TH at 1:250 dilution (magenta) and anti-GFP at 1:200 dilution (green). Inset shows increased GFP intensity to highlight expression in DA neurons. Scale bar = 20 μm.

3.1.9 Characterisation of expression of MEF2 in DA neurons

The expression of *MEF2* in DA neurons was assessed by anti-MEF2 immunohistochemistry on brains in which DA neurons were labelled with GFP. This approach was taken because both anti-TH and anti-MEF2 antibodies were raised in rabbit, preventing direct co-labelling with both. Due to MEF2's potential involvement in neurodegeneration (discussed in section 1.4.2), GFP was expressed in the *Ddc-GAL4* driver pattern, which was then compared to *MEF2's* endogenous expression pattern to determine whether *MEF2* is expressed in DA neurons. Figure 3.14 shows *MEF2* is expressed across the whole brain, with the highest expression in the KCs. Since MEF2 is located primarily in the nucleus while CD8::GFP is distributed to the cell membrane, the colocalization is not obvious. Closer analysis of the expression pattern shown in Figure 3.14 shows MEF2 is present in all *Ddc-GAL4* expressing neurons, indicating that *MEF2* is endogenously expressed in DA neurons. As *HDAC4* and *MEF2* are endogenously expressed in these neurons, it suggests the possibility that the interaction between these proteins could increase susceptibility to α-synuclein-mediated neurodegeneration.

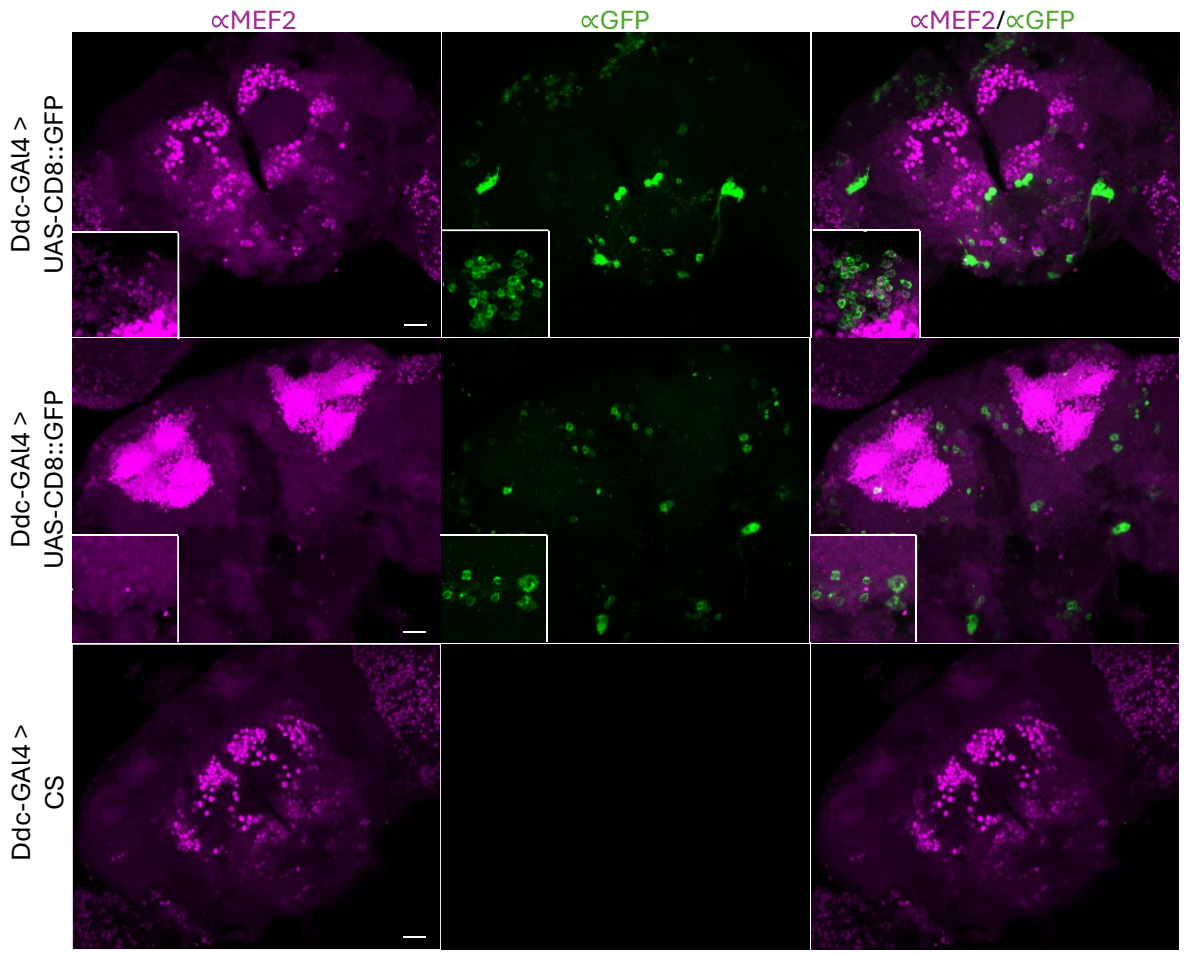

Figure 3.14 – Characterisation of expression of endogenous MEF2 in DA neurons

Maximum projections of whole mount anterior and posterior *Ddc-GAL4 >UAS-CD8::GFP* and *Ddc-GAL4 CS* brains following immunohistochemistry anti-MEF2 at 1:500 dilution (magenta) and anti-GFP at 1:200 dilution (green). Inset shows enlarged section with increased MEF2 and GFP intensity to highlight MEF2 expression in DA neurons. Scale bar = 20 μm.

3.1.10 Assessment of climbing defects induced by *SNCA* and HDAC4

The previous experiments determined an experimental protocol in which α-synuclein could be robustly expressed in DA neurons via *Ddc-GAL4* driving expression of CO *SNCA* transgene. The impact of expression of α-synuclein on climbing ability was then re-assessed. *HDAC4* overexpression was also assessed, alongside the expression of $HDAC4^{M1\text{-}L285}$, which is a truncated HDAC4 that only contains the first 285 amino acids. As described in section 1.4.2, this truncated protein still binds MEF2, as the MEF2 binding domain is in the N-terminal region however it does not contain the deacetylase domain or nuclear export domain, resulting in nuclear accumulation and binding of MEF2 without any deacetylase activity (Chan et al., 2003; Fitzsimons et al., 2013; Zhao et al., 2001).

It was expected that the expression of $HDAC4^{M1\text{-}L285}$ would have a limited impact on climbing ability; therefore, it could be tested as a potential therapy to reduce nuclear HDAC4-induced neurodegeneration by outcompeting it for binding to MEF2. A decline in motor function was observed for both α-synuclein and HDAC4-expressing flies compared to the w^{1118} control flies (Figure 3.15). The decline in climbing of HDAC4-expressing flies was significantly different to the control at all time points and α-synuclein showed a significant decrease by 4 weeks. The controls held a climbing index of over 0.7 for 35 days, whereas both *HDAC4* and *SNCA* declined to under 0.7 in 12 days or less and continued to decline steadily. These data show that the expression of *HDAC4* and *SNCA* in DA neurons results in a progressive decline in motor function.

The motor function of $HDAC4^{M1\text{-}L285}$ flies declined more slowly than HDAC4-expressing flies. While *HDAC4* and *SNCA* expressing flies showed a significant decline by 16 days, it took 28 days for flies expressing $HDAC4^{M1\text{-}L285}$ to do so. After 28 days, $HDAC4^{M1\text{-}L285}$ flies showed similar motor decline to α-synuclein and HDAC4 flies and declined faster than w^{1118} control flies over the course of the assay. This suggests that the truncated protein does impair normal locomotor function, but at a slower rate.

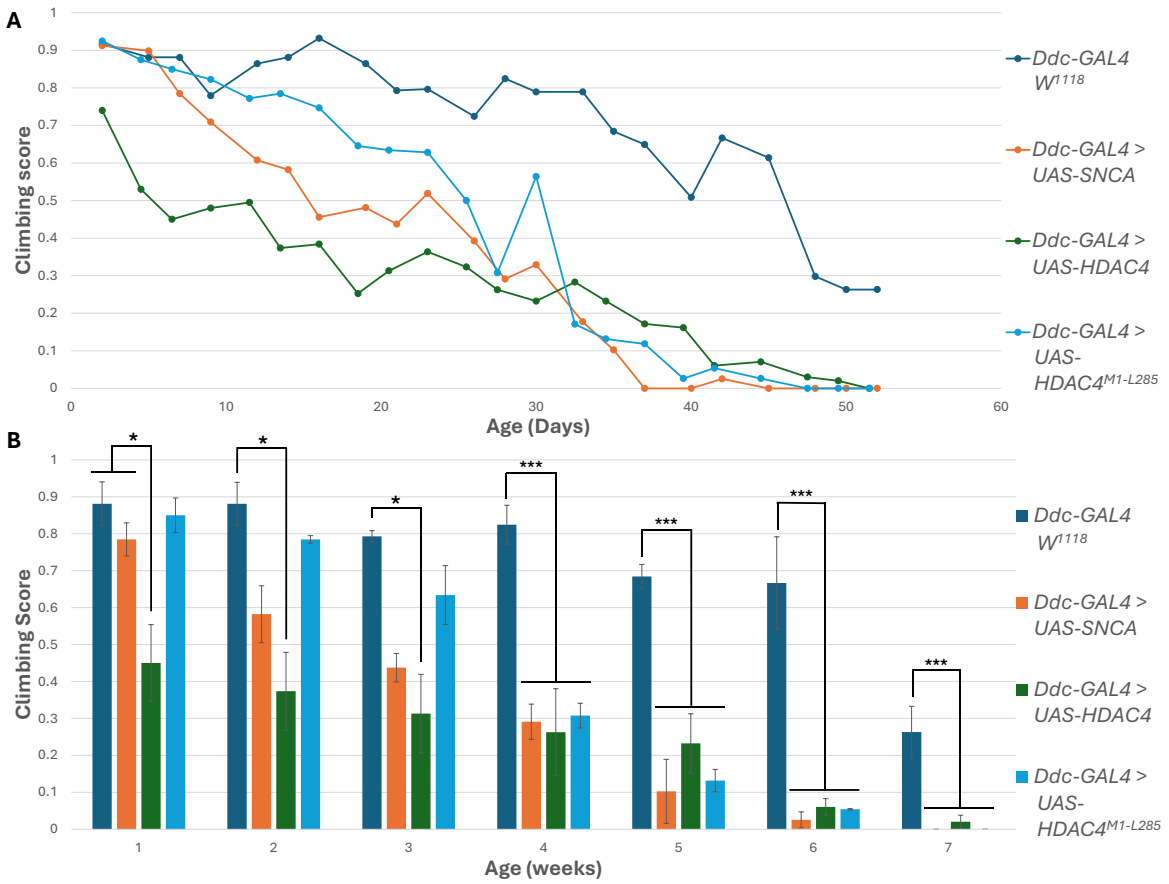

Figure 3.15 - Assessment of climbing defects induced by *SNCA* and HDAC4

Testing motor function of *Ddc-GAL4 CS, Ddc-GAL4>UAS-SNCA, Ddc-GAL4>UAS-HDAC4WT, and Ddc-GAL4>UAS-HDAC4M1-L285* flies over 52 days. Data is shown both via a line graph over days (A) and a bar graph of motor function at each week (B). Climbing score = the percentage of flies climbed above 5cm in 10 seconds. Error bars indicate mean ± standard error of the mean. w^{1118} = wildtype strain. (one-way ANOVA, Week 1: $F(3,12) = 5.7199$, $p = 0.0115$, Week 2: $F(3,12) = 6.0479$, $p = 0.0095$, Week 3: $F(3,12) = 5.2112$, $p = 0.0156$, Week 4: $F(3,12) = 7.0086$, $p = 0.0056$, Week 5: $F(3,12) = 9.7372$, $p = 0.0015$, Week 6: $F(3,12) = 25.371$, $p = 2x10^{-5}$, Week 7: $F(3,12) = 13.931$, $p = 0.00032$. Post-hoc Tukey's HSD, $p<0.5$ = *, $p<0.1$ = **, $p<0.01$ = ***).

3.2 CHARACTERISATION OF EXPRESSION OF HDAC4, MEF2 AND A-SYNUCLEIN IN DA NEURONS

3.2.1 Characterisation of the distribution of HDAC4 and α-synuclein *in Kenyon cells of the mushroom body*

Next, the impact of α-synuclein on HDAC4 distribution was investigated. α-synuclein has been shown to dysregulate HDAC4 nuclear localisation, promoting neurotoxicity (Kontopoulos et al., 2006). Induced pluripotent stem cell (iPSC)-derived DA neurons from PD patients exhibited HDAC4 mislocalisation to the nucleus, leading to dysregulated gene expression, and downregulation of neuronal development and synaptic activity genes (Lang et al., 2019).

HDAC4 displays a relatively heterogeneous subcellular distribution in many neuronal subtypes, and its distribution in DA neurons has not yet been characterised. Changes in HDAC4 subcellular distribution have, however, been thoroughly characterised in this laboratory in the KCs of the MB. Increased nuclear accumulation of HDAC4 results in an increase in the size of condensates in the nucleus in a dose-dependent manner, as a result of coalescence or smaller condensates as the concentration of HDAC4 increases (Hawley et al., 2025). For these reasons, the distribution of HDAC4 was first examined in KCs to determine whether it was altered in the presence of α-synuclein.

The *OK107-GAL4* driver promotes expression in KCs (Connolly et al., 1996). Virgin *OK107-GAL4* females were crossed to males for expression of either α-synuclein or HDAC4, or both together. HDAC4 condensates were observed in brains of flies expressing HDAC4 alone, as well as HDAC4 and α-synuclein, however, the brains expressing both HDAC4 and α-synuclein appeared to have fewer condensates per cell, but they appeared larger than in HDAC4-only brains (Figure 3.16). A small number of aggresomes were also seen in HDAC4/α-synuclein brains, which have been previously observed when the levels of nuclear HDAC4 reach a specific threshold (Hawley, 2024). This suggests that the presence of α-synuclein results in nuclear accumulation of HDAC4 and leads to the hypothesis that HDAC4 dysregulation may contribute to neurodegenerative processes. This interpretation is based on observation thus far as the number of condensates has yet to be quantified. The WT distribution

of HDAC4 in DA neurons is still to be assessed, as is whether the presence of α-synuclein alters its distribution. This experiment was attempted, however the co-expression of α-synuclein and HDAC4 in DA neurons was lethal.

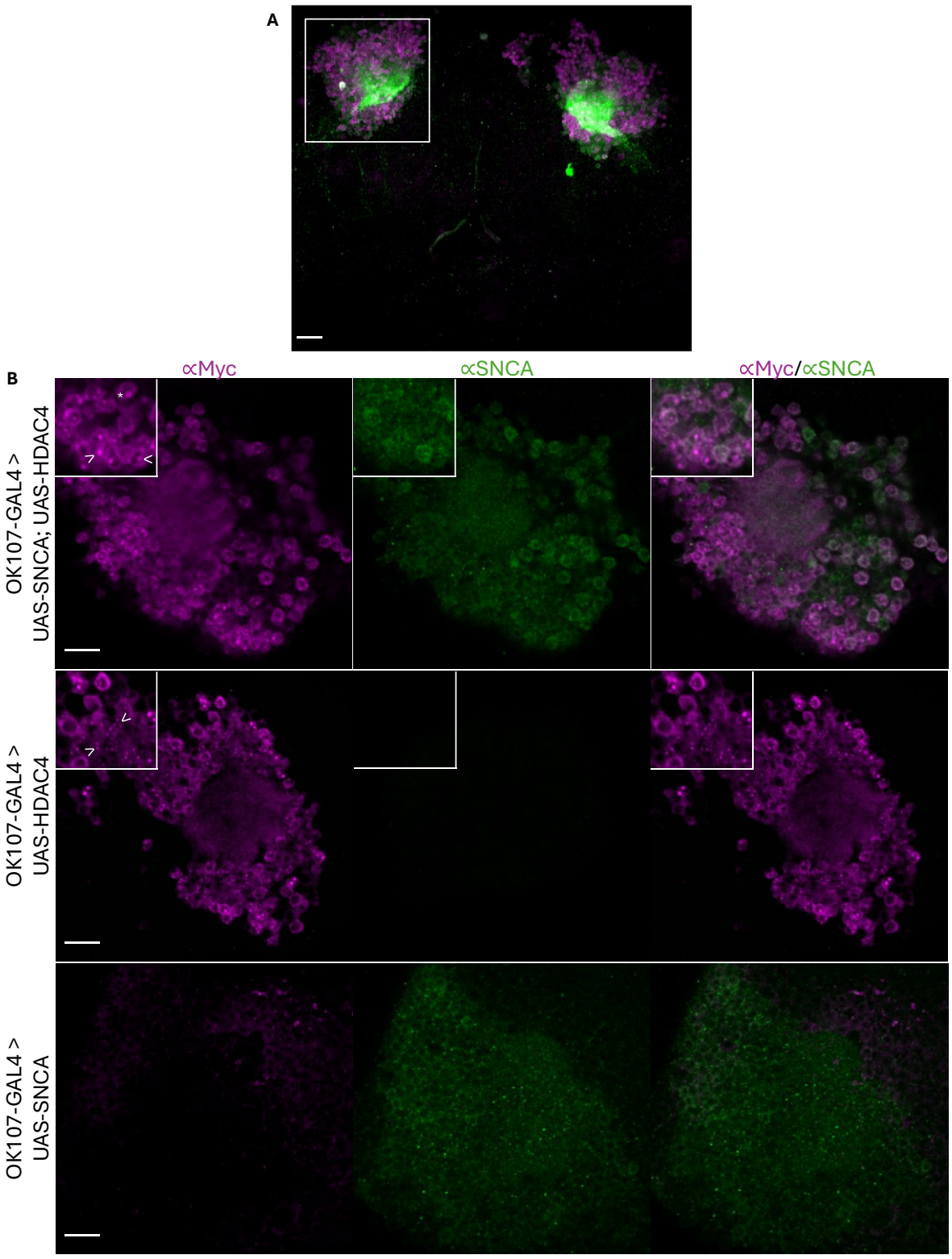

Figure 3.16 – Characterisation of HDAC4 and α-synuclein distribution in Kenyon cells

Figure 3.17 (cont.) – Characterisation of HDAC4 and α-synuclein distribution in Kenyon cells

(A) *OK107-GAL4 > UAS-SNCA; UAS-HDAC4^{WT}* brains following immunohistochemistry anti-Myc at 1:250 dilution (magenta) and anti-*SNCA* (green) at 1:200 dilution. White box indicates Kenyon cells and Calyx imaged in (B). Scale bar = 20 μm. **(B)** Snapshots of Kenyon cells of a whole mount brains expressing *UAS-SNCA; UAS-HDAC4, UAS-HDAC4,* or *UAS-SNCA* under the *OK107-GAL4* driver. Immunohistochemistry was done with anti-Myc at 1:250 dilution (magenta) and anti-*SNCA* (green) at 1:200 dilution. Inset shows enlarged section to highlight HDAC4 condensates. Arrowheads point to enlarged condensates in Kenyon cells expressing α-synuclein and HDAC4, and smaller condensates in Kenyon cells expressing HDAC4 only. Asterisk shows the presence of an aggresome, which forms as a cellular response to aggregated protein, identified by ring shaped condensates with a hollow core. Scale bar = 10 μm.

3.2.2 Characterising expression and distribution of SNCA and HDAC4 rescue constructs in motor neurons

To determine whether reduced expression or nuclear accumulation of HDAC4 can decrease the α-synuclein-mediated neurodegeneration resulting, fly lines were generated in which *UAS-SNCA* was combined with *UAS-HDAC4^{WT}* as well as *UAS-HDAC4^{F65A}, UAS-HDAC4$^{M1-L285}$, UAS-HDAC4 RNAi*, and *UAS-CD8::GFP* as a control. HDAC4^{F65A} is a mutant with a reduced capacity to oligomerise. It is hypothesised that HDAC4^{F65A} would bind endogenous HDAC4, which would lead to decreased efficiency of endogenous HDAC4 oligomerisation. This would lead to decreased nuclear entry of HDAC4, since oligomerisation is required for MEF2-dependent nuclear entry. HDAC4$^{M1-L285}$ contains only the N-terminal 285 amino acids of HDAC4, which includes the oligomerisation domain and MEF2 binding site. This mutant localises to the nucleus where it binds MEF2 (Hawley, 2024). It is hypothesised that HDAC4$^{M1-L285}$ will titrate MEF2, preventing endogenous HDAC4 from binding. This will prevent nuclear entry of HDAC4, as this requires its binding to MEF2. As HDAC4^{F65A} disrupts oligomerisation, HDAC4$^{M1-L285}$ reduces MEF2 binding, and HDAC4 RNAi reduces *HDAC4* expression, one or more of these constructs may rescue the deficits observed from α-synuclein expression (Section 1.3.4; Section 1.4.2). For simplicity, these will hereafter be referred to as the "rescue constructs". Firstly, the expression of these new constructs was confirmed by crossing *Ddc-GAL4* virgin females to flies carrying the following transgene combinations: 1. *UAS-SNCA; UAS-HDAC4^{WT}*, 2. *UAS-SNCA; UAS-HDAC4$^{M1-L285}$*, 3. *UAS-SNCA; UAS-HDAC4^{F65A}*, 4. *UAS-SNCA; UAS-RNAi*, and 5. *UAS-SNCA; UAS-GFP* and then assessing expression in brains of progeny via immunohistochemistry. α-synuclein was detected in all lines, along with GFP, HDAC4^{F65A}, and HDAC4$^{M1-L285}$ (Figure 3.17). There is not an available antibody that detects endogenous HDAC4 via immunohistochemistry, therefore, knockdown of HDAC4 could not be confirmed; however, this RNAi line was previously validated in our lab, in which it decreased HDAC4 by approximately 50% via western blotting (Fitzsimons et al., 2013).

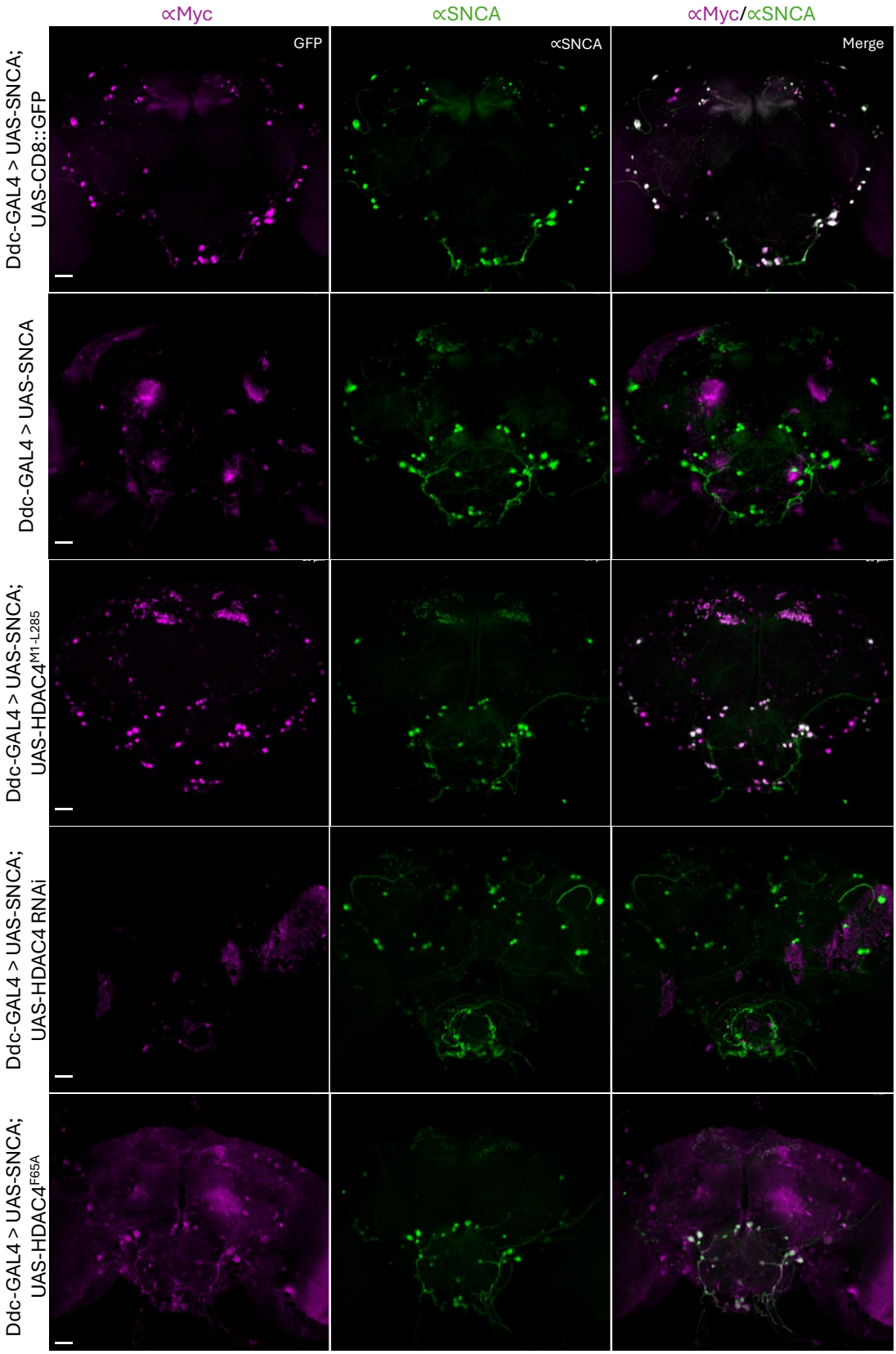
∝Myc
∝SNCA
∝Myc/∝SNCA
GFP
∝SNCA
Merge
Ddc-GAL4 > UAS-SNCA; UAS-CD8::GFP
Ddc-GAL4 > UAS-SNCA
Ddc-GAL4 > UAS-SNCA; UAS-HDAC4M1-L285
Ddc-GAL4 > UAS-SNCA; UAS-HDAC4 RNAi
Ddc-GAL4 > UAS-SNCA; UAS-HDAC4F65A

Figure 3.18 - Confirmation of expression of α-synuclein and the rescue constructs

Maximum projections of whole mount brains co-expressing SNCA and CD8::GFP or rescue constructs (HDAC4^{F65A}, HDAC4$^{M1\text{-}L285}$, or HDAC4 RNAi). Immunohistochemistry was done with anti-Myc at 1:250 dilution (magenta) and anti-SNCA at 1:200 dilution (green). Scale bar = 20 μm.

3.3 DETERMINATION OF WHETHER DISRUPTION OF HDAC4 OLIGOMERISATION, MEF2 BINDING, OR REDUCED EXPRESSION OF HDAC4 ARE PROTECTIVE IN THE A-SYNUCLEIN PD MODEL

3.3.1 Assessment of climbing deficits induced by co-expressing α-synuclein and HDAC4 rescue constructs

After the co-expression of α-synuclein and the rescue constructs was confirmed, the motor function of flies expressing these constructs was then assessed and compared to α-synuclein expression alone. The rate of climbing decline in flies expressing the rescue constructs in DA neurons was carried out to determine whether disrupting HDAC4 could improve motor function seen in the PD model. Expression of α-synuclein significantly impaired climbing at 4 and 6 weeks and the climbing ability of all rescue constructs declined at a similar rate to α-synuclein expression only (Figure 3.18). The lack of improvement in climbing ability indicates that strategies to decrease nuclear accumulation of HDAC4, or total HDAC4 levels were not therapeutic. The co-expression of α-synuclein and GFP expression resulted in a consistently slower decline in motor function than *SNCA* alone. This control was included to account for the expression of a second UAS-linked transgene, and the slower decline suggests that the amount of GAL4 may have been limiting, therefore possibly reducing expression of α-synuclein when *UAS-CD8::GFP* was also present.

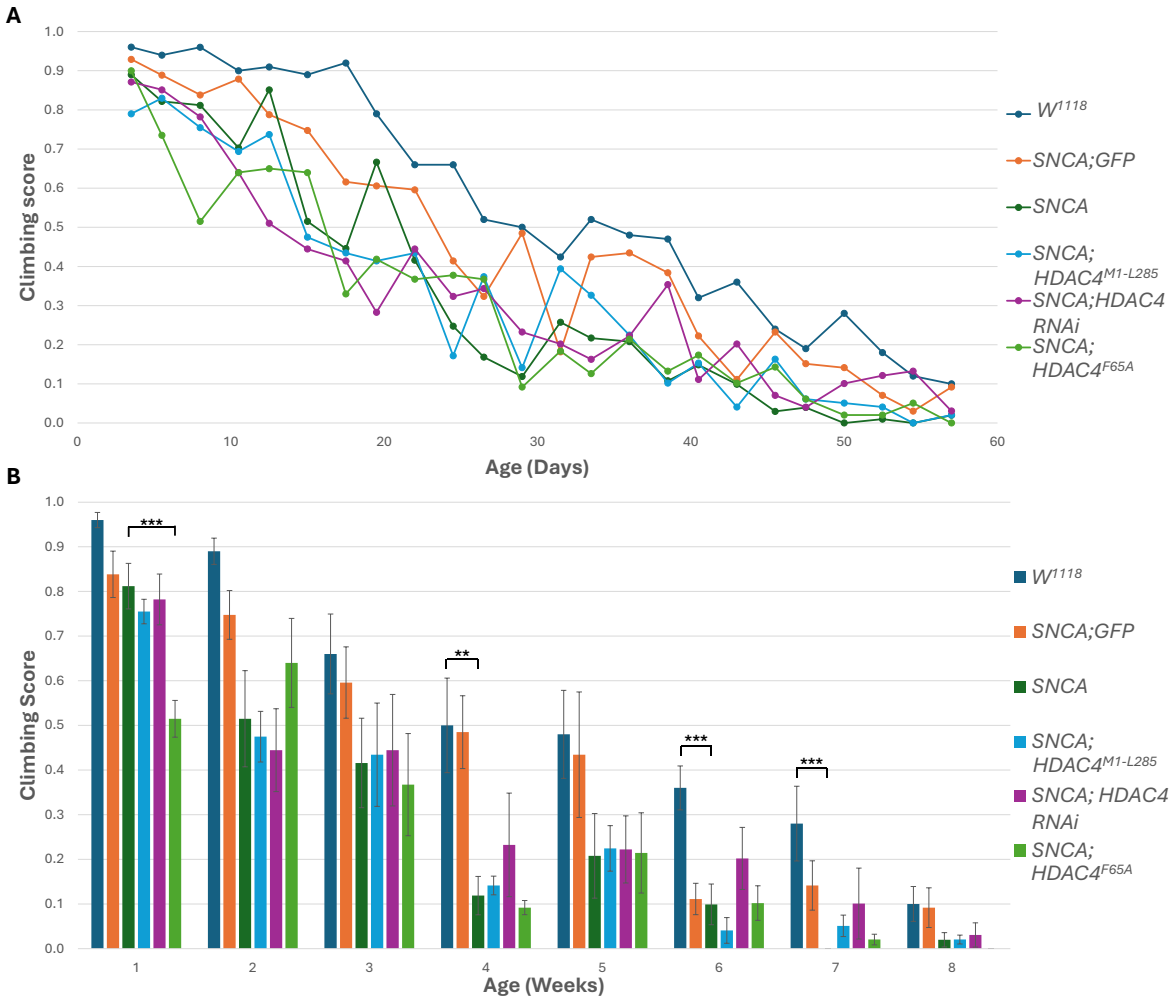

Figure 3.19 - Assessment of climbing deficits induced by co-expressing SNCA and HDAC4 rescue constructs.

Assessment of the motor function of *SNCA* co-expressed with HDAC4 rescue constructs (HDAC4 M1-L285, HDAC4 RNAi and HDAC4 F65A) via a negative geotaxis assay. 100 flies of each genotype were tested over 50 days. Data is shown both via a line graph over days (A) and a bar graph of motor function at each week (B). Climbing score = the percentage of flies climbed above 5cm in 10 seconds. Error bars indicate mean ± standard error of the mean. w^{1118} = control strain. (one-way ANOVA, Week 1: $F(5,29) = 8.7236$, $p = 3.867 \times 10^{-5}$, Week 2: $F(5,29) = 3.975$, $p = 0.00722$, Week 3: $F(5,29) = 1.2162$, $p = 0.3266$, Week 4: $F(5,29) = 4.762$, $p = 0.0027$, Week 5: $F(5,29) = 1.6019$, $p = 0.191$, Week 6; $F(5,29) = 5.2787$, $p = 0.0014$, Week 7: $F(5,29) = 3.8143$, $p = 0.0089$, Week 8: $F(5,29) = 1.7759$, $p = 0.1492$. Post-hoc Tukey's HSD, $p<0.5$ = *, $p<0.1$ = **, $p<0.01$ = ***).

3.3.2 Assessment of neurodegeneration induced by co-expressing SNCA and HDAC4 rescue constructs

To evaluate age-dependent neurodegeneration, TH fluorescence intensity was measured in DA neurons in brains of flies of the same genotypes as the climbing assay, at day 1 and day 42 post-eclosion (Figure 3.19). Previous studies have shown that α-synuclein expression causes progressive DA neuron loss from around 28–30 days of age, while WT flies show stable TH levels over time (Chen et al., 2009; Liu et al., 2022; Mohite et al., 2018; White et al., 2010). Brains expressing α-synuclein alone showed relatively low TH fluorescence at both day 1 and day 42 (Figure 3.19; Figure 3.20). This suggests that developmental α-synuclein expression can impact DA neuron integrity and PD-like phenotypes in *Drosophila* requires high α-synuclein expression levels. Co-expression of the rescue constructs with α-synuclein did not improve TH levels at day 42; instead, all combinations exhibited a significant reduction in TH intensity compared to day 1, consistent with substantial neurodegeneration. (Figure 3.19; Figure 3.20). In agreement with the climbing assay data, flies co-expressing α-synuclein and GFP had consistently higher TH levels than α-synuclein alone at both timepoints. Overall, the data show that strategies designed to decrease nuclear HDAC4 or total HDAC4 did not rescue α-synuclein-mediated DA neurodegeneration and instead may exacerbate it, suggesting a potential requirement for endogenous HDAC4 in maintaining DA neuron health and motor function.

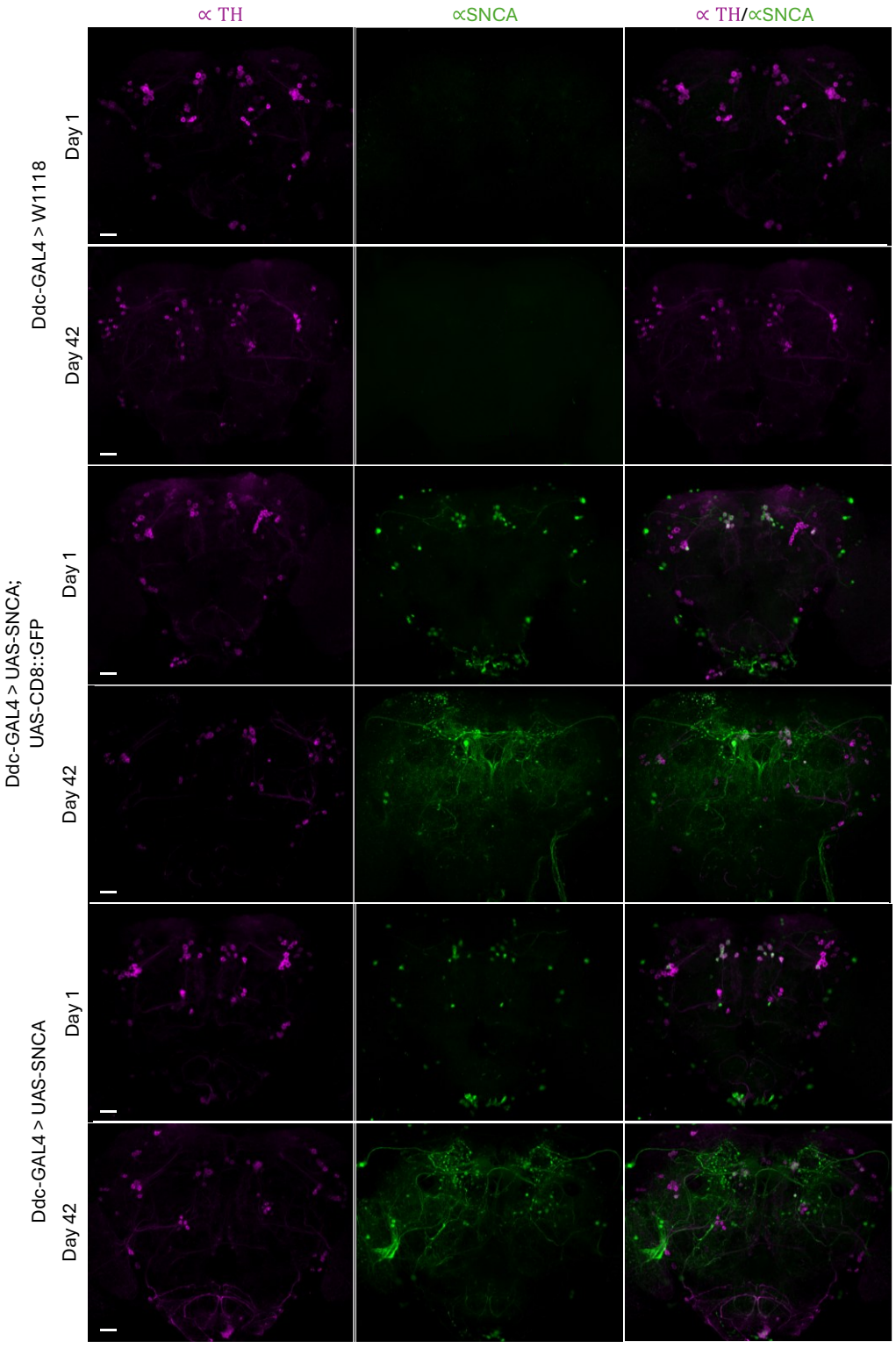

Figure 3.20 - Assessment of neurodegeneration induced by co-expressing *SNCA* and HDAC4 rescue constructs

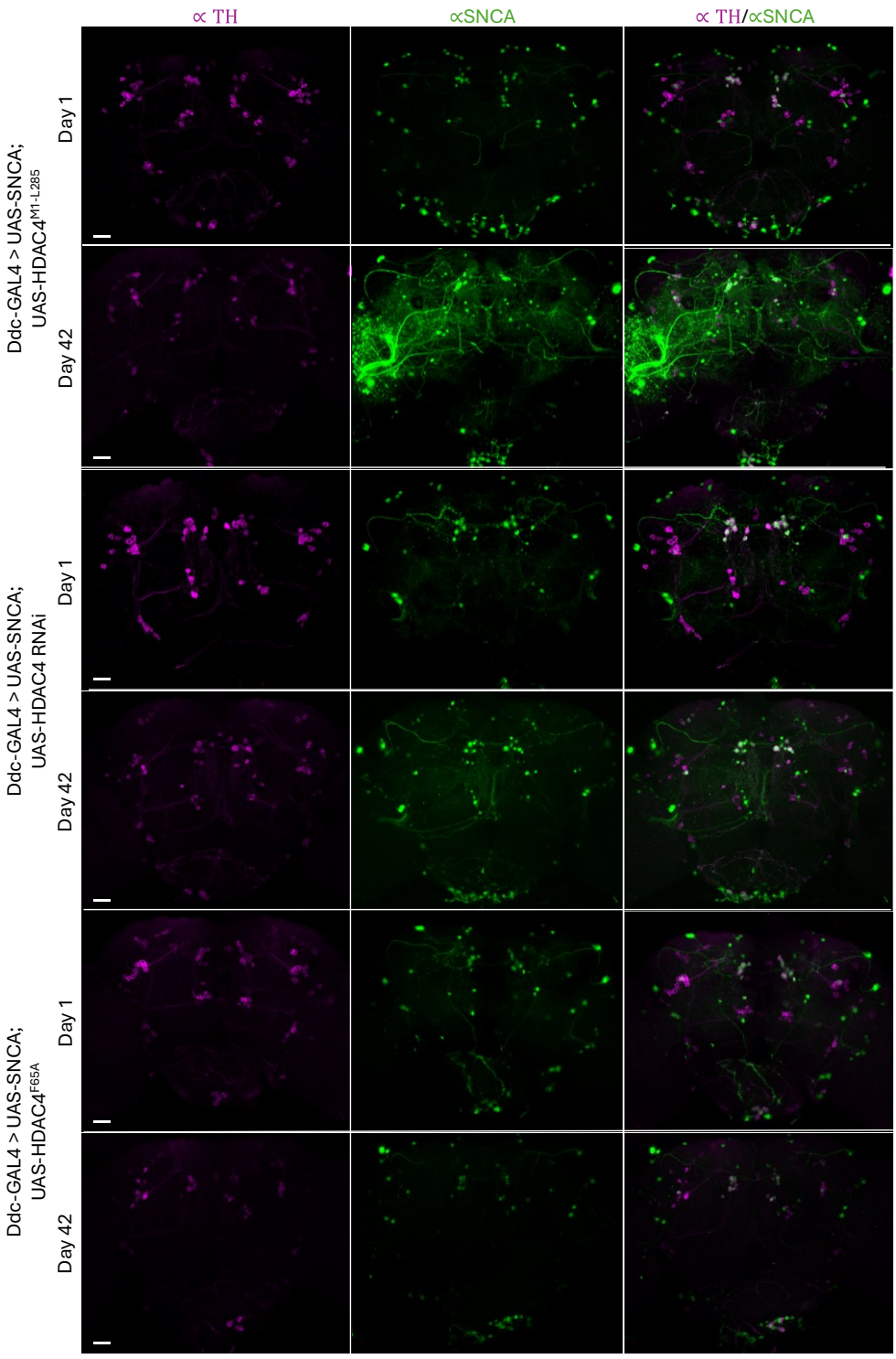

Figure 3.19 (cont.) - Assessment of neurodegeneration induced by co-expressing SNCA and HDAC4 rescue constructs in *Drosophila*

Figure 3.19 (cont.) - Assessment of neurodegeneration induced by co-expressing SNCA and HDAC4 rescue constructs in Drosophila

Maximum projections of whole mount brains expressing *UAS-SNCA*, along with *UAS-CD8::GFP, UAS-HDAC4*$^{M1\text{-}L285}$*, UAS-HDAC4 RNAi,* or *UAS_HDAC4*^{F65A} with the *Ddc-GAL4* driver. Brains were imaged at 1 day (or 42 days) post eclosion following immnohistochemistry with anti-TH at 1:250 dilution (magenta) and anti-*SNCA* at 1:200 dilution (green). w^{1118} = control strain. Scale bar = 20 µm.

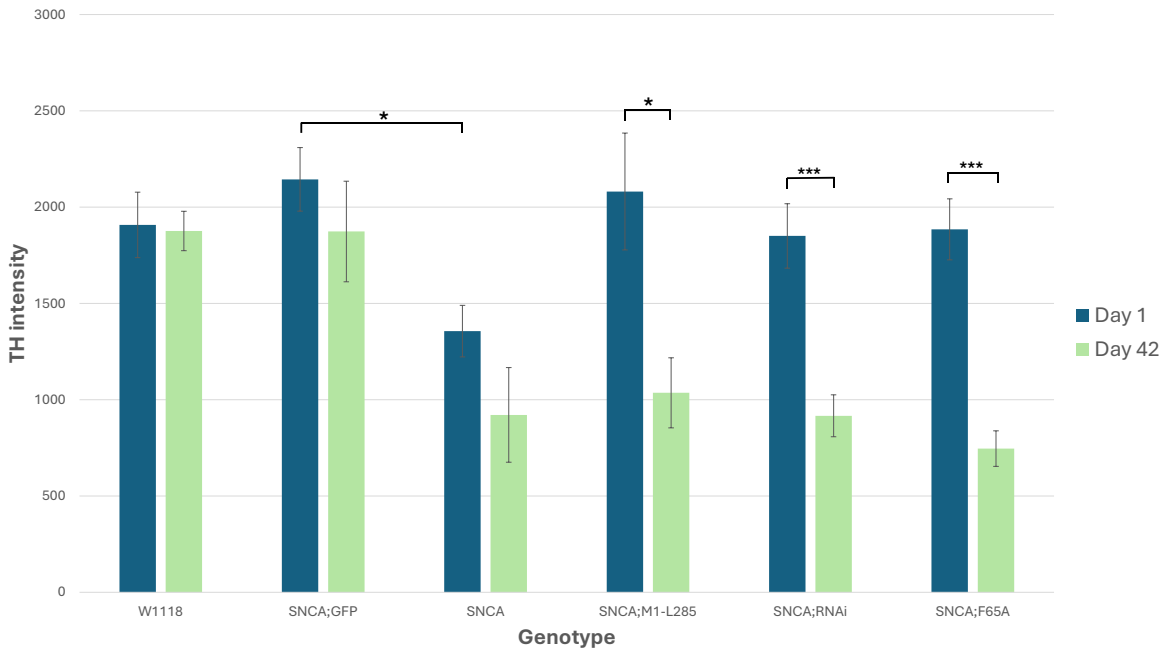

Figure 3.21 - Measurement of TH fluorescence of 1-day and 42-day old brains co-expressing SNCA and HDAC4 rescue constructs

Measurement of TH fluorescence intensity of brains 1 day (or 42 days) post eclosion that are co-expressing SNCA with HDAC4 rescue constructs (HDAC4$^{M1\text{-}L285}$, HDAC4 RNAi and HDAC4^{F65A}) as an assessment of neurodegeneration. Error bars indicate mean ± standard error of the mean. (Unpaired t-test, * $p < 0.05$, ** $p < 0.01$, *** $p < 0.001$).

4 DISCUSSION AND FUTURE DIRECTIONS

A *Drosophila* model of PD, involving the expression of human α-synuclein in DA neurons, was validated in this study to result in a significant and progressive deficit in locomotor function, along with degeneration of DA neurons. This model can be used for future research in this laboratory to investigate the pathological effects of α-synuclein further.

Both *HDAC4* and *MEF2* were determined to be expressed in DA neurons in *Drosophila*. Preliminary investigations revealed that, in the presence of α-synuclein in KCs, HDAC4 becomes more nuclear, forming large condensates, indicating that its distribution was disrupted. This mirrors findings in a rodent model of PD and in human iPSCs derived from human PD patients, although similar changes in *Drosophila* DA neurons have not yet been confirmed.

Furthermore, increased expression of *HDAC4* in *Drosophila* DA neurons led to a progressive decline in motor function, suggesting that dysregulation of HDAC4 may contribute to PD-related neurodegeneration. Together, these findings support the use of this *Drosophila* model to investigate the relative roles of HDAC4 and MEF2 in the pathogenesis of PD.

However, reducing *HDAC4* expression or employing strategies to reduce its nuclear distribution did not improve motor function or increase survival of DA neurons. Further research is required to understand the direct interaction of MEF2 and HDAC4 fully, and to determine whether this interaction plays an important role in the progression of PD.

4.1 EXPRESSION OF CODON OPTIMISED *SNCA* RESULTS IN PD-LIKE PHENOTYPES

Previous studies have demonstrated the changes in motor function, lifespan, neuronal function, and cellular function in *Drosophila* upon expression of human α-synuclein. However, literature review reveals that the phenotypes vary greatly depending on the specific *SNCA* transgene expressed and the selection of the driver (Table 2.1). Because of these inconsistencies, it was important to validate a model of PD in our laboratory, prior to testing therapeutic strategies. The level and distribution of α-synuclein expression were important to consider; therefore, multiple GAL4 drivers and α-synuclein-expressing constructs were compared. *nSyb-GAL4*, *elav-GAL4*, and *Ddc-GAL4* are the most common drivers that have been used to express WT human α-synuclein for assessing neurodegeneration and motor function in PD models (Table 2.1); therefore, they were directly compared in this study. *nSyb-GAL4* and *elav-GAL4* both drove pan-neuronal expression in the brain. However, with both drivers, very low α-synuclein expression was detected in most neurons (Figure 3.6) and the decline of motor function was also insignificant. Other studies have shown that the expression of WT α-synuclein does not result in significant retinal degeneration, motor function decline, or neurodegeneration (Karpinar et al., 2009; Pesah, 2005). Interestingly, some studies observed a significant change in some but not all of these phenotypes. Jahromi et al. (2021) observed neurodegeneration and a climbing deficit when WT α-synuclein was expressed with *Ddc-GAL4*, but there was no significant decrease in longevity with *elav-GAL4*. Sakai et al. (2019) demonstrated no significant retinal degeneration but showed that expression of WT α-synuclein resulted in a progressive decline in motor function when driven with *nSyb-GAL4*. One study did show consistent results, with a decline in climbing ability, retinal degeneration, and neurodegeneration (Feany & Bender, 2000). Interestingly, Liu et al. (2022) showed expression of WT α-synuclein in DA neurons exhibited no significant neurodegeneration, nor decreased motor function or survival, but when WT α-synuclein was expressed in the intestine there was a large change in all these phenotypes.

Confounding the lack of a significant decline in climbing was the fact that the WT *CS* strain that was used as a control also displayed an unexpected rapid decline in climbing ability

compared to our previous studies and to the literature (Haywood & Staveley, 2004; Pesah, 2005; Sakai et al., 2019), indicating reduced physiological vigour. These issues were subsequently addressed by outcrossing all transgenic lines into the WT w^{1118} control strain, which maintained normal climbing activity, and obtaining a fly line carrying *UAS-SNCA*^{WT} that had been codon optimised for expression in *Drosophila*.

It was also noticed that the flies had inadvertently been placed under constant light, rather than the standard 12h:12h light-dark cycle. Control *nSyb-GAL4* flies exhibited a slow decrease in motor function over 25 days, followed by a very sharp decline in motor function, whereas under a 12h:12h light-dark cycle, the same genotype displayed a much more consistent decline. Constant light conditions can disrupt circadian rhythms and locomotor function in *Drosophila*, abolishing normal rhythmic patterns and resulting in arrhythmic behaviour. Initially, flies may exhibit hyperactivity, but this is often followed by random or dampened movements, leading to a sharp reduction in activity (Cho et al., 2016; Dunlap, 1999; Konopka et al., 1989; Leloup & Goldbeter, 2000; Tataroglu & Emery, 2014). Neurons that regulate circadian locomotor activity rely on light information to maintain rhythmicity, and when flies are placed in constant light, both morning and evening peaks in activity disappear (Tataroglu & Emery, 2014). This highlights the potential influence constant light had on the *nSyb-GAL4* and *CS* flies in Figure 3.2

Codon optimisation of WT α-synuclein has been previously shown to result in a higher level of expression, and this has been associated with retinal degeneration, motor function decline, and degeneration of PPM1/2 and PPL1 DA neurons (Chouhan et al., 2016; Narwal et al., 2024). A fly line for expression of codon-optimised α-synuclein was therefore obtained, which resulted in significantly increased expression driven by *Ddc-GAL4*, and a progressive decline in locomotor function. Neurodegeneration, as shown by the level of TH in neurons, was assessed, which revealed a small decrease in staining of PPM1, PPM2, PPL1, and PPL2 neurons in 30-day-old flies compared to 1-day-old flies, suggesting the higher expression from codon-optimised α-synuclein resulted in neurodegeneration. This change was not quantified, and a small sample size was tested; therefore, further testing and quantification are required to confirm neurodegeneration in these clusters. It was questioned whether 30 days was enough time to observe significant neurodegeneration; however, multiple studies observe

neurodegeneration after 21 – 30 days (Agostini et al., 2023; Mohite et al., 2018; Trinh et al., 2008). Together, this data indicates that expressing codon-optimised α-synuclein with *Ddc-GAL4* results in α-synuclein-mediated dysfunction via degeneration of DA neurons with an associated decline in motor function, and therefore, this model could be used to test therapeutic strategies.

4.2 HDAC4 AND MEF2 ARE EXPRESSED IN *DROSOPHILA* DA NEURONS, AND INCREASED HDAC4 IMPAIRS LOCOMOTOR FUNCTION

Previous studies have investigated the roles of HDAC4 and MEF2 in mammalian models of PD, and both nuclear accumulation of HDAC4 and altered expression of MEF2 have been associated with PD (Section 1.3.4 and 1.4.2). HDAC4 has also been studied in developmental contexts in *Drosophila*, in which its nuclear accumulation impairs neurodevelopment, long-term memory, and mushroom body (MB) morphogenesis (Main et al., 2021; Tan et al., 2024). Moreover, these HDAC4-induced developmental defects in the MB are dependent on the presence of MEF2, confirmed through the expression of $HDAC4^{M1\text{-}L285}$, which prevented nuclear accumulation of HDAC4 and decreased MB defects (Section 1.4.2). *HDAC4* and *MEF2* expression were examined in relation to DA neurons to assess potential spatial overlap. Due to the lack of a reliable antibody for detecting endogenous HDAC4 in *Drosophila* tissue, expression was visualised using the *NP3588-GAL4* driver, which drives UAS-dependent expression in HDAC4-expressing cells. Future studies would instead aim to validate and refine these findings using either a specific anti-HDAC4 antibody or the HDAC4::GFP protein trap line, in which GFP is inserted in-frame within the endogenous HDAC4 locus to allow direct visualisation of the protein (Fitzsimons et al., 2013; Knowles-Barley et al., 2010). Visualisation revealed that *HDAC4* expression was strongest in KCs, where signal intensity was high enough to cause oversaturation, making it difficult to detect *HDAC4* expression in other brain regions. Despite this, partial co-localisation with tyrosine hydroxylase DA neurons was observed across multiple clusters, including PPL2, PPM3, PPL1, and PPM1/2. These clusters are known to undergo degeneration in *Drosophila* models of PD (Table 2.1), suggesting that HDAC4 may play a role in DA neuron vulnerability and the progression of PD-related pathology in this

model. As anti-TH and anti-MEF2 antibodies both required rabbit secondary antibodies, MEF2 was instead compared to *Ddc-GAL4* driving CD8::GFP. Detection of endogenous MEF2 showed more widespread expression, including expression in *Ddc-GAL4*-driven cells. These data show that both are expressed in the same neurons; however, more information about the subcellular distribution of HDAC4 was required. This was examined in subsequent experiments, where WT *HDAC4* was expressed.

Expression of WT *Drosophila HDAC4* resulted in a significant impairment in climbing ability. This motor function deficit is likely due to increased nuclear HDAC4, as nuclear accumulation is observed in human iPSCs derived from human patients and leads to dysregulated gene expression (Lang et al., 2019). This result fits in with other animal models where increased nuclear HDAC4 is observed. Wu et al. (2017) showed HDAC4 is typically localised in the cytoplasm and when mice DA neuron cell cultures and PC12 cells expressing α-synuclein^{A53T} are treated with MPP^+, it accumulates in the nucleus, correlating with altered gene expression patterns, impaired neuronal function, neuronal toxicity, and cell death. The results presented here confirm *HDAC4* overexpression may have a toxic effect; however, this requires further research to determine the mechanism by which HDAC4 is impairing motor functions, and whether it is attributable to the nuclear activity of HDAC4. This could include expressing mutants that restrict HDAC4 to the nucleus (HDAC4^{3SA}), or the cytoplasm (HDAC4$^{\Delta MEF2}$), and measuring the motor function of these flies to compare to *HDAC4* overexpression (Cohen et al., 2007; Hawley et al., 2025).

Both *HDAC4* and *MEF2* expression were observed in TH-positive DA neurons, and further investigation revealed that increased WT HDAC4 results in impaired climbing ability. This aligns with findings in mammalian PD models and suggests that elevated nuclear HDAC4 may contribute to motor deficits and DA neuron vulnerability in the α-synuclein model of PD.

4.3 REGULATION OF HDAC4 DISTRIBUTION BY A-SYNUCLEIN

To evaluate whether α-synuclein expression influences the subcellular localisation of HDAC4, both proteins were co-expressed in *Drosophila* neurons. This aimed to determine whether α-synuclein induces a shift of HDAC4 from the cytoplasm to the nucleus, as observed in mammalian PD models (Wang et al., 2023; Wu et al., 2017). Demonstrating a change in distribution would strengthen the validity of this *Drosophila* model for investigating the role of HDAC4 in PD. This was first examined in KCs, which are the intrinsic neurons of the MB (Section 1.5.2). Previous research in this laboratory has thoroughly characterised the nuclear-cytoplasmic distribution of WT HDAC4 in KCs, and alterations in distribution (such as resulting from overexpression or knockdown of *MEF2*) can be measured in these cells (Main, 2019). Previous HDAC4 characterisation in KCs makes it suitable for analysing the effect α-synuclein may have.

It was determined that HDAC4 distribution shifted towards nuclear accumulation when α-synuclein was co-expressed. *HDAC4* expression alone resulted in small nuclear condensates, with cytoplasmic halos around the nuclei indicating cytoplasmic distribution as well. α-synuclein co-expression resulted in fewer but much larger HDAC4 condensates in the nucleus, with less in the cytoplasm. It appears that α-synuclein may have localised more to the axons around the KCs when solely expressed and shifted more towards the KCs with *HDAC4* expression. An analysis of HDAC4 distribution in the presence of α-synuclein in DA neurons could not be performed as co-expression was toxic, resulting in no adult progeny.

More research is still required to determine whether nuclear accumulation of HDAC4 increases vulnerability in PD. This could potentially occur through multiple interrelated mechanisms that involve transcriptional repression, synaptic dysfunction, and/or impaired stress responses. HDAC4 nuclear localisation causes repression of pro-survival transcription factors such as MEF2 and CREB, in turn repressing MEF2 and CREB-dependent transcription, accelerating cell death (Bolger & Yao, 2005). HDAC4 also silences neuroprotective genes by acting as a co-repressor with NCoR/SMRT complexes, contributing to global transcriptional repression, which can compromise neuronal stress responses under pathological conditions such as α-synuclein accumulation (Wu et al., 2017; Yang et al., 2011). While it is understood that

HDAC4 is likely dysregulating gene expression, further research is required to understand the mechanism behind the dysregulation.

4.4 ALTERING HDAC4 DISTRIBUTION DOES NOT RESCUE THE DEFICITS INDUCED BY A-SYNUCLEIN EXPRESSION IN DA NEURONS

HDAC4 has been linked to PD in previous studies (El-Saiy et al., 2022; Lang et al., 2019; Takahashi-Fujigasaki & Fujigasaki, 2006; Wu et al., 2017), and our findings show that its overexpression impairs climbing ability. Moreover, it accumulates in the nucleus, forming larger condensates in the presence of α-synuclein. These data suggest that decreasing nuclear accumulation or condensation of HDAC4 may be therapeutic. Three strategies were employed: expression of an HDAC4 RNAi to reduce expression, expression of HDAC4$^{M1\text{-}L285}$ truncated protein that was shown to bind and titrate MEF2, preventing nuclear entry of HDAC4, and expression of HDAC4^{F65A}, a mutant with reduced capacity to oligomerise. It was hypothesised that HDAC4^{F65A} would bind endogenous HDAC4, leading to decreased oligomerisation. This would lead to decreased nuclear entry of HDAC4, since oligomerisation is required for MEF2-dependent nuclear entry (Hawley et al., 2025). The negative geotaxis assay results showed these constructs did not rescue the climbing deficit resulting from α-synuclein expression. At some time points, the RNAi-expressing flies appeared to have better climbing; however, the overall trajectory of motor decline remained indistinguishable from α-synuclein alone. While at least 100 flies were tested for each genotype in all climbing assays, 20 flies were allocated to each vial, making a sample size of only 5 per genotype. This small sample size may have resulted in an underestimation of significance. For a more accurate evaluation of significance, either a smaller number of flies per vial or more flies overall should be tested. Co-expression of GFP with α-synuclein unexpectedly improved the climbing deficit. This was employed to control for the presence of two UAS-driven constructs. If GAL4 is not in excess, then co-expressing a second transgene (in addition to α-synuclein) could result in less GAL4 available to bind *UAS-SNCA*, resulting in lower α-synuclein expression. If α-synuclein expression is reduced with an additional UAS construct, this would further confirm that the expression of

the HDAC4 rescue constructs is contributing to an even more severe phenotype. To investigate this, α-synuclein expression would be quantitatively measured.

The evaluation of neurodegeneration through measuring TH intensity of the brains expressing the rescue constructs further validates these results. WT, and α-synuclein; GFP brains did not show a significant decrease in TH levels between day 1 and day 42 brains; however, expressing the rescue constructs resulted in large reductions of TH. The TH intensity was lower at day 1 in α-synuclein expressing brains however this is not clear why. Consistent with the negative geotaxis assay results, co-expressing α-synuclein and GFP had consistently higher TH levels than α-synuclein alone and displayed no neurodegeneration, highlighting the possibility of decreased α-synuclein expression. If the decreased α-synuclein expression hypothesis is correct, this result would also validate the lack of PD phenotypes observed when WT human α-synuclein was expressed. It was shown that codon-optimised expression of *SNCA* was much higher than WT α-synuclein, supporting the hypothesis that the severity of PD-like phenotypes in *Drosophila* is sensitive to α-synuclein expression levels. The low TH intensity of day 1 brains suggests that developmental α-synuclein expression may impact DA neuron development, however this TH intensity measurement requires repetition to confirm if it is reproducible. This developmental sensitivity has not been explored in *Drosophila* but could explain the diversity in phenotypes reported across studies. Due to time constraints, more extensive quantification of neurodegeneration, such as analysing the number of TH neurons, likely caused an underestimation of significance. If time wasn't an issue, this limitation would have been addressed through measuring a larger quantity of brains and performing more extensive quantification. Taken together, these findings point to a complex interplay between α-synuclein expression, HDAC4 activity, and neuronal development and degeneration, where even subtle changes in protein levels or localisation may have significant consequences for neuronal survival and motor function.

Many studies suggest that inhibition of HDACs is neuroprotective (Li et al., 2021; Wang et al., 2023); however, one study found inhibiting HDACs exacerbated neurodegeneration (Harrison & Dexter, 2013). HDAC4 may be required in DA neurons for normal locomotor function, and its loss also results in a progressive decline in performance. Both increased and reduced HDAC4 impaired climbing ability, indicating neurons may require a fine balance of HDAC4

for normal function. HDAC4 could instead be contributing to PD progression indirectly through transcriptional regulation of autophagy and vesicle trafficking, neuronal function, stress responses, and gene expression patterns in ways that worsen α-synuclein toxicity, mitochondrial dysfunction, proteosome dysfunction, and neuroinflammation. Mitochondrial stress has been found to result in hyperacetylation and decreased levels of HDAC4, altering gene expression and contributing to DA neuron vulnerability in PD (Huang et al., 2024). Furthermore, single-cell sequencing of iPSC-derived DA neurons from idiopathic PD patients demonstrated elevated nuclear HDAC4 localisation can indirectly impair mitochondrial function via downregulation of HDAC4-controlled genes involving mitochondrial function and upregulation of ER stress genes (Lang et al., 2019). These studies establish a clear functional link between mitochondrial impairment and HDAC4 nuclear relocalisation in PD models, which can be explored further in *Drosophila*. Proteosome function could also be impaired by HDAC4 to exacerbate neurodegeneration in PD indirectly. HDAC4 has been implicated in impairing protein clearance pathways, particularly autophagy, contributing to the accumulation of misfolded proteins such as α-synuclein in models of PD (Ciechanover & Kwon, 2015; El-Saiy et al., 2022; Wang et al., 2023). While HDAC4 is known to act as a transcriptional repressor, direct regulation of proteasome gene expression by HDAC4 has not been demonstrated. Both mitochondrial and proteosome dysfunction in PD could also be caused by HDAC4 interacting with MEF2, causing MEF2 to contribute to neurodegeneration directly. Larger condensates may be overwhelming these quality control systems, contributing to the pathological effects of α-synuclein. As HDAC4 represses MEF2 in the nucleus, this changes gene expression through MEF2 (Wu et al., 2017). When MEF2 is repressed by HDAC4, these pathways are dysregulated, resulting in reduced Complex I activity, elevated reactive oxygen species, ATP depletion, and impaired clearance of toxic proteins like α-synuclein (She et al., 2011; Yang et al., 2009; Yao et al., 2012; Zhang et al., 2014). This is yet to be explored in the *Drosophila* model of PD.

4.5 FUTURE DIRECTIONS

Expression of codon optimised α-synuclein resulted in a significant climbing deficit and neurodegeneration of DA neurons, however further characterisation of this model is required. α-synuclein has previously been shown to form aggregates in *Drosophila* models (Agostini et al., 2023; Auluck et al., 2002; Chen & Feany, 2005); therefore, measuring insoluble α-synuclein accumulation and aggregation would provide further information on the effect of *SNCA* expression in *Drosophila*. A more extensive time course measuring the loss of TH in DA neurons would be beneficial to quantify the neurodegeneration caused by α-synuclein expression. As late-stage neurodegeneration has been shown to result in a 30% - 75% decrease in TH signal of affected neuronal clusters (Agostini et al., 2023; Auluck et al., 2005; Chen & Feany, 2005; Jahromi et al., 2021; Liu et al., 2022; Periquet et al., 2007), quantification would include comparing survival of DA neurons (via TH staining) between α-synuclein expressing and WT flies at 5–10-day intervals starting from 1-day post eclosion ranging to 60 days post eclosion. This would give significant insight into which neurons are most affected, at what age the neurons begin to degenerate and the extent at which TH signal is lost. To explore the effect of HDAC4 on mitochondrial and proteosome function, the PD model should incorporate relative assessments. Multiple markers for assessing mitochondrial function could be measured, such as reactive oxygen species, mitochondrial biogenesis markers such as PGC1α, or the MitoTimer- reporter gene, which measures mitochondrial biogenesis, stress, and degradation (Laker et al., 2014; Wu et al., 2024; Zhao et al., 2003). Proteosome function could also be measured through chymotrypsin-like proteasomal activity, or polyubiquitinated proteins (Fernández-Cruz et al., 2020; Ikeda et al., 2019; Tonoki et al., 2009).

The expression of *MEF2* in *Drosophila* DA neurons was confirmed in this research project; however, the role MEF2 potentially plays in the progression of PD was not studied further due to time constraints. MEF2 functions as a critical survival factor for DA neurons through transcriptional support of cell survival and mitochondrial function, in which disrupting MEF2's ability to regulate transcription makes neurons more vulnerable either directly or through Complex I dysfunction (She et al., 2011; Smith et al., 2006). Additionally, the analysis of the rat α-synuclein overexpression model found that levels of nuclear and cytoplasmic MEF2D were significantly decreased, correlating with reduced TH expression (Chu et al.,

2011). This suggests MEF2 may play a role in the progression of PD. The next step in understanding PD mechanisms in *Drosophila* is to investigate whether MEF2 activity is altered by α-synuclein expression and *HDAC4* overexpression. This could be assessed by examining MEF2-chromatin binding dynamics using chromatin immunoprecipitation followed by sequencing (ChIP-seq) (Furey, 2012), or by measuring transcriptional activity through a luciferase reporter assay in transgenic flies carrying a MEF2-responsive element linked to a luciferase gene (Caine et al., 2014; Lu et al., 2000a). These approaches would provide insight into whether α-synuclein and HDAC4 impair MEF2-mediated gene regulation in this PD model.

To better understand the role of HDAC4 in PD, it is important to examine its distribution in DA neurons and how this is altered when α-synuclein is present. Co-expression of *HDAC4* and *SNCA* in DA neurons with *Ddc-GAL4* resulted in no adult progeny, indicating developmental toxicity. *HDAC4* overexpression or nuclear accumulation impairs neural morphogenesis, eye development, and long-term memory when expressed during development (Fitzsimons et al., 2013; Main, 2019; Tan et al., 2024). As HDAC4 has been shown to accumulate in the nucleus when α-synuclein is expressed, it is likely causing defects in neuronal development, resulting in death before emerging as an adult. To circumvent this, the GAL80ts system can be used to express *HDAC4* and *SNCA* in DA neurons in adulthood only. In this system, the larvae and pupae would be raised at 18ºC, at which temperature GAL80 represses GAL4, and then moved to 25ºC after eclosion to induce adult-specific expression. This would also allow for the examination of the impact HDAC4 has on DA neurons, including the changes in gene expression, mitochondrial and proteosome function, and protein interactions important for these cellular functions. This could be compared with mutants that cause HDAC4 to accumulate in the nucleus, such as HDAC4^{3SA}, which contains three serine to alanine substitutions, preventing phosphorylation required for the nuclear export and causing HDAC4 to accumulate in the nucleus (Sando et al., 2012).

Due to time constraints, the HDAC4 rescue constructs were only assessed in the presence of α-synuclein. Given that they appeared to worsen the α-synuclein-induced climbing phenotype, assessing their individual impacts on climbing and DA neuron survival would provide further understanding of the results seen in Figure 3.18. The role of HDAC4 in DA neurons in

Drosophila has not yet been investigated. HDAC4$^{M1\text{-}L285}$ and HDAC4^{F65A} were designed to reduce nuclear HDAC4 to restore a more WT distribution. However, if a certain level of nuclear HDAC4 is required for normal function of DA neurons, excessive reduction could impair normal HDAC4 function and may explain the more severe climbing deficit. Although the current data do not show a rescue effect, they could point to an unrecognised role for HDAC4 in DA neuron physiology. The impact of HDAC4^{F65A} and HDAC4$^{M1\text{-}L285}$ on the distribution of endogenous HDAC4 was not examined in DA neurons. It was hypothesised that they would result in reduced nuclear entry as this has been shown in KCs (Hawley et al., 2025; Tan et al., 2024); however, this has not yet been confirmed in DA neurons. HDAC4^{F65A} is not completely deficient in oligomerisation (Hawley et al., 2025), and if it is binding to endogenous HDAC4, it will be disrupting its ability to form oligomers, which is hypothesised to be a requirement for normal HDAC4 function (Dai et al., 2024). HDAC4$^{M1\text{-}L285}$ may also disrupt function; however, it was also shown in a previous study to have no impact on MB development when expressed in KCs (Tan et al., 2024). The subcellular localisation of HDAC4, as well as the stoichiometry between MEF2 and HDAC4, may be different in DA neurons. High expression of *HDAC4$^{M1\text{-}L285}$* may not only titrate MEF2 as observed in KCs (Hawley et al., 2025), but it may also oligomerise with HDAC4, which would prevent the formation of normal HDAC4 oligomers, disrupting normal interactions. Titrating out MEF2 itself may also impact normal function, as the binding of HDAC4$^{M1\text{-}L285}$ to MEF2 would impair MEF2's normal interactions with other proteins. Testing HDAC4 RNAi, HDAC4^{F65A}, and HDAC4$^{M1\text{-}L285}$ in the absence of α-synuclein would clarify whether they independently impair locomotor function. If so, further experiments could be carried out to examine *HDAC4* expression levels and whether altered protein interactions cause these deficits.

This further research would provide a well-characterised PD model that allows for the comparison of many cellular mechanisms and pathways and provide a baseline for how these may change with the expression of both *SNCA* and *HDAC4*. Using a well-characterised PD model, the role of HDAC4 in inducing oxidative stress through mitochondrial function can be examined to better understand the mechanisms by which HDAC4 exacerbates PD progression.

5 CONCLUSION

This study characterises the use of *Drosophila* as a model for investigating PD mechanisms, particularly regarding α-synuclein and HDAC4 interactions. WT α-synuclein expression was too low to reliably detect or induce PD-like phenotypes, especially when driven pan-neuronally by *elav-GAL4* or *nSyb-GAL4*, which resulted in minimal expression in DA (TH-positive) neurons and no significant motor impairment. In contrast, codon-optimised α-synuclein expression driven by *Ddc-GAL4* produced robust phenotypes, including climbing deficits, neurodegeneration, and eye defects, validating its use as a model. Similarly, *HDAC4* overexpression independently impaired locomotor function, and both *HDAC4* and *MEF2* were shown to be expressed in TH-positive neurons. Co-expression of HDAC4 with α-synuclein led to the formation of larger nuclear HDAC4 condensates, suggesting enhanced nuclear accumulation and potential transcriptional dysregulation. However, genetic disruption of HDAC4 using HDAC4 RNAi, $HDAC4^{F65A}$, or $HDAC4^{M1\text{-}L285}$ failed to rescue *SNCA*-induced motor and neuronal defects, and instead potentially worsened outcomes. This unexpected exacerbation underscores the complexity of HDAC4's role in neuronal function and interaction with α-synuclein. To further refine the model and elucidate underlying mechanisms, future work should focus on quantifying *SNCA* expression levels, characterising the extent of α-synuclein-induced neurodegeneration, and assessing mitochondrial and proteasomal function. Importantly, MEF2 activity should be directly assessed to determine whether it is impaired by α-synuclein and HDAC4 co-expression. As the combined expression of α-synuclein and HDAC4 was toxic in DA neurons, adult-specific expression using the GAL80ts system will be critical for further evaluating this interaction. Lastly, testing the HDAC4 rescue constructs individually for their effects on motor function and DA neuron survival will help clarify their distinct contributions and potential as therapeutic targets in the PD model.

6 REFERENCES

Aasly, J. O. (2020). Long-term outcomes of genetic Parkinson's disease. *Journal of movement disorders*, *13*(2), 81. https://doi.org/10.14802/jmd.19080

Abeliovich, A., Schmitz, Y., Fariñas, I., Choi-Lundberg, D., Ho, W.-H., Castillo, P. E., Shinsky, N., Verdugo, J. M. G., Armanini, M., & Ryan, A. (2000). Mice lacking α-synuclein display functional deficits in the nigrostriatal dopamine system. *Neuron*, *25*(1), 239-252. https://doi.org/10.1016/S0896-6273(00)80886-7

Agostini, F., Bubacco, L., Chakrabarti, S., & Bisaglia, M. (2023). α-Synuclein Toxicity in *Drosophila melanogaster* Is Enhanced by the Presence of Iron: Implications for Parkinson's Disease. *Antioxidants*, *12*(2). https://doi.org/10.3390/antiox12020261

Alam, G., & Richardson, J. R. (2020). Regulation of tyrosine hydroxylase: relevance to Parkinson's disease. In *Genetics, Neurology, Behavior, and Diet in Parkinson's Disease* (pp. 51-66). Elsevier. https://doi.org/10.1016/B978-0-12-815950-7.00004-7

Antrobus, J., & Parsons, J. L. (2022). Histone deacetylases and their potential as targets to enhance tumour radiosensitisation. *Radiation*, *2*(1), 149-167. https://doi.org/10.3390/radiation2010011

Armstrong, M. J., & Okun, M. S. (2020). Diagnosis and treatment of Parkinson disease: a review. *Jama*, *323*(6), 548-560. https://doi.org/10.1001/jama.2019.22360

Arsac, J., Sedru, M., Dartiguelongue, M., Vulin, J., Davoust, N., Baron, T., & Mollereau, B. (2021). Chronic Exposure to Paraquat Induces Alpha-Synuclein Pathogenic Modifications in *Drosophila*. *International Journal of Molecular Sciences*, *22*(21). https://doi.org/10.3390/ijms222111613

Aso, Y., Grübel, K., Busch, S., Friedrich, A. B., Siwanowicz, I., & Tanimoto, H. (2009). The mushroom body of adult *Drosophila* characterized by GAL4 drivers. *Journal of Neurogenetics*, *23*(1-2), 156-172. https://doi.org/10.1080/01677060802471718

Aso, Y., Hattori, D., Yu, Y., Johnston, R. M., Iyer, N. A., Ngo, T.-T., Dionne, H., Abbott, L., Axel, R., & Tanimoto, H. (2014). The neuronal architecture of the mushroom body provides a logic for associative learning. *eLife*, *3*, e04577. https://doi.org/10.7554/eLife.04577

Auluck, P. K., Chan, H. Y. E., Trojanowski, J. Q., Lee, V., & Bonni, N. M. (2002). Chaperone Suppression of α-Synuclein Toxicity in a *Drosophila* Model for Parkinson's Disease. *Science*, *295*, 865-868. https://doi.org/10.1126/science.1067389

Auluck, P. K., Meulener, M. C., & Bonini, N. M. (2005). Mechanisms of suppression of α-synuclein neurotoxicity by geldanamycin in *Drosophila*. *Journal of Biological Chemistry*, *280*(4), 2873-2878. https://doi.org/10.1074/jbc.M412106200

Ayano, G. (2016). Dopamine: receptors, functions, synthesis, pathways, locations and mental disorders: review of literatures. *J Ment Disord Treat*, *2*(120), 2. https://doi.org/10.4172/2471-271X.1000120

Balzano, T., Del Rey, N. L.-G., Esteban-García, N., Reinares-Sebastián, A., Pineda-Pardo, J. A., Trigo-Damas, I., Obeso, J. A., & Blesa, J. (2024). Neurovascular and immune factors of vulnerability of substantia nigra dopaminergic neurons in non-human primates. *npj Parkinson's Disease*, *10*(1), 118. https://doi.org/10.1038/s41531-024-00735-w

Bandhyopadhyay, U., & Cuervo, A. M. (2007). Chaperone-mediated autophagy in aging and neurodegeneration: Lessons from α-synuclein. *Experimental gerontology*, *42*(1-2), 120-128. https://doi.org/10.1016/j.exger.2006.05.019

Barbosa, A. C., Kim, M.-S., Ertunc, M., Adachi, M., Nelson, E. D., McAnally, J., Richardson, J. A., Kavalali, E. T., Monteggia, L. M., & Bassel-Duby, R. (2008). MEF2C, a transcription factor that facilitates learning and memory by negative regulation of synapse numbers and function. *Proceedings of the National Academy of Sciences*, *105*(27), 9391-9396. https://doi.org/10.1073/pnas.0802679105

Barone, M. C., & Bohmann, D. (2013). Assessing neurodegenerative phenotypes in *Drosophila* dopaminergic neurons by climbing assays and whole brain immunostaining. *Journal of visualized experiments: JoVE*(74), 50339. https://doi.org/10.3791/50339

Basso, V., Döbrössy, M. D., Thompson, L. H., Kirik, D., Fuller, H. R., & Gates, M. A. (2024). State of the Art in Sub-Phenotyping Midbrain Dopamine Neurons. *Biology*, *13*(9), 690. https://doi.org/10.3390/biology13090690

Bellani, S., Sousa, V. L., Ronzitti, G., Valtorta, F., Meldolesi, J., & Chieregatti, E. (2010). The regulation of synaptic function by alpha-synuclein. *Commun Integr Biol*, *3*(2), 106-109. https://doi.org/10.4161/cib.3.2.10964

Bertos, N. R., Wang, A. H., & Yang, X.-J. (2001). Class II histone deacetylases: structure, function, and regulation. *Biochemistry and Cell Biology*, *79*(3), 243-252. https://doi.org/10.1139/o01-032

Bertram, L., & Tanzi, R. E. (2005). The genetic epidemiology of neurodegenerative disease. *The Journal of Clinical Investigation*, *115*(6), 1449-1457. https://doi.org/10.1172/JCI24761

Black, B. L., & Olson, E. N. (1998). Transcriptional control of muscle development by myocyte enhancer factor-2 (MEF2) proteins. *Annual review of cell and developmental biology*, *14*(1), 167-196. https://doi.org/10.1146/annurev.cellbio.14.1.167

Bolger, T. A., & Yao, T. P. (2005). Intracellular trafficking of histone deacetylase 4 regulates neuronal cell death. *The Journal of Neuroscience*, *25*(41), 9544 - 9553. https://doi.org/10.1523/JNEUROSCI.1826-05.2005

Borghi, S., Molinari, S., Razzini, G., Parise, F., Battini, R., & Ferrari, S. (2001). The nuclear localization domain of the MEF2 family of transcription factors shows member-specific features and mediates the nuclear import of histone deacetylase 4. *Journal of Cell Science*, *114*(24), 4477-4483. https://doi.org/10.1242/jcs.114.24.4477

Brand, A. H., & Perrimon, N. (1993). Targeted gene expression as a means of altering cell fates and generating dominant phenotypes. *development*, *118*(2), 401-415. https://doi.org/10.1242/dev.118.2.401

Bronstein, J. M., Tagliati, M., Alterman, R. L., Lozano, A. M., Volkmann, J., Stefani, A., Horak, F. B., Okun, M. S., Foote, K. D., & Krack, P. (2011). Deep brain stimulation for Parkinson disease: an expert consensus and review of key issues. *Archives of neurology*, *68*(2), 165-165. https://doi.org/10.1001/archneurol.2010.260

Cabin, D. E., Shimazu, K., Murphy, D., Cole, N. B., Gottschalk, W., McIlwain, K. L., Orrison, B., Chen, A., Ellis, C. E., & Paylor, R. (2002). Synaptic vesicle depletion correlates with attenuated synaptic responses to prolonged repetitive stimulation in mice lacking α-synuclein. *Journal of Neuroscience*, *22*(20), 8797-8807. https://doi.org/10.4161/cib.3.2.10964

Cagan, R. L., & Ready, D. F. (1989). The emergence of order in the *Drosophila* pupal retina. *Developmental biology*, *136*(2), 346-362. https://doi.org/10.1016/0012-1606(89)90261-3

Caine, C., Kasherov, P., Silber, J., & Lalouette, A. (2014). Mef2 interacts with the Notch pathway during adult muscle development in *Drosophila melanogaster*. *PLoS ONE*, *9*(9), e108149. https://doi.org/10.1371/journal.pone.0108149

Calabresi, P., Mechelli, A., Natale, G., Volpicelli-Daley, L., Di Lazzaro, G., & Ghiglieri, V. (2023). Alpha-synuclein in Parkinson's disease and other synucleinopathies: from overt neurodegeneration back to early synaptic dysfunction. *Cell Death & Disease*, *14*(3), 176. https://doi.org/10.1038/s41419-023-05672-9

Campos, E. I., & Reinberg, D. (2009). Histones: annotating chromatin. *Annual review of genetics*, *43*(1), 559-599. https://doi.org/10.1146/annurev.genet.032608.103928

Chan, J. K., Sun, L., Yang, X.-J., Zhu, G., & Wu, Z. (2003). Functional characterization of an amino-terminal region of HDAC4 that possesses MEF2 binding and transcriptional repressive activity. *Journal of Biological Chemistry*, *278*(26), 23515-23521. https://doi.org/10.1074/jbc.M301922200

Chan, S. F., Sances, S., Brill, L. M., Okamoto, S.-i., Zaidi, R., McKercher, S. R., Akhtar, M. W., Nakanishi, N., & Lipton, S. A. (2014). ATM-dependent phosphorylation of MEF2D promotes neuronal survival after DNA damage. *Journal of Neuroscience*, *34*(13), 4640-4653. https://doi.org/10.1523/JNEUROSCI.2510-12.2014

Chartier-Harlin, M. C., Kachergus, J., Roumier, C., Mouroux, V., Douay, X., Lincoln, S., Levecque, C., Larvor, L., Andrieux, J., Hulihan, M., Waucquier, N., Defebvre, L., Amouyel, P., Farrer, M., & Destée, A. (2004). α-synuclein locus duplication as a cause of familial Parkinson's disease. *The Lancet*, *364*(9440), 1167-1169. https://doi.org/10.1016/S0140-6736(04)17103-1

Chaudhary, R., Agarwal, V., Kaushik, A. S., & Rehman, M. (2021). Involvement of myocyte enhancer factor 2c in the pathogenesis of autism spectrum disorder. *Heliyon*, *7*(4). https://doi.org/10.1016/j.heliyon.2021.e06854

Chawla, S., Vanhoutte, P., Arnold, F. J. L., Huang, C. L. H., & Bading, H. (2003). Neuronal activity-dependent nucleocytoplasmic shuttling of HDAC4 and HDAC5. *Journal of Neurochemistry*, *85*(1), 151-159. https://doi.org/10.1046/j.1471-4159.2003.01648.x

Chen, A., Wilburn, P., Hao, X., & Tully, T. (2014a). Walking deficits and centrophobism in an α-synuclein fly model of Parkinson's disease. *Genes, Brain and Behavior*, *13*(8), 812-820. https://doi.org/10.1111/gbb.12172

Chen, A., Y, Xia, S., Wilburn, P., & Tully, T. (2014b). Olfactory deficits in an alpha-synuclein fly model of Parkinson's disease. *PLoS ONE*, *9*(5). https://doi.org/10.1371/journal.pone.0097758

Chen, D., Xu, M., Wu, B., & Chen, L. (2017a). Histone deacetylases in hearing loss: Current perspectives for therapy. *Journal of Otology*, *12*(2), 47-54. https://doi.org/10.1016/j.joto.2017.04.002

Chen, L., & Feany, M. (2005). α-Synuclein phosphorylation controls neurotoxicity and inclusion formation in a *Drosophila* model of Parkinson disease. . *Nat Neurosci 8*, 657–663. https://doi.org/10.1038/nn1443

Chen, L., Periquet, M., Wang, X., Negro, A., McLean, P. J., Hyman, B. T., & Feany, M. B. (2009). Tyrosine and serine phosphorylation of α-synuclein have opposing effects on neurotoxicity and soluble oligomer formation. *The Journal of Clinical Investigation*, *119*(11), 3257-3265. https://doi.org/10.1172/JCI39088

Chen, X., Gao, B., Ponnusamy, M., Lin, Z., & Liu, J. (2017b). MEF2 signaling and human diseases. *Oncotarget*, *8*(67), 112152. https://doi.org/10.18632/oncotarget.22899

Chen, Y., Wang, Y., Modrusan, Z., Sheng, M., & Kaminker, J. S. (2014c). Regulation of neuronal gene expression and survival by basal NMDA receptor activity: a role for histone deacetylase 4. *Journal of Neuroscience*, *34*(46), 15327-15339. https://doi.org/10.1523/JNEUROSCI.0569-14.2014

Chinta, S. J., & Andersen, J. K. (2005). Dopaminergic neurons. *The International Journal of Biochemistry & Cell Biology*, *37*(5), 942-946. https://doi.org/10.1016/j.biocel.2004.09.009

Cho, E., Oh, J. H., Lee, E., Do, Y. R., & Kim, E. Y. (2016). Cycles of circadian illuminance are sufficient to entrain and maintain circadian locomotor rhythms in *Drosophila*. *Scientific Reports*, *6*(1), 37784. https://doi.org/10.1038/srep37784

Choudhary, C., Kumar, C., Gnad, F., Nielsen, M. L., Rehman, M., Walther, T. C., Olsen, J. V., & Mann, M. (2009). Lysine acetylation targets protein complexes and co-regulates major cellular functions. *Science*, *325*(5942), 834-840. https://doi.org/10.1126/science.1175371

Chouhan, A. K., Guo, C., Hsieh, Y.-C., Ye, H., Senturk, M., Zuo, Z., Li, Y., Chatterjee, S., Botas, J., & Jackson, G. R. (2016). Uncoupling neuronal death and dysfunction in *Drosophila* models of neurodegenerative disease. *Acta Neuropathologica Communications*, *4*, 1-15. https://doi.org/10.1186/s40478-016-0333-4

Chu, Y., Mickiewicz, A. L., & Kordower, J. H. (2011). α-synuclein aggregation reduces nigral myocyte enhancer factor-2D in idiopathic and experimental Parkinson's disease. *Neurobiology of Disease*, *41*(1), 71-82. https://doi.org/10.1016/j.nbd.2010.08.022

Ciechanover, A., & Kwon, Y. T. (2015). Degradation of misfolded proteins in neurodegenerative diseases: therapeutic targets and strategies. *Experimental & molecular medicine*, *47*(3), e147-e147. https://doi.org/10.1038/emm.2014.117

Cohen, T. J., Waddell, D. S., Barrientos, T., Lu, Z., Feng, G., Cox, G. A., Bodine, S. C., & Yao, T.-P. (2007). The histone deacetylase HDAC4 connects neural activity to muscle transcriptional reprogramming. *Journal of Biological Chemistry*, *282*(46), 33752-33759. https://doi.org/10.1074/jbc.M706268200

Connolly, J. B., Roberts, I. J., Armstrong, J. D., Kaiser, K., Forte, M., Tully, T., & O'Kane, C. J. (1996). Associative learning disrupted by impaired Gs signaling in *Drosophila* mushroom bodies. *Science*, *274*(5295), 2104-2107. https://doi.org/10.1126/science.274.5295.2104

Crowther, D. C., Kinghorn, K. J., Miranda, E., Page, R., Curry, J. A., Duthie, F. A. I., Gubb, D. C., & Lomas, D. A. (2005). Intraneuronal Aβ, non-amyloid aggregates and neurodegeneration in a *Drosophila* model of Alzheimer's disease. *Neuroscience*, *132*(1), 123-135. https://doi.org/10.1016/j.neuroscience.2004.12.025

Dai, S., Guo, L., Dey, R., Guo, M., Zhang, X., Bates, D., Cayford, J., Jiang, L., Wei, H., & Chen, Z. (2024). Structural insights into the HDAC4–MEF2A–DNA complex and its implication in long-range transcriptional regulation. *Nucleic Acids Research*, *52*(5), 2711-2723. https://doi.org/10.1093/nar/gkae036

Darcy, M. J., Calvin, K., Cavnar, K., & Ouimet, C. C. (2010). Regional and subcellular distribution of HDAC4 in mouse brain. *Journal of Comparative Neurology*, *518*(5), 722-740. https://doi.org/10.1002/cne.22241

Dasgupta, A. (2016). Association between polymorphisms in genes encoding various receptors, transporters, and enzymes and alcohol/drug addiction. In A. Dasgupta (Ed.), *Alcohol, drugs, genes and the clinical laboratory: an overview for healthcare and safety professionals* (pp. 135-154). https://doi.org/10.1016/B978-0-12-805455-0.00008-7

Dauer, W., & Przedborski, S. (2003). Parkinson's disease: mechanisms and models. *Neuron*, *39*, 889-909. https://doi.org/10.1016/S0896-6273(03)00568-3

De Belle, J. S., & Heisenberg, M. (1994). Associative odor learning in *Drosophila* abolished by chemical ablation of mushroom bodies. *Science*, *263*(5147), 692-695. https://doi.org/10.1126/science.8303280

Deep-Brain Stimulation for Parkinson's Disease Study Group. (2001). Deep-brain stimulation of the subthalamic nucleus or the pars interna of the globus pallidus in Parkinson's disease. *New England Journal of Medicine*, *345*(13), 956-963. https://doi.org/10.1056/NEJMoa000827

Devi, L., Raghavendran, V., Prabhu, B. M., Avadhani, N. G., & Anandatheerthavarada, H. K. (2008). Mitochondrial import and accumulation of α-synuclein impair complex I in human dopaminergic neuronal cultures and Parkinson disease brain. *Journal of Biological Chemistry*, *283*(14), 9089-9100. https://doi.org/10.1074/jbc.M710012200

Dickstein, D. L., Kabaso, D., Rocher, A. B., Luebke, J. I., Wearne, S. L., & Hof, P. R. (2007). Changes in the structural complexity of the aged brain. *Aging Cell*, *6*(3), 275-284. https://doi.org/10.1111/j.1474-9726.2007.00289.x

Dubnau, J., Grady, L., Kitamoto, T., & Tully, T. (2001). Disruption of neurotransmission in *Drosophila* mushroom body blocks retrieval but not acquisition of memory. *Nature*, *411*(6836), 476-480. https://doi.org/10.1038/35078077

Duffy, J. B. (2002). GAL4 system in *Drosophila*: a fly geneticist's Swiss army knife. *Genesis*, *34*(1-2), 1-15. https://doi.org/10.1002/gene.10150

Dumbhare, O., & Gaurkar, S. S. (2023). A review of genetic and gene therapy for Parkinson's disease. *Cureus*, *15*(2). https://doi.org/10.7759/cureus.34657

Dunlap, J. C. (1999). Molecular bases for circadian clocks. *Cell*, *96*(2), 271-290. https://doi.org/10.1016/S0092-8674(00)80566-8

Ebrahimi-Fakhari, D., Wahlster, L., & McLean, P. J. (2012). Protein degradation pathways in Parkinson's disease: curse or blessing. *Acta neuropathologica*, *124*(2), 153-172. https://doi.org/10.1007/s00401-012-1004-6

El-Saiy, K. A., Sayed, R. H., El-Sahar, A. E., & Kandil, E. A. (2022). Modulation of histone deacetylase, the ubiquitin proteasome system, and autophagy underlies the neuroprotective effects of venlafaxine in a rotenone-induced Parkinson's disease model in rats. *Chemico-Biological Interactions*, *354*, 109841. https://doi.org/10.1016/j.cbi.2022.109841

Ericsson, J., Stephenson-Jones, M., Pérez-Fernández, J., Robertson, B., Silberberg, G., & Grillner, S. (2013). Dopamine differentially modulates the excitability of striatal neurons of the direct and indirect pathways in lamprey. *Journal of Neuroscience*, *33*(18), 8045-8054. https://doi.org/10.1523/JNEUROSCI.5881-12.2013

Fan, G.-H., Zhou, H.-Y., Yang, H., & Chen, S.-D. (2006). Heat shock proteins reduce α-synuclein aggregation induced by MPP+ in SK-N-SH cells. *FEBS letters*, *580*(13), 3091-3098. https://doi.org/10.1016/j.febslet.2006.04.057

Farrer, M., Kachergus, J., Forno, L., Lincoln, S., Wang, D. S., Hulihan, M., Maraganore, D., Gwinn-Hardy, K., Wszolek, Z., Dickson, D., & Langston, J. W. (2004). Comparison of kindreds with parkinsonism and α-synuclein genomic multiplications. *Annals of Neurology: Official Journal of the American Neurological Association and the Child Neurology Society*, *55*(2), 174-179. https://doi.org/10.1002/ana.10846

Feany, M. B., & Bender, W. W. (2000). A *Drosophila* model of Parkinson's disease. *Nature*, *404*(6776), 394-398. https://doi.org/10.1038/35006074

Fearnley, J. M., & Lees, A. J. (1991). Ageing and Parkinson's disease: substantia nigra regional selectivity. *Brain*, *114*(5), 2283-2301. https://doi.org/10.1093/brain/114.5.2283

Federspiel, J. D., Greco, T. M., Lum, K. K., & Cristea, I. M. (2019). Hdac4 Interactions in Huntington's Disease Viewed Through the Prism of Multiomics. *Molecular & Cellular Proteomics*, *18*(8), 92-113. https://doi.org/10.1074/mcp.RA118.001253

Fernández-Cruz, I., Sánchez-Díaz, I., Narváez-Padilla, V., & Reynaud, E. (2020). Rpt2 proteasome subunit reduction causes Parkinson's disease like symptoms in *Drosophila*. *IBRO reports*, *9*, 65-77. https://doi.org/10.1016/j.ibror.2020.07.001

Fernandez-Funez, P., Nino-Rosales, M. L., de Gouyon, B., She, W. C., Luchak, J. M., Martinez, P., Turiegano, E., Benito, J., Capovilla, M., Skinner, P. J., McCall, A., Canal, I., Orr, H. T., Zoghbi, H. Y., & Botas, J. (2000). Identification of genes that modify ataxin-1 induced neurodegeneration. *Nature*, *408*(6808), 101-106. https://doi.org/10.1038/35040584

Fischbach, K.-F., & Dittrich, A. (1989). The optic lobe of *Drosophila melanogaster*. I. A Golgi analysis of wild-type structure. *Cell and tissue research*, *258*, 441-475. https://doi.org/10.1007/BF00218858

Fischer, J. A., Giniger, E., Maniatis, T., & Ptashne, M. (1988). GAL4 activates transcription in *Drosophila*. *Nature*, *332*(6167), 853-856. https://doi.org/10.1038/332853a0

Fischle, W., Emiliani, S., Hendzel, M. J., Nagase, T., Nomura, N., Voelter, W., & Verdin, E. (1999). A new family of human histone deacetylases related tosaccharomyces cerevisiae hda1p. *Journal of Biological Chemistry*, *274*(17), 11713-11720. https://doi.org/10.1074/jbc.274.17.11713

Fischle, W., Kiermer, V., Dequiedt, F., & Verdin, E. (2001). The emerging role of class II histone deacetylases. *Biochemistry and Cell Biology*, *79*(3), 337-348. https://doi.org/10.1139/o01-116

Fishilevich, E., & Vosshall, L. B. (2005). Genetic and functional subdivision of the *Drosophila* antennal lobe. *Current Biology*, *15*(17), 1548-1553. https://doi.org/10.1016/j.cub.2005.07.066

Fitzsimons, H. L. (2015). The class IIa histone deacetylase HDAC4 and neuronal function: nuclear nuisance and cytoplasmic stalwart? *Neurobiology of Learning and Memory*, *123*, 149-158. https://doi.org/10.1016/j.nlm.2015.06.006

Fitzsimons, H. L., Schwartz, S., Given, F. M., & Scott, M. J. (2013). The histone deacetylase HDAC4 regulates long-term memory in *Drosophila*. *PLoS ONE*, *8*(12), e83903. https://doi.org/10.1371/journal.pone.0083903

Friggi-Grelin, F., Coulom, H., Meller, M., Gomez, D., Hirsh, J., & Birman, S. (2003). Targeted gene expression in *Drosophila* dopaminergic cells using regulatory sequences from tyrosine hydroxylase. *Journal of neurobiology*, *54*(4), 618-627. https://doi.org/10.1002/neu.10185

Furey, T. S. (2012). ChIP–seq and beyond: new and improved methodologies to detect and characterize protein–DNA interactions. *Nature reviews genetics*, *13*(12), 840-852. https://doi.org/10.1038/nrg3306

Gajula Balija, M. B., Griesinger, C., Herzig, A., Zweckstetter, M., & Jackle, H. (2011). Pre-fibrillar α-synuclein mutants cause Parkinson's disease-like non-motor symptoms in *Drosophila*. *PLoS ONE*, *6*(9). https://doi.org/10.1371/journal.pone.0024701

Gao, L., She, H., Li, W., Zeng, J., Zhu, J., Jones, D. P., Mao, Z., Gao, G., & Yang, Q. (2014). Oxidation of survival factor MEF2D in neuronal death and Parkinson's disease. *Antioxid Redox Signal*, *20*(18), 2936-2948. https://doi.org/10.1089/ars.2013.5399

German, D. C., Manaye, K., Smith, W. K., Woodward, D. J., & Saper, C. B. (1989). Midbrain dopaminergic cell loss in Parkinson's disease: computer visualization. *Annals of Neurology: Official Journal of the American Neurological Association and the Child Neurology Society*, *26*(4), 507-514. https://doi.org/10.1002/ana.410260403

Giniger, E., Varnum, S. M., & Ptashne, M. (1985). Specific DNA binding of GAL4, a positive regulatory protein of yeast. *Cell*, *40*(4), 767-774. https://doi.org/10.1016/0092-8674(85)90336-8

Goldman, S. M. (2014). Environmental toxins and Parkinson's disease. *Annual review of pharmacology and toxicology*, *54*(1), 141-164. https://doi.org/10.1146/annurev-pharmtox-011613-135937

Grozinger, C. M., Hassig, C. A., & Schreiber, S. L. (1999). Three proteins define a class of human histone deacetylases related to yeast Hda1p. *Proceedings of the National Academy of Sciences*, *96*(9), 4868-4873. https://doi.org/10.1073/pnas.96.9.4868

Grozinger, C. M., & Schreiber, S. L. (2000). Regulation of histone deacetylase 4 and 5 and transcriptional activity by 14-3-3-dependent cellular localization. *Proceedings of the National Academy of Sciences*, *97*(14), 7835-7840. https://doi.org/10.1073/pnas.140199597

Guo, L., Han, A., Bates, D. L., Cao, J., & Chen, L. (2007). Crystal structure of a conserved N-terminal domain of histone deacetylase 4 reveals functional insights into glutamine-rich domains. *Proceedings of the National Academy of Sciences*, *104*(11), 4297-4302. https://doi.org/10.1073/pnas.0608041104

Gustafsson, C., Govindarajan, S., & Minshull, J. (2004). Codon bias and heterologous protein expression. *Trends in biotechnology*, *22*(7), 346-353. https://doi.org/10.1016/j.tibtech.2004.04.006

Harrison, I. F., & Dexter, D. T. (2013). Epigenetic targeting of histone deacetylase: therapeutic potential in Parkinson's disease? *Pharmacology & therapeutics*, *140*(1), 34-52. https://doi.org/10.1111/jnc.14599

Hawley, H. R. (2024). *Investigating HDAC4 aggregation in a Drosophila model of neuronal development: a dissertation presented in partial fulfilment of the requirements for the degree of Doctor of Philosophy in Biochemistry at Massey University, Manawatū, New Zealand* https://mro.massey.ac.nz/handle/10179/70051

Hawley, H. R., Roberts, C. J., & Fitzsimons, H. L. (2023). Comparison of neuronal GAL4 drivers along with the AGES (auxin-inducible gene expression system) and TARGET (temporal and regional gene expression targeting) systems for fine tuning of neuronal gene expression in *Drosophila*. *Micropublication Biology*, *2023*, 10.17912/micropub. biology. 000885. https://doi.org/10.17912/micropub.biology.000885

Hawley, H. R., Sutherland-Smith, A. J., Savoian, M. S., & Fitzsimons, H. L. (2025). N-terminal oligomerization drives HDAC4 nuclear condensation and neurodevelopmental dysfunction in *Drosophila*. *bioRxiv*, 2025.2003.2010.642474. https://doi.org/10.1101/2025.03.10.642474

Hay, B. A., Maile, R., & Rubin, G. M. (1997). P element insertion-dependent gene activation in the *Drosophila* eye. *Proceedings of the National Academy of Sciences*, *94*(10), 5195-5200. https://doi.org/10.1073/pnas.94.10.5195

Haywood, A., & Staveley, B. (2004). parkin counteracts symptoms in a *Drosophila* model of Parkinson's disease. *BMC Neuroscience*, *5*(14). https://doi.org/10.1186/1471-2202-5-14

Heisenberg, M., Borst, A., Wagner, S., & Byers, D. (1985). *Drosophila* mushroom body mutants are deficient in olfactory learning. *Journal of Neurogenetics*, *2*(1), 1-30. https://doi.org/10.3109/01677068509100140

Henrich, M. T., Oertel, W. H., Surmeier, D. J., & Geibl, F. F. (2023). Mitochondrial dysfunction in Parkinson's disease–a key disease hallmark with therapeutic potential. *Molecular neurodegeneration*, *18*(1), 83. https://doi.org/10.1186/s13024-023-00676-7

Hodgetts, R. B., & O'Keefe, S. L. (2006). Dopa decarboxylase: a model gene-enzyme system for studying development, behavior, and systematics. *Annual Review of Entomology*, *51*(1), 259-284. https://doi.org/10.1146/annurev.ento.51.110104.151143

Huang, M., Jin, H., Anantharam, V., Kanthasamy, A., & Kanthasamy, A. G. (2024). Mitochondrial stress-induced H4K12 hyperacetylation dysregulates transcription in Parkinson's disease. *Frontiers in Cellular Neuroscience*, *18*, 1422362. https://doi.org/10.3389/fncel.2024.1422362

Ikeda, A., Nishioka, K., Meng, H., Takanashi, M., Hasegawa, I., Inoshita, T., Shiba-Fukushima, K., Li, Y., Yoshino, H., & Mori, A. (2019). Mutations in CHCHD2 cause α-synuclein aggregation. *Human molecular genetics*, *28*(23), 3895-3911. https://doi.org/10.1093/hmg/ddz241

Iyer, J., Wang, Q., Le, T., Pizzo, L., Grönke, S., Ambegaokar, S. S., Imai, Y., Srivastava, A., Troisí, B. L., & Mardon, G. (2016). Quantitative assessment of eye phenotypes for functional genetic studies using *Drosophila melanogaster*. *G3: Genes, Genomes, Genetics*, *6*(5), 1427-1437. https://doi.org/10.1534/g3.116.027060

Jahromi, S. R., Ramesh, S. R., Finkelstein, D. I., & Haddadi, M. (2021). α-Synuclein E46K Mutation and Involvement of Oxidative Stress in a *Drosophila* model of Parkinson's Disease. *Parkinson's Disease*, *2021*(1). https://doi.org/10.1155/2021/6621507

Jakes, R., Spillantini, M. G., & Goedert, M. (1994). Identification of two distinct synucleins from human brain. *FEBS letters*, *345*(1), 27-32. https://doi.org/10.1016/0014-5793(94)00395-5

Jeibmann, A., & Paulus, W. (2009). *Drosophila melanogaster* as a model organism of brain diseases. *International Journal of Molecular Sciences*, *10*(2), 407- 440. https://doi.org/10.3390/ijms10020407

Kahle, P. J., Neumann, M., Ozmen, L., Müller, V., Jacobsen, H., Schindzielorz, A., Okochi, M., Leimer, U., van der Putten, H., Probst, A., Kremmer, E., Kretzschmar, H. A., & Haass, C. (2000). Subcellular localization of wild-type and Parkinson's disease-associated mutant α-synuclein in human and transgenic mouse brain. *The Journal of Neuroscience*, *20*(17), 6365-6373. https://doi.org/10.1523/JNEUROSCI.20-17-06365.2000

Karpinar, D. P., Balija, M. B. G., Kügler, S., Opazo, F., Rezaei-Ghaleh, N., Wender, N., Kim, H. Y., Taschenberger, G., Falkenburger, B. H., & Heise, H. (2009). Pre-fibrillar α-synuclein variants with impaired β-structure increase neurotoxicity in Parkinson's disease models. *The EMBO Journal*, *28*(20), 3256-3268. https://doi.org/10.1038/emboj.2009.257

Kastner, A., Hirsch, E., Herrero, M., Javoy-Agid, F., & Agid, Y. (1993). Immunocytochemical quantification of tyrosine hydroxylase at a cellular level in the mesencephalon of control subjects and patients with Parkinson's and

Alzheimer's disease. *Journal of Neurochemistry*, *61*(3), 1024-1034. https://doi.org/10.1111/j.1471-4159.1993.tb03616.x

Kasuya, J., Ishimoto, H., & Kitamoto, T. (2009). Neuronal mechanisms of learning and memory revealed by spatial and temporal suppression of neurotransmission using shibirets1, a temperature-sensitive dynamin mutant gene in *Drosophila melanogaster*. *Frontiers in Molecular Neuroscience*, *2*, 861. https://doi.org/10.3389/neuro.02.011.2009

Kelly, M. A., Chellgren, B. W., Rucker, A. L., Troutman, J. M., Fried, M. G., Miller, A.-F., & Creamer, T. P. (2001). Host− guest study of left-handed polyproline II helix formation. *Biochemistry*, *40*(48), 14376-14383. https://doi.org/10.1021/bi011043a

Kim, M. S., Akhtar, M. W., Adachi, M., Mahgoub, M., Bassel-Duby, R., Kavalali, E. T., Olson, E. N., & Monteggia, L. M. (2012). An essential role for histone deacetylase 4 in synaptic plasticity and memory formation. *The Journal of Neuroscience*, *32*(32), 10879 - 10886. https://doi.org/10.1523/JNEUROSCI.2089-12.2012

Kim, S. (2025). Chemical Synapse: Steps of Synaptic Transmission. In.

Klein, C., & Westenberger, A. (2012). Genetics of Parkinson's disease. *Cold Spring Harbor perspectives in medicine*, *2*(1), a008888. https://doi.org/10.1101/cshperspect.a008888

Knowles-Barley, S., Longair, M., & Armstrong, J. D. (2010). BrainTrap: a database of 3D protein expression patterns in the *Drosophila* brain. *Database*, *2010*, baq005. https://doi.org/10.1093/database/baq005

Konopka, R. J., Pittendrigh, C., & Orr, D. (1989). Reciprocal behaviour associated with altered homeostasis and photosensitivity of *Drosophila* clock mutants. *Journal of Neurogenetics*, *6*(1), 1-10. https://doi.org/10.3109/01677068909107096

Konrad, K. D., & Marsh, J. L. (1987). Developmental expression and spatial distribution of dopa decarboxylase in *Drosophila*. *Developmental biology*, *122*(1), 172-185. https://doi.org/10.1016/0012-1606(87)90343-5

Kontopoulos, E., Parvin, J. D., & Feany, M. B. (2006). α-synuclein acts in the nucleus to inhibit histone acetylation and promote neurotoxicity. *Human molecular genetics*, *15*(20), 3012-3023. https://doi.org/10.1093/hmg/ddl243

Kumer, S. C., & Vrana, K. E. (1996). Intricate regulation of tyrosine hydroxylase activity and gene expression. *Journal of Neurochemistry*, *67*(2), 443-462. https://doi.org/10.1046/j.1471-4159.1996.67020443.x

Kuzuhara, S., Mori, H., Izumiyama, N., Yoshimura, M., & Ihara, Y. (1988). Lewy bodies are ubiquitinated: a light and electron microscopic immunocytochemical study. *Acta neuropathologica*, *75*, 345-353. https://doi.org/10.1007/BF00687787

Lahiri, A. K., & Bevan, M. D. (2020). Dopaminergic transmission rapidly and persistently enhances excitability of D1 receptor-expressing striatal projection neurons. *Neuron*, *106*(2), 277-290. e276. https://doi.org/10.1016/j.neuron.2020.01.028

Lahm, A., Paolini, C., Pallaoro, M., Nardi, M. C., Jones, P., Neddermann, P., Sambucini, S., Bottomley, M. J., Lo Surdo, P., Carfı, A., & Koch, U. (2007). Unraveling the hidden catalytic activity of vertebrate class IIa histone deacetylases. *Proceedings*

of the National Academy of Sciences, *104*(44), 17335-17340. https://doi.org/10.1073/pnas.0706487104

Laker, R. C., Xu, P., Ryall, K. A., Sujkowski, A., Kenwood, B. M., Chain, K. H., Zhang, M., Royal, M. A., Hoehn, K. L., & Driscoll, M. (2014). A novel MitoTimer reporter gene for mitochondrial content, structure, stress, and damage in vivo. *Journal of Biological Chemistry*, *289*(17), 12005-12015. https://doi.org/10.1074/jbc.M113.530527

Lang, C., Campbell, K. R., Ryan, B. J., Carling, P., Attar, M., Vowles, J., Perestenko, O. V., Bowden, R., Baig, F., Kasten, M., Hu, M. T., Cowley, S. A., Webber, C., & Wade-Martins, R. (2019). Single-cell sequencing of iPSC-dopamine neurons reconstructs disease progression and identifies HDAC4 as a regulator of Parkinson cell phenotypes. *Cell stem cell*, *24*(1), 93-106. https://doi.org/10.1016/j.stem.2018.10.023

Lee, S.-J., Jeon, H., & Kandror, K. (2008). Alpha-synuclein is localized in a subpopulation of rat brain synaptic vesicles. *Acta neurobiologiae experimentalis*, *68*(4), 509-515.

Lee, T., & Luo, L. (1999). Mosaic analysis with a repressible cell marker for studies of gene function in neuronal morphogenesis. *Neuron*, *22*(3), 451-461. https://doi.org/10.1016/S0896-6273(00)80701-1

Leifer, D., Krainc, D., Yu, Y. T., McDermott, J., Breitbart, R. E., Heng, J., Neve, R. L., Kosofsky, B., Nadal-Ginard, B., & Lipton, S. A. (1993). MEF2C, a MADS/MEF2-family transcription factor expressed in a laminar distribution in cerebral cortex. *Proceedings of the National Academy of Sciences*, *90*(4), 1546-1550. https://doi.org/10.1073/pnas.90.4.1546

Leloup, J. C., & Goldbeter, A. (2000). Modeling the molecular regulatory mechanism of circadian rhythms in *Drosophila*. *BioEssays*, *22*(1), 84-93. https://doi.org/10.1002/(SICI)1521-1878(200001)22:1<84::AID-BIES13>3.0.CO;2-I

Lemercier, C., Verdel, A., Galloo, B., Curtet, S., Brocard, M.-P., & Khochbin, S. (2000). mHDA1/HDAC5 histone deacetylase interacts with and represses MEF2A transcriptional activity. *Journal of Biological Chemistry*, *275*(20), 15594-15599. https://doi.org/10.1074/jbc.M908437199

LeWitt, P. A. (2008). Levodopa for the treatment of Parkinson's disease. *New England Journal of Medicine*, *359*(23), 2468-2476. https://doi.org/10.1056/NEJMct0800326

Li, F., Lindsey, J. W., Marin, E. C., Otto, N., Dreher, M., Dempsey, G., Stark, I., Bates, A. S., Pleijzier, M. W., & Schlegel, P. (2020). The connectome of the adult *Drosophila* mushroom body provides insights into function. *eLife*, *9*, e62576. https://doi.org/10.7554/eLife.62576

Li, H., Shi, G., Zha, H., Zheng, L., Luo, Z., & Wang, Y. (2021). Inhibition of histone deacetylase promotes a neuroprotective mechanism in an experimental model of Parkinson's disease. *Archives of Medical Science: AMS*, *20*(2), 664. https://doi.org/10.5114/aoms/130287

Lin, X., Shah, S., & Bulleit, R. F. (1996). The expression of MEF2 genes is implicated in CNS neuronal differentiation. *Molecular brain research*, *42*(2), 307-316. https://doi.org/10.1016/S0169-328X(96)00135-0

Lisek, M., Przybyszewski, O., Zylinska, L., Guo, F., & Boczek, T. (2023). The role of MEF2 transcription factor family in neuronal survival and degeneration. *International Journal of Molecular Sciences*, *24*(4), 3120. https://doi.org/10.3390/ijms24043120

Liu, C., Plaçais, P.-Y., Yamagata, N., Pfeiffer, B. D., Aso, Y., Friedrich, A. B., Siwanowicz, I., Rubin, G. M., Preat, T., & Tanimoto, H. (2012). A subset of dopamine neurons signals reward for odour memory in *Drosophila*. *Nature*, *488*(7412), 512-516. https://doi.org/10.1038/nature11304

Liu, W., Lim, K. L., & Tan, E. K. (2022). Intestine-derived α-synuclein initiates and aggravates pathogenesis of Parkinson's disease in *Drosophila*. *Translational neurodegeneration*, *11*(44). https://doi.org/10.1186/s40035-022-00318-w

Lu, J., McKinsey, T. A., Nicol, R. L., & Olson, E. N. (2000a). Signal-dependent activation of the MEF2 transcription factor by dissociation from histone deacetylases. *Proceedings of the National Academy of Sciences*, *97*(8), 4070-4075. https://doi.org/10.1073/pnas.080064097

Lu, J., McKinsey, T. A., Zhang, C.-L., & Olson, E. N. (2000b). Regulation of skeletal myogenesis by association of the MEF2 transcription factor with class II histone deacetylases. *Molecular Cell*, *6*(2), 233-244. https://doi.org/10.1016/S1097-2765(00)00025-3

Magistrelli, L., Contaldi, E., & Comi, C. (2021). The impact of SNCA variations and its product alpha-synuclein on non-motor features of Parkinson's disease. *Life*, *11*(8), 804. https://doi.org/10.3390/life11080804

Magwire, M. M., Yamamoto, A., Carbone, M. A., Roshina, N. V., Symonenko, A. V., Pasyukova, E. G., Morozova, T. V., & Mackay, T. F. (2010). Quantitative and molecular genetic analyses of mutations increasing *Drosophila* life span. *PLoS Genetics*, *6*(7), e1001037. https://doi.org/10.1371/journal.pgen.1001037

Main, P., Tan, W. J., Wheeler, D., & Fitzsimons, H. L. (2021). Increased abundance of nuclear HDAC4 impairs neuronal development and long-term memory. *Frontiers in Molecular Neuroscience*, *14*, 616642. https://doi.org/10.3389/fnmol.2021.616642

Main, P. J. (2019). *Investigating the role of HDAC4 subcellular distribution in Drosophila development and memory: a thesis presented in partial fulfilment of the requirements for the degree of Doctor of Philosophy (PhD) in Biochemistry at Massey University, Manawatū, New Zealand* Massey University]. http://hdl.handle.net/10179/15578

Maiti, P., Manna, J., & Dunbar, G. L. (2017). Current understanding of the molecular mechanisms in Parkinson's disease: Targets for potential treatments. *Translational neurodegeneration*, *6*, 1-35. https://doi.org/10.1186/s40035-017-0099-z

Mao, Z., Bonni, A., Xia, F., Nadal-Vicens, M., & Greenberg, M. E. (1999). Neuronal activity-dependent cell survival mediated by transcription factor MEF2. *Science*, *286*(5440), 785-790. https://doi.org/10.1126/science.286.5440.785

Mao, Z., & Davis, R. L. (2009). Eight different types of dopaminergic neurons innervate the *Drosophila* mushroom body neuropil: anatomical and physiological heterogeneity. *Frontiers in neural circuits*, *3*, 612. https://doi.org/10.3389/neuro.04.005.2009

Maor, G., Dubreuil, R. R., & Feany, M. B. (2023). α-Synuclein promotes neuronal dysfunction and death by disrupting the binding of ankyrin to β-spectrin. *Journal of Neuroscience*, *43*(9), 1614-1626. https://doi.org/10.1523/JNEUROSCI.1922-22.2022

McBride, S. M., Giuliani, G., Choi, C., Krause, P., Correale, D., Watson, K., Baker, G., & Siwicki, K. K. (1999). Mushroom body ablation impairs short-term memory and long-term memory of courtship conditioning in *Drosophila melanogaster*. *Neuron*, *24*(4), 967-977. https://doi.org/10.1016/S0896-6273(00)81043-0

McGuire, S. E., Mao, Z., & Davis, R. L. (2004). Spatiotemporal gene expression targeting with the TARGET and gene-switch systems in *Drosophila*. *Science's STKE*. https://doi.org/10.1126/stke.2202004pl6

McGurk, L., Berson, A., & Bonini, N. M. (2015). *Drosophila* as an in vivo model for human neurodegenerative disease. *Genetics*, *201*(2), 377-402. https://doi.org/10.1534/genetics.115.179457

McKinsey, T. A., Zhang, C. L., & Olson, E. N. (2002). MEF2: a calcium-dependent regulator of cell division, differentiation and death. *Trends in biochemical sciences*, *27*(1), 40-47. https://doi.org/10.1016/S0968-0004(01)02031-X

McNaught, K. S. P., Olanow, C. W., Halliwell, B., Isacson, O., & Jenner, P. (2001). Failure of the ubiquitin–proteasome system in Parkinson's disease. *Nature Reviews Neuroscience*, *2*(8), 589-594. https://doi.org/10.1038/35086067

Melki, R. (2015). Role of different alpha-synuclein strains in synucleinopathies, similarities with other neurodegenerative diseases. *Journal of Parkinson's disease*, *5*(2), 217-227. https://doi.org/10.3233/JPD-150543

Mielcarek, M., Zielonka, D., Carnemolla, A., Marcinkowski, J. T., & Guidez, F. (2015). HDAC4 as a potential therapeutic target in neurodegenerative diseases: a summary of recent achievements. *Frontiers in Cellular Neuroscience*, *9*, 42. https://doi.org/10.3389/fncel.2015.00042

Miska, E. A., Karlsson, C., Langley, E., Nielsen, S. J., Pines, J., & Kouzarides, T. (1999). HDAC4 deacetylase associates with and represses the MEF2 transcription factor. *The EMBO Journal*. https://doi.org/10.1093/emboj/18.18.5099

Mitchell, K. J. (2011). The genetics of neurodevelopmental disease. *Current Opinion in Neurobiology*, *21*(1), 197-203. https://doi.org/10.1016/j.conb.2010.08.009

Mohite, G. M., Dwivedi, S., Das, S., Kumar, R., Paluri, S., Mehra, S., Ruhela, N., S, A., Jha, N. N., & Maji, S. K. (2018). Parkinson's disease associated α-synuclein familial mutants promote dopaminergic neuronal death in *Drosophila melanogaster*. *ACS chemical neuroscience*, *9*(11), 2628-2638. https://doi.org/10.1021/acschemneuro.8b00107

Myall, D. J., Pitcher, T. L., Pearson, J. F., Dalrymple-Alford, J. C. A., T.J, & MacAskill, M. R. (2017). Parkinson's in the oldest old: Impact on estimates of future disease burden. *Parkinsonism & Related Disorders*, *42*, 78-84. https://doi.org/10.1016/j.parkreldis.2017.06.018

Nam, J., & Gwon, Y. (2023). Neuronal biomolecular condensates and their implications in neurodegenerative diseases. *Frontiers in Aging Neuroscience*, *15*, 1145420. https://doi.org/10.3389/fnagi.2023.1145420

Narwal, S., Singh, A., & Tare, M. (2024). Analysis of α-syn and parkin interaction in mediating neuronal death in *Drosophila* model of Parkinson's disease. *Frontiers in Cellular Neuroscience*, *17*, 1295805. https://doi.org/10.3389/fncel.2023.1295805

Nässel, D., & Elekes, K. (1992). Aminergic neurons in the brain of blowflies and *Drosophila*: dopamine-and tyrosine hydroxylase-immunoreactive neurons and their relationship with putative histaminergic neurons. *Cell and tissue research*, *267*, 147-167. https://doi.org/10.1007/BF00318701

Nitta, Y., & Sugie, A. (2022). Studies of neurodegenerative diseases using *Drosophila* and the development of novel approaches for their analysis. *Fly*, *16*(1), 275-298. https://doi.org/10.1080/19336934.2022.2087484

Nuytemans, K., Theuns, J., Cruts, M., & Van Broeckhoven, C. (2010). Genetic etiology of Parkinson disease associated with mutations in the SNCA, PARK2, PINK1, PARK7, and LRRK2 genes: a mutation update. *Human mutation*, *31*(7), 763-780. https://doi.org/0.1002/humu.21277

Olsen, A. L., Clemens, S. G., & Feany, M. B. (2023). Nicotine-Mediated Rescue of α-Synuclein Toxicity Requires Synaptic Vesicle Glycoprotein 2 in *Drosophila*. *Movement Disorders*, *38*(2), 244-255. https://doi.org/10.1002/mds.29283

Olsen, A. L., & Feany, M. B. (2019). Glial α-synuclein promotes neurodegeneration characterized by a distinct transcriptional program in vivo. *Glia*, *67*(10), 1933-1957. https://doi.org/10.1002/glia.23671

Ordonez, D. G., Lee, M. K., & Feany, M. B. (2018). α-synuclein induces mitochondrial dysfunction through spectrin and the actin cytoskeleton. *Neuron*, *97*(1), 108-124. https://doi.org/10.1016/j.neuron.2017.11.036

Pandey, U. B., & Nichols, C. D. (2011). Human disease models in *Drosophila melanogaster* and the role of the fly in therapeutic drug discovery. *Pharmacological reviews*, *63*(2), 411-436. https://doi.org/10.1124/pr.110.003293

Parihar, M. S., Parihar, A., Fujita, M., Hashimoto, M., & Ghafourifar, P. (2009). Alpha-synuclein overexpression and aggregation exacerbates impairment of mitochondrial functions by augmenting oxidative stress in human neuroblastoma cells. *The International Journal of Biochemistry & Cell Biology*, *41*(10), 2015-2024. https://doi.org/10.1016/j.biocel.2009.05.008

Park, S.-Y., & Kim, J.-S. (2020). A short guide to histone deacetylases including recent progress on class II enzymes. *Experimental & molecular medicine*, *52*(2), 204-212. https://doi.org/10.1038/s12276-020-0382-4

Periquet, M., Fulga, T., Myllykangas, L., Schlossmacher, M. G., & Feany, M. B. (2007). Aggregated α-synuclein mediates dopaminergic neurotoxicity in vivo. *Journal of*

Neuroscience, *27*(12), 3338-3346. https://doi.org/10.1523/JNEUROSCI.0285-07.2007

Perrin, R., Payton, J., Barnett, D., Wraight, C., Woods, W., Ye, L., & George, J. (2003). Epitope mapping and specificity of the anti-α-synuclein monoclonal antibody Syn-1 in mouse brain and cultured cell lines. *Neuroscience Letters*, *349*(2), 133-135. https://doi.org/10.1016/S0304-3940(03)00781-X

Pesah, Y., Burgess, H., Middlebrooks, B., Ronningen, K., Prosser, J., Tirunagaru, V., Zysk, J., Mardon, G. (2005). Whole-mount analysis reveals normal numbers of dopaminergic neurons following misexpression of α-Synuclein in *Drosophila*. *Genesis*, *41*(4), 154-159. https://doi.org/10.1002/gene.20106

Petit, P., Berger, F., Bonneterre, V., & Vuillerme, N. (2025). Investigating Parkinson's disease risk across farming activities using data mining and large-scale administrative health data. *npj Parkinson's Disease*, *11*(1), 13. https://doi.org/10.1038/s41531-024-00864-2

Pezzoli, G., & Cereda, E. (2013). Exposure to pesticides or solvents and risk of Parkinson disease. *Neurology*, *80*(22), 2035-2041. https://doi.org/10.1212/WNL.0b013e318294b3c8

Piper, M. D., & Partridge, L. (2018). *Drosophila* as a model for ageing. *Biochimica et Biophysica Acta (BBA)-Molecular Basis of Disease*, *1864*(9), 2707-2717. https://doi.org/10.1016/j.bbadis.2017.09.016

Poewe, W., Seppi, K., Tanner, C. M., Halliday, G. M., Brundin, P., Volkmann, J., Schrag, A.-E., & Lang, A. E. (2017). Parkinson disease. *Nature Reviews Disease Primers*, *3*(1). https://doi.org/10.1038/nrdp.2017.13

Polymeropoulos, M. H., Lavedan, C., Leroy, E., Ide, S. E., Dehejia, A., Dutra, A., Pike, B., Root, H., Rubenstein, J., & Boyer, R. (1997). Mutation in the α-synuclein gene identified in families with Parkinson's disease. *Science*, *276*(5321), 2045-2047. https://doi.org/10.1126/science.276.5321.2045

Raji, J. I., & Potter, C. J. (2021). The number of neurons in *Drosophila* and mosquito brains. *PLoS ONE*, *16*(5), e0250381. https://doi.org/10.1371/journal.pone.0250381

Ready, D. F., Hanson, T. E., & Benzer, S. (1976). Development of the *Drosophila* retina, a neurocrystalline lattice. *Developmental biology*, *53*(2), 217-240. https://doi.org/10.1016/0012-1606(76)90225-6

Rein, K., Zöckler, M., Mader, M. T., Grübel, C., & Heisenberg, M. (2002). The *Drosophila* standard brain. *Current Biology*, *12*(3), 227-231. https://doi.org/10.1016/S0960-9822(02)00656-5

Reiter, L. T., Potocki, L., Chien, S., Gribskov, M., & Bier, E. (2001). A systematic analysis of human disease-associated gene sequences in *Drosophila melanogaster*. *Genome research*, *11*(6), 1114-1125. https://doi.org/10.1101/gr.169101.

Riemensperger, T., Isabel, G., Coulom, H., Neuser, K., Seugnet, L., Kume, K., Iché-Torres, M., Cassar, M., Strauss, R., & Preat, T. (2011). Behavioral consequences of dopamine deficiency in the *Drosophila* central nervous system. *Proceedings of the National Academy of Sciences*, *108*(2), 834-839. https://doi.org/10.1073/pnas.1010930108

Rose, M. R. (2009). Adaptation, aging, and genomic information. *Aging*, *1*(5), 444-450. https://doi.org/10.18632/aging.100053

Rubin, G. M., Yandell, M. D., Wortman, J. R., Gabor, G. L., Miklos, Nelson, C. R., Hariharan, I. K., Fortini, M. E., Li, P. W., & Apweiler, R. (2000). Comparative genomics of the eukaryotes. *Science*, *287*(5461), 2204-2215. https://doi.org/10.1126/science.287.5461.2204

Ryan, S. D., Dolatabadi, N., Chan, S. F., Zhang, X., Akhtar, M. W., Parker, J., Soldner, F., Sunico, C. R., Nagar, S., & Talantova, M. (2013). Isogenic human iPSC Parkinson's model shows nitrosative stress-induced dysfunction in MEF2-PGC1α transcription. *Cell*, *155*(6), 1351-1364. https://doi.org/10.1016/j.cell.2013.11.009

Sakai, R., Suzuki, M., Ueyama, M., Takeuchi, T., Minakawa, E. N., Hayakawa, H., Baba, K., Mochizuki, H., & Nagai, Y. (2019). E46K mutant α-synuclein is more degradation resistant and exhibits greater toxic effects than wild-type α-synuclein in *Drosophila* models of Parkinson's disease. *PLoS ONE*, *14*(6), e0218261. https://doi.org/10.1371/journal.pone.0218261

Salles, P., Tirapegui, J., & Chaná-Cuevas, P. (2024). Genetics of Parkinson's disease: Dominant forms and GBA. *Neurology Perspectives*, *4*(3), 100153. https://doi.org/10.1016/j.neurop.2024.100153

Sando, R., Gounko, N., Pieraut, S., Liao, L., Yates, J., & Maximov, A. (2012). HDAC4 governs a transcriptional program essential for synaptic plasticity and memory. *Cell*, *151*(4), 821-834. https://doi.org/10.1016/j.cell.2012.09.037

Sasaki, K., & Harano, K.-i. (2010). Multiple regulatory roles of dopamine in behavior and reproduction of social insects. *Trends Entomol*, *6*, 1-13. https://doi.org/10.5555/20113273165

Schwartz, S., Truglio, M., Scott, M. J., & Fitzsimons, H. L. (2016). Long-term memory in *Drosophila* is influenced by histone deacetylase HDAC4 interacting with SUMO-conjugating enzyme Ubc9. *Genetics*, *203*(3), 1249-1264. https://doi.org/10.1534/genetics.115.183194

Seong, K.-H., Uemura, T., & Kang, S. (2023). Road to sexual maturity: Behavioral event schedule from eclosion to first mating in each sex of *Drosophila melanogaster*. *Iscience*, *26*(9). https://doi.org/10.1016/j.isci.2023.107502

Seto, E., & Yoshida, M. (2014). Erasers of Histone Acetylation: The Histone Deacetylase Enzymes. *Cold Spring Harbor Perspectives in Biology*, *6*(4). https://doi.org/10.1101/cshperspect.a018713

She, H., Yang, Q., Shepherd, K., Smith, Y., Miller, G., Testa, C., & Mao, Z. (2011). Direct regulation of complex I by mitochondrial MEF2D is disrupted in a mouse model of Parkinson disease and in human patients. *The Journal of Clinical Investigation*, *121*(3), 930-940. https://doi.org/10.1172/JCI43871

Shen, X., Chen, J., Li, J., Kofler, J., & Herrup, K. (2016). Neurons in vulnerable regions of the Alzheimer's disease brain display reduced ATM signaling. *Eneuro*, *3*(1). https://doi.org/10.1523/ENEURO.0124-15.2016

Shi, L., Li, B., Chen, G., Huang, Y., Tian, Z., Zhang, L., Tian, L., & Fu, Q. (2022). MEF2D participates in microglia-mediated neuroprotection in cerebral ischemia-

reperfusion rats. *Shock*, *57*(1), 118-130. https://doi.org/10.1097/SHK.0000000000001844

Siju, K., De Backer, J.-F., & Grunwald Kadow, I. C. (2021). Dopamine modulation of sensory processing and adaptive behavior in flies. *Cell and tissue research*, *383*(1), 207-225. https://doi.org/10.1007/s00441-020-03371-x

Silbering, A. F., Okada, R., Ito, K., & Galizia, C. G. (2008). Olfactory information processing in the *Drosophila* antennal lobe: anything goes? *Journal of Neuroscience*, *28*(49), 13075-13087. https://doi.org/10.1523/JNEUROSCI.2973-08.2008

Smith, P. D., Mount, M. P., Shree, R., Callaghan, S., Slack, R. S., Anisman, H., Vincent, I., Wang, X., Mao, Z., & Park, D. S. (2006). Calpain-regulated p35/cdk5 plays a central role in dopaminergic neuron death through modulation of the transcription factor myocyte enhancer factor 2. *Journal of Neuroscience*, *26*(2), 440-447. https://doi.org/10.1523/JNEUROSCI.2875-05.2006

Sparrow, D. B., Miska, E. A., Langley, E., Reynaud-Deonauth, S., Kotecha, S., Towers, N., Spohr, G., Kouzarides, T., & Mohun, T. J. (1999). MEF-2 function is modified by a novel co-repressor, MITR. *The EMBO Journal*. https://doi.org/10.1093/emboj/18.18.5085

Spillantini, M. G., Crowther, R. A., Jakes, R., Hasegawa, M., & Goedert, M. (1998). α-Synuclein in filamentous inclusions of Lewy bodies from Parkinson's disease and dementia with Lewy bodies. *Proceedings of the National Academy of Sciences*, *95*(11), 6469-6473. https://doi.org/10.1073/pnas.95.11.6469

St Johnston, D. (2002). The art and design of genetic screens: *Drosophila melanogaster*. *Nature reviews genetics*, *3*(3), 176-188. https://doi.org/10.1038/nrg751

Stocker, R., Lienhard, M., Borst, A., & Fischbach, K. (1990). Neuronal architecture of the antennal lobe in *Drosophila melanogaster*. *Cell and tissue research*, *262*, 9-34. https://doi.org/10.1007/BF00327741

Takahashi-Fujigasaki, J., & Fujigasaki, H. (2006). Histone deacetylase (HDAC) 4 involvement in both Lewy and Marinesco bodies. *Neuropathology and Applied Neurobiology*, *32*(5), 562-566. https://doi.org/10.1111/j.1365-2990.2006.00733.x

Takahashi, M., Suzuki, M., Fukuoka, M., Fujikake, N., Watanabe, S., Murata, M., Wada, K., Naga, Y., & Hohjoh, H. (2015). Normalization of Overexpressed α-Synuclein Causing Parkinson's Disease By a Moderate Gene Silencing With RNA interference. *Molecular Therapy—Nucleic Acids*, *4*. https://doi.org/10.1038/mtna.2015.14

Takemura, S. Y., Lu, Z., & Meinertzhagen, I. A. (2008). Synaptic circuits of the *Drosophila* optic lobe: the input terminals to the medulla. *Journal of Comparative Neurology*, *509*(5), 493-513. https://doi.org/10.1002/cne.21757

Tan, W. J., Hawley, H. R., Wilson, S. J., & Fitzsimons, H. L. (2024). Deciphering the roles of subcellular distribution and interactions involving the MEF2 binding region, the ankyrin repeat binding motif and the catalytic site of HDAC4 in *Drosophila* neuronal morphogenesis. *BMC biology*, *22*(1), 2. https://doi.org/10.1186/s12915-023-01800-1

Tataroglu, O., & Emery, P. (2014). Studying circadian rhythms in *Drosophila melanogaster*. *Methods*, *68*(1), 140-150. https://doi.org/10.1016/j.ymeth.2014.01.001

Taylor, J. P., Hardy, J., & Fischbeck, K. H. (2002). Toxic proteins in neurodegenerative disease. *Science*, *296*(5575), 1991-1995. https://doi.org/10.1126/science.1067122

Tonoki, A., Kuranaga, E., Tomioka, T., Hamazaki, J., Murata, S., Tanaka, K., & Miura, M. (2009). Genetic evidence linking age-dependent attenuation of the 26S proteasome with the aging process. *Molecular and Cellular Biology*, *29*(4), 1095-1106. https://doi.org/10.1128/MCB.01227-08

Trinh, K., Moore, K., Wes, P. D., Muchowski, P. J., Dey, J., Andrews, L., & Pallanck, L. J. (2008). Induction of the phase II detoxification pathway suppresses neuron loss in *Drosophila* models of Parkinson's disease. *Journal of Neuroscience*, *28*(2), 465-472. https://doi.org/10.1523/JNEUROSCI.4778-07.2008

Tsachaki, M., & Sprecher, S. G. (2012). Genetic and developmental mechanisms underlying the formation of the *Drosophila* compound eye. *Developmental Dynamics*, *241*(1), 40-56. https://doi.org/10.1002/dvdy.22738

Tsien, R. Y. (1998). The green fluorescent protein. *Annual review of biochemistry*, *67*(1), 509-544. https://doi.org/10.1146/annurev.biochem.67.1.509

Uversky, V. N. (2003). A Protein-Chameleon: Conformational Plasticity of α-Synuclein, a Disordered Protein Involved in Neurodegenerative Disorders. *Journal of Biomolecular Structure and Dynamics*, *21*(2), 211-234. https://doi.org/10.1080/07391102.2003.10506918

Van Maele-Fabry, G., Hoet, P., Vilain, F., & Lison, D. (2012). Occupational exposure to pesticides and Parkinson's disease: a systematic review and meta-analysis of cohort studies. *Environment international*, *46*, 30-43. https://doi.org/10.1016/j.envint.2012.05.004

Wang, A. H., Bertos, N. R., Vezmar, M., Pelletier, N., Crosato, M., Heng, H. H., Th'ng, J., Han, J., & Yang, X.-J. (1999). HDAC4, a human histone deacetylase related to yeast HDA1, is a transcriptional corepressor. *Molecular and Cellular Biology*, *19*(11), 7816-7827. https://doi.org/10.1128/MCB.19.11.7816

Wang, A. H., Kruhlak, M. J., Wu, J., Bertos, N. R., Vezmar, M., Posner, B. I., Bazett-Jones, D. P., & Yang, X.-J. (2000). Regulation of histone deacetylase 4 by binding of 14-3-3 proteins. *Molecular and Cellular Biology*, *20*(18), 6904-6912. https://doi.org/10.1128/MCB.20.18.6904-6912.2000

Wang, B., Cai, Z., Lu, F., Li, C., Zhu, X., Su, L., Gao, G., & Yang, Q. (2014). Destabilization of survival factor MEF2D mRNA by neurotoxin in models of Parkinson's disease. *Journal of Neurochemistry*, *130*(5), 720-728. https://doi.org/10.1111/jnc.12765

Wang, L., Liu, L., Han, C., Jiang, H., Ma, K., Guo, S., Xia, Y., Wan, F., Huang, J., & Xiong, N. (2023). Histone deacetylase 4 inhibition reduces rotenone-induced alpha-synuclein accumulation via autophagy in SH-SY5Y cells. *Brain Sciences*, *13*(4), 670. https://doi.org/10.3390/brainsci13040670

Welberg, L. (2009). Dopamine drives the circuit. *Nature Reviews Neuroscience*, *10*(12), 832-832. https://doi.org/10.1038/nrn2764

White, K. E., Humphrey, D. M., & Hirth, F. (2010). The dopaminergic system in the aging brain of *Drosophila*. *Frontiers in Neuroscience*, *4*, 205. https://doi.org/10.3389/fnins.2010.00205

Whitworth, A. J. (2011). *Drosophila* models of Parkinson's disease. *Advances in genetics*, *73*, 1-50. https://doi.org/10.1016/B978-0-12-380860-8.00001-X

Withers, G. S., George, J. M., Banker, G. A., & Clayton, D. F. (1997). Delayed localization of synelfin (synuclein, NACP) to presynaptic terminals in cultured rat hippocampal neurons. *Developmental brain research*, *99*(1), 87-94. https://doi.org/10.1016/S0165-3806(96)00210-6

Wu, K. L. H., Liu, W.-C., Wu, C.-W., Fu, M.-H., Huang, H.-M., Tain, Y.-L., Liang, C.-K., Hung, C.-Y., Chen, I.-C., & Hung, P.-L. (2024). Butyrate reduction and HDAC4 increase underlie maternal high fructose-induced metabolic dysfunction in hippocampal astrocytes in female rats. *The Journal of Nutritional Biochemistry*, *126*, 109571. https://doi.org/10.1016/j.jnutbio.2024.109571

Wu, Q., Yang, X., Zhang, L., Zhang, Y., & Feng, L. (2017). Nuclear accumulation of histone deacetylase 4 (HDAC4) exerts neurotoxicity in models of Parkinson's disease. *Molecular Neurobiology*, *54*, 6970-6983. https://doi.org/10.1007/s12035-016-0199-2

Wyttenbach, A. (2004). Role of heat shock proteins during polyglutamine neurodegeneration: mechanisms and hypothesis. *Journal of Molecular Neuroscience*, *23*, 69-95. https://doi.org/10.1385/JMN:23:1-2:069

Xie, T., Ho, M. C., Liu, Q., Horiuchi, W., Lin, C.-C., Task, D., Luan, H., White, B. H., Potter, C. J., & Wu, M. N. (2018). A genetic toolkit for dissecting dopamine circuit function in *Drosophila*. *Cell Reports*, *23*(2), 652-665. https://doi.org/10.1016/j.celrep.2018.03.068

Xiong, Y., & Yu, J. (2018). Modeling Parkinson's disease in *Drosophila*: what have we learned for dominant traits? *Frontiers in Neurology*, *9*, 228. https://doi.org/10.3389/fneur.2018.00228

Yang, Q., She, H., Gearing, M., Colla, E., Lee, M., Shacka, J., & Mao, Z. (2009). Regulation of Neuronal Survival Factor MEF2D by Chaperone-Mediated Autophagy. *Science*, *323*, 124-127. https://doi.org/10.1126/science.1166088

Yang, X., Ma, Z., Lian, P., Wu, Y., Liu, K., Zhang, Z., Tang, Z., Xu, Y., & Cao, X. (2025). Disruption of axonal transport in Parkinson's disease: the role of pathological α-Syn and AMPK/p38 MAPK signaling. *npj Parkinson's Disease*, *11*(1), 114. https://doi.org/10.1038/s41531-025-00926-z

Yang, Y., Qin, X., Liu, S., Li, J., Zhu, X., Gao, T., & Wang, X. (2011). Peroxisome proliferator-activated receptor γ is inhibited by histone deacetylase 4 in cortical neurons under oxidative stress. *Journal of Neurochemistry*, *118*(3), 429-439. https://doi.org/10.1111/j.1471-4159.2011.07316.x

Yankner, B. A., Lu, T., & Loerch, P. (2008). The aging brain. *Annu. Rev. Pathol. Mech. Dis.*, *3*(1), 41-66. https://doi.org/10.4103/0377-4929.71995

Yao, L., Li, W., She, H., Dou, J., Jia, L., He, Y., Yang, Q., Zhu, J., Cápiro, N. L., & Walker, D. I. (2012). Activation of transcription factor MEF2D by bis (3)-cognitin protects dopaminergic neurons and ameliorates Parkinsonian motor defects. *Journal of*

Biological Chemistry, *287*(41), 34246-34255. https://doi.org/10.1074/jbc.M112.367540

Yarali, A., & Gerber, B. (2010). A neurogenetic dissociation between punishment-, reward-, and relief-learning in *Drosophila*. *Frontiers in behavioral neuroscience*, *4*(189).

Yasuyama, K., Meinertzhagen, I. A., & Schürmann, F. W. (2002). Synaptic organization of the mushroom body calyx in *Drosophila melanogaster*. *Journal of Comparative Neurology*, *445*(3), 211-226. https://doi.org/10.1002/cne.10155

Youn, H.-D., Grozinger, C. M., & Liu, J. O. (2000). Calcium regulates transcriptional repression of myocyte enhancer factor 2 by histone deacetylase 4. *Journal of Biological Chemistry*, *275*(29), 22563-22567. https://doi.org/10.1074/jbc.C000304200

Youn, H.-D., Sun, L., Prywes, R., & Liu, J. O. (1999). Apoptosis of T cells mediated by Ca2+-induced release of the transcription factor MEF2. *Science*, *286*(5440), 790-793. https://doi.org/10.1126/science.286.5440.790

Zhang, L., Sun, Y., Fei, M., Tan, C., Wu, J., Zheng, J., Tang, J., Sun, W., Lv, Z., & Bao, J. (2014). Disruption of chaperone-mediated autophagy-dependent degradation of MEF2A by oxidative stress-induced lysosome destabilization. *Autophagy*, *10*(6), 1015-1035. https://doi.org/10.4161/auto.28477

Zhao, H., Kalivendi, S., Zhang, H., Joseph, J., Nithipatikom, K., Vásquez-Vivar, J., & Kalyanaraman, B. (2003). Superoxide reacts with hydroethidine but forms a fluorescent product that is distinctly different from ethidium: potential implications in intracellular fluorescence detection of superoxide. *Free Radical Biology and Medicine*, *34*(11), 1359-1368. https://doi.org/10.1016/s0891-5849(03)00142-4

Zhao, X., Ito, A., Kane, C. D., Liao, T.-S., Bolger, T. A., Lemrow, S. M., Means, A. R., & Yao, T.-P. (2001). The modular nature of histone deacetylase HDAC4 confers phosphorylation-dependent intracellular trafficking. *Journal of Biological Chemistry*, *276*(37), 35042-35048. https://doi.org/10.1074/jbc.M105086200

Zhao, Z., & McBride, C. S. (2020). Evolution of olfactory circuits in insects. *Journal of Comparative Physiology A*, *206*(3), 353-367. https://doi.org/10.1007/s00359-020-01399-6

Zigmond, R. E., Schwarzschild, M. A., & Rittenhouse, A. R. (1989). Acute regulation of tyrosine hydroxylase by nerve activity and by neurotransmitters via phosphorylation. *Annual review of neuroscience*, *12*(1), 415-461. https://doi.org/10.1146/annurev.neuro.12.1.415